Influence of the E3 ligase Trim33 on the development and the therapy resistance of liver cancer

Dissertation

der Mathematisch-Naturwissenschaftlichen Fakultät
der Eberhard Karls Universität Tübingen
zur Erlangung des Grades eines
Doktors der Naturwissenschaften
(Dr. rer. nat.)

vorgelegt von
Vanessa Rousseau
aus Lindau

Tübingen
2021

Gedruckt mit Genehmigung der Mathematisch-Naturwissenschaftlichen Fakultät der Eberhard Karls Universität Tübingen.

Tag der mündlichen Qualifikation:	21.12.2021
Stellvertretender Dekan:	Prof. Dr. Thilo Stehle
1. Berichterstatter:	Prof. Dr. Tassula Proikas-Cezanne
2. Berichterstatter:	Prof. Dr. Nikita Popov

Table of contents

Abbreviations

Prefixes:

µ	micro
m	mili
k	kilo

Units:

°C	degree celsius
g	gramm
h	hour
m	meter
min	minute
sec	second

Additionals:

4-OHT	4-hydroxytamoxifen
ALD	alcoholic liver disease
AV	Annexin-V
DDR	DNA damage response
DM	Dermatomyositis
DSB	double strand break
DUBs	deubiquitinases
EBs	embryonic bodies
ER	estrogen receptor
ESC	embryonic stem cells
EtOH	Ethanol
Etop	etoposide
GESA	gene set enrichment analysis
HBV/HCV	hepatitis B/C virus
HCC	Hepatocellular carcinoma
HU	hydroxyurea
KD	knock down
KO	knock out
NALFD	Nonalcoholic fatty liver disease
NES	nuclear export signal
NLS	nuclear localization signal
Noc	nocodazole
ON	overnight
OS	overall survival
PEI	Polyethyleneimine
PHD	Plant Homeo Domain
PI	propidiumiodid
PolII	RNA polymerase II
ROS	reactive oxygen species
rpm	rotations per minute
RS	replicative stress
RT	room temperature
SCTF	stem cell transcription factor
TACE	transarterial chemoembolization
TF	transcription factor
TIF1	transcriptional intermediary factor 1
TRIM	Tripartite motif-containing

Summary

Myc is an oncogenic transcription factor (TF), promoting the growth and aggressiveness of many different cancer types, including liver cancer. Despite its tumorigenic function, Myc activation can induce DNA damage and replicative stress (RS), thereby promoting the apoptotic response. Hence, Myc would be an attractive target for cancer therapy. However, Myc does not have enzymatic activity or defined binding pockets, which makes it difficult to target it with small molecule inhibitors. Taken together, there is an urgent need to find new indirect mechanisms regulating Myc, to be able to design novel therapeutic strategies. Previous data from our working group showed that the ubiquitin E3 ligase Trim33 is a regulator of Myc-induced apoptosis (Popov *et al.,* 2007). I could show during this thesis that Myc is not a substrate of Trim33 in liver cancer cells and that Trim33 does not influence Myc levels through its already known connections to the Wnt and TGFβ pathways. Furthermore, I demonstrated that Trim33 knockout (Trim33KO) cells can replicate DNA more efficiently, reenter cell cycle faster and proliferate more upon RS compared to control cells. Additionally, upon Trim33KO, DNA damage is induced later after induction of RS and is repaired faster during recovery from RS. These effects could be seen when RS was induced by Myc overexpression or by the treatment with the genotoxic drugs hydroxyurea (HU) and etoposide (Etop). Hence, the function of Trim33 is not limited to the regulation of Myc-induced apoptosis, but it is rather more generally modulating the response of cells to RS. Subsequently, RNA-Sequencing analysis revealed that the target genes of the TF E2F4 were strongly upregulated in Trim33KO cells compared to control cells. E2F4 is known to be involved in DNA replication and cell cycle control, making it a very promising candidate. I could show that E2F4 is a novel substrate of Trim33 and that its overexpression in control cells mimicked the RS phenotype observed in Trim33KO cells, demonstrating the E2F4 dependency of the mechanism. Finally, mass spectrometry analysis revealed that the binding of E2F4 to the helicase RecQL was enhanced upon Trim33KO, which could be validated by proximity ligation assays (PLAs). RecQL is known to stabilize replication forks and to be involved in DNA damage repair. Hence, RecQL could strongly simplify the handling of RS for cells. I could demonstrate that RecQL as well as E2F4 binding to chromatin is enhanced upon Trim33KO, suggesting that E2F4 recruits RecQL to DNA. Moreover, the overexpression of RecQL in control cells mimicked the enhanced fork rate observed in Trim33KO cells, whereas an inactive RecQL mutant (K119A) overexpressed in Trim33KO cells significantly impaired replication fork progression under RS. Two E2F4 mutants, one which cannot bind to DNA (E2F4-DB) and one which lacks a part of its C-terminus (E2F4-ΔC), cannot recruit RecQL to chromatin and revert the RS phenotype of Trim33KO cells. Taken together, our data suggest a model in which E2F4 recruits RecQL to chromatin, which in turn makes cells less sensitive to RS.

Zusammenfassung

Myc ist ein onkogener Transkriptionsfaktor (TF), welcher sowohl das Wachstum als auch die Aggressivität vieler Krebsarten, einschließlich Leberkrebs, verstärkt. Trotz seiner tumor unterstützenden Funktion, kann die Aktivierung von Myc DNA Schäden und replikativen Stress (RS) induzieren und dadurch Apoptose fördern. Demnach wäre Myc ein vielversprechendes Ziel für Krebstherapien. Es besitzt allerdings keine enzymatische Aktivität oder definierte Bindetaschen, was es erschwert niedermolekulare Inhibitoren gegen Myc zu entwickeln. Zusammenfassend besteht ein dringender Bedarf an neuen indirekt Myc regulierenden Mechanismen, um mögliche neue therapeutische Strategien zu verwirklichen. Bereits publizierte Daten unserer Arbeitsgruppe zeigten, dass die Ubiquitin-E3-Ligase Trim33 ein Regulator der Myc-induzierten Apoptose ist (Popov *et al.,* 2007). Ich konnte während dieser Thesis zeigen, dass Myc kein Substrat von Trim33 in Leberkrebszellen ist und dass Trim33 nicht über ihre bereits bekannte Verbindung zu den Wnt und TGFβ Signalwegen das Myc Protein Level beeinflusst. Weiterhin konnte ich demonstrieren, dass Trim33 knockout (KO) Zellen im Vergleich zu Kontrollzellen unter RS DNA schneller replizieren, den Zellzyklus schneller starten und sich effektiver vermehren. Zusätzlich werden DNA Schäden unter RS später induziert und während der Erholung von RS effizienter repariert. Diese Effekte konnten beobachtet werden, wenn RS sowohl durch die Überexpression von Myc, als auch durch die Behandlung der Zellen mit genotoxischen Mitteln wie HU oder Etop ausgelöst wurde. Demnach ist die Funktion von Trim33 nicht auf die Regulation der Myc-induzierten Apoptose beschränkt, sondern Trim33 moduliert eher die generelle Antwort von Zellen auf RS. Anschließend konnte ein RNA-Sequenzierungsexperiment zeigen, dass die Zielgene von E2F4 stark induziert werden, wenn Trim33 ausgeknockt ist. E2F4 ist ein TF welcher bereits dafür bekannt ist, an der DNA Replikation und dem Zellzyklus beteiligt zu sein, was E2F4 zu einem sehr interessanten Kandidaten macht. Ich konnte zeigen, dass E2F4 ein neues Substrat von Trim33 ist und dass dessen Überexpression in Kontrollzellen den RS Phänotyp der Trim33KO Zellen imitieren kann, was die E2F4-Abhängigkeit des Mechanismus verdeutlicht. Schlussendlich konnte ein Massenspektrometer-Experiment demonstrieren, dass die Bindung von E2F4 an die Helikase RecQL in Trim33KO Zellen verglichen mit Kontrollzellen verstärkt ist, was durch proximity ligation assays (PLAs) validiert werden konnte. RecQL ist dafür bekannt, Replikationsgabeln zu stabilisieren und in die DNA Schadensreparatur involviert zu sein. Demnach könnte RecQL die Handhabung von RS für Zellen massiv vereinfachen. Ich konnte zeigen, dass sowohl RecQL als auch E2F4 in Trim33KO Zellen stärker an Chromatin binden, was darauf hindeutet, dass E2F4 RecQL an DNA rekrutieren könnte. Darüber hinaus imitiert die Überexpression von RecQL in Kontrollzellen die erhöhte Replikation, welche in Trim33KO Zellen beobachtet werden konnte. Die Überexpression einer inaktiven RecQL Mutante (K119A) in Trim33KO Zellen hingegen reduzierte das Fortschreiten der

Replikationsgabeln signifikant. Zwei E2F4 Mutanten, eine, die nicht an DNA binden kann (E2F4-DB) und eine, der ein Teil ihres C-Terminus fehlt (E2F4-ΔC), können RecQL nicht an Chromatin rekrutieren und heben den RS Phänotyp in Trim33KO Zellen auf. Zusammenfassend schlagen unsere Daten ein Modell vor, indem E2F4 RecQL an Chromatin rekrutiert, welches im Gegenzug Zellen weniger sensibel gegen RS macht.

1 Introduction

1.1 Hepatocellular carcinoma (HCC)

HCC represents 80 % of all primary liver cancers worldwide and is considered as the fourth leading cause of cancer related death (Villanueva 2019, El-Serag et al., 2007). The majority of HCC patients are diagnosed only at advanced stages and the numbers and severity of HCC cases continue to increase. For example, the incidence rates increased in the last 30 years two- to threefold in the USA (Yang et al., 2019; Altekruse *et al.*, 2009). There are several known risk factors for the development of HCC, whereas there are only very limited treatment options, especially for advanced stages.

1.1.1 Factors elevating the risk of HCC development

The infection with hepatitis B/C (HBV/HCV) is categorized as one of the most important causes of HCC as it is detected in 80 % of cases (Levrero *et al*., 2016; El-Serag., 2012; Yuen *et al.*, Yang *et al*., 2010). Moreover, the most common liver disease NALFD (Nonalcoholic fatty liver disease) is a strong risk factor for the development of HCC, as 10-20 % of cases show NALFD burden in the USA (Yang and Mohammed *et al*., 2017; Younossi, Blissett *et al*., 2016; Younossi, Koenig *et al*., 2016; Younassi *et al*., 2015). Furthermore, alcohol abuse can lead to alcoholic liver disease (ALD), which increases the hepatocarcinogenic potential threefold (Park *et al*., 2017; West *et al*., 2017). Finally, exposure to different toxins such as aflatoxin or aristolochic acid can lead to the development of HCC (Yang *et al*., 2019). Aflatoxin is a mycotoxin, which can be found in staple cereals as well as oilseeds. In regions with high rates of HCC, aflatoxin contaminations can often be observed (Gouas *et al*., 2019; Wild *et al*., 2015). Aristolochic acid can be found in worldwide growing plants as Aristolichia and Asarum, which are traditionally being used in Chinese medicine (Arlt *et al*., 2002). Consistent with the high mutagenic potential of aristolochic acid, many HCC patients from Asia have mutations typical for aristolochic acid exposure (Ng *et al*., 2017; Rosenquist *et al*., 2016).

1.1.2 Treatment options to counteract HCC tumor progression

The most recommended option to treat HCC is the resection of the tumor tissue, as this surgical option is potentially curative. However, this method is only possible in early diagnosed patients and after resection nearly 70 % of patients show a recurrence of the tumor (Yang *et al*., 2019; Roayaie *et al*., 2015; Tabrizian *et al*., 2015). Nevertheless, the most promising therapy option is the transplantation of a healthy liver, which is not used frequently because of the limited availability of donation organs (Yang *et al*., 2019; Yang, Larson *et al*., 2017; Mazzaferro *et al*., 1996). This method does not only remove the tumor tissue, but additionally the challenged liver tissue with a higher potential to develop tumors, which is why HCC is the leading reason for liver transplantations in the USA (Yang, Larson *et al*., 2017). A percutaneous

method to fight HCC tumors would be the local radio-frequency ablation or microwave ablation, which both are potentially curative strategies. These therapies can only be used in early diagnosed cases and induce tumor necrosis, which makes them not the most used strategies (Yang *et al*., 2019; Shiina *et* al., 2018; Yu *et al*., 2017; Cucchetti *et al*., 2013). Moreover, the transarterial chemoembolization (TACE) can be utilized for treating patients at intermediate HCC stage. Here, cytotoxic chemotherapeutics as doxorubicin or cisplatin are being delivered in the tumor feeding artery by embolization particles to induce necrosis and hence slowing down the tumor growth (Lencioni and de Baere *et al*., 2016; Lo *et al*., 2002; Llovet *et al*., 2002). Finally, HCC can be treated with pharmacological drugs, which may reduce the proliferation of the tumor. The most commonly used drug is sorafenib, followed by its derivatives lenvatinib, regorafenib and cabozantinib (Villanueva 2019; Yang *et al*., 2019). They all can moderately prolong the patient survival alone or in combination with others, but none is considered as a curative therapy option (Abou- Alfa *et al*., 2018; Kudo *et al*., 2018; Bruix *et al*., 2017; Lencioni and Llovet *et al*., 2016; Cheng *et al*., 2009; Llovet *et al*., 2008).

However, in reality only very few curative options are available these days. Liver cancer has only a 5-year survival of 18 %, which makes it very important to find new putative curative therapy options (Jemal *et al.*, 2017).

An often-deregulated pathway in liver cancer is the DNA damage response (DDR) (Gillman *et al*., 2021; Lin *et al*., 2019; Yang *et al*., 2014). DDR should arrest the cell cycle allowing cells to repair the DNA damage before resuming to the cell cycle or inducing apoptosis (Awasthi *et al*., 2015). In liver cancer, this mechanism is often deregulated and can induce genomic instability or uncontrolled tumor growth (Gillman *et al*.,2021). One of the most often deregulated TFs in HCC is the onco-protein Myc, which is known to promote DNA damage, to interfere with DNA replication and to trigger genomic instability (Zheng *et al*., 2017; Qu *et al*., 2014; Dang *et al*., 2012). Additionally, the risk of liver cancer caused by hepatitis virus, ALD or NAFLD increases significantly when Myc is overexpressed (Wang *et al*., 2019; Zheng *et al*., 2017; Nevzorova *et al*., 2016; Higgs *et al*., 2013; Balsano *et al*., 1991). In summary, targeting Myc in HCC could be a promising strategy to develop new putative curative therapy options.

1.2 The Myc oncoprotein

The MYC gene is one of the most analyzed genetic alteration in cancer biology worldwide as it is known to be genomically amplified in 28 % of tumors and transcriptionally overexpressed in about 50 % of tumors (Schaub *et al.*, 2018; Zheng *et al*., 2017). This oncogene was first described to be altered in human cancer 1982 (Dalla-Favera *et al*., 1982; Taub *et al*.; 1982). In the decades of analysis, Myc was found to be involved in the regulation of 15 % of the human genome and has an impact on multiple cellular processes such as the cell cycle progression, proliferation, apoptosis, differentiation, genome stability and metabolism (Chen *et*

al., 2018; Gabay *et al*., 2014; Dang *et al*., 2012; Miller *et al*., 2012; Hoffmann *et al*., 2008; Meyer *et al*., 2008; Pelengaris *et al.*, 2003; Dang, 1999).

1.2.1 The influence of Myc on HCC progression

The role of Myc in HCC was intensely studied since many working groups showed that Myc levels are upregulated in HCC cell lines as well as in tumors derived from mice or humans (Dang *et al*. 2012; Srivasrava *et al*., 2004; Wang *et al*., 2002). High levels of Myc correlate with promotion of HCC, shorter overall survival (OS) and poor prognosis (Chen *et al*., 2020; Dhanasekaran *et al*., 2020; Huang *et al*., 2020; Liu *et al*., 2020; Min *et al*., 2020; Shi *et al*., 2020; Wei *et al*., 2020; Wu *et al*., 2020; Nevzorova *et* al., 2013; Lin *et al*., 2010). Furthermore, it was shown that the expression of Myc is sufficient to induce HCC (Zheng and Cubero *et al*., 2017; Wahlström *et al*., 2015; Muakkassah-Kelly *et al*., 1988) as for example 80 % of mice overexpressing Myc developed HCC (Freimuth *et al*., 2010). Corresponding to these findings, the reduction of Myc protein inhibits cell cycle progression as well as growth of HCC and can in addition completely arrest invasive hepatic cancers (Qu *et al*., 2014; Shachaf *et al*., 2004; Simile *et al*., 2004).

1.2.2 Apoptosis induction by the overexpression of Myc

Paradoxically, Myc is known to induce proliferation of tumor cells, as well as it is known to induce RS, double strand breaks (DSBs) and hence apoptosis when overexpressed (Curti *et al*., 2021; King et al., 2020; Zheng et al., 2017; Zimonjic et al., 2012; Bouchard et al., 2007; Wu et al., 2007; Dang et al., 2006; Finch et al., 2006; Pelengaris et al., 2003). The ability of Myc to stimulate replication genome-wide can cause RS, which in turn leads to DSBs. The increased number of DNA damage then activates the Arf/p53 pathway, which initiates the controlled cell death, also known as apoptosis (Chen et al., 2018; Zheng et al., 2017; Gabay et al., 2014). Accordingly, Myc overexpression can sensitize cells to drugs increasing DNA damage, which was already shown for Parp1 or Chk1/2 inhibitors (Carracciolo *et al*., 2021; King *et al*., 2020; Ning *et al*., 2019; Ferraro *et al*., 2011). Similarly, increasing levels of RS can be more lethal in Myc overexpressing cells (Curti *et al*., 2021; King *et al*., 2020).

One big family which is important in stabilizing replication forks and hence minimizing RS when overexpressed is the RecQ family of helicases, which are known as the caretakers of the genome (Chu *et al*., 2003). The most abundant member in humans is RecQL, also known as RecQ1 or RecQL1 (Debnath *et al*., 2020, Chu *et al*., 2009). RecQL binds to DNA intermediates during replication and repair, unwinds the DNA duplex and executes different functions (Bachrati *et al*., 2008; Sharma *et al*., 2005; Cui *et al*., 2003). These are the initiation of DNA replication, the stabilization of fragile DNA sites as well as the help in damage repair (Qiu *et al.,* 2021; Viziteu *et al*., 2017; Bertie *et al*., 2013; Lu *et al*., 2013; Parvathaneni *et al*., 2013;

Popuri *et al*., 2012; Thangavel *et al*., 2010). KD of such RS-reducing proteins as RecQL could enhance the function of Myc to induce apoptosis.

1.2.3 Targeting Myc as a therapeutic strategy

Regulating Myc levels play an essential role in manipulating the growth of tumors and hence Myc represents an obvious target for cancer therapies. Unfortunately, developing a small molecule inhibitor against Myc raised structural and functional problems as it is known to be a disordered protein with a mainly unstructured surface (Madden *et al*., 2019). Small molecule inhibitors typically target specific sites such as enzymatic pockets or defined binding pockets. Myc does not have this kind of pockets and is additionally not easily accessible due to its strong nuclear localization (Madden *et* al., 2019). Hence, indirectly targeting Myc function is of immense scientific interest. Different strategies to achieve this goal have emerged over the last decades, focusing on manipulation of either the expression of Myc, its post-translational modifications or its binding to partner proteins (Allen-Petersen *et al*., 2019).

For example, the well-known interaction of Myc and Max was shown to be essential for efficient Myc function (Chen *et al*., 2018). Additionally, other proteins were described to be important for Myc function. For example, the TF E2F4 was shown to share many binding sites with Myc (Bhawe *et al*., 2018) and to be essential for the development of Myc-induced lymphomagenesis (Rempel *et al*., 2009). Moreover, Myc overexpression correlates with E2F4 overexpression in cancer (Dai *et al*., 2019), making it a promising target to indirectly influence Myc function.

E2F4 belongs to the E2F family of TFs, which is involved in the control of cell cycle, DNA repair and apoptosis (Attwooll *et al*., 2014; Bertoli *et al*., 2013; Van Den Heuvel *et al*., 2008; Tsantoulis *et al*., 2005). The members of this family are known to be highly dependent on numerous interaction partners such as the RB protein family (pRb, p107, p130). E2F proteins are generally divided into three groups, the activators (E2F1-3), the canonical repressors (E2F4-6) and the atypical repressors (E2F7-8) (Kent *et al*., 2019; Hsu *et al*., 2016; Chen *et al*., 2009; Tsantoulis *et al.,* 2005; Trimarchi *et al*., 2002). The atypical repressors were discovered the lates and are the less investigated group, whereas activator E2Fs are the best characterized members of the family. However, E2F4 belongs to the canonical repressors and executes its canonical function during the G0/1 phase of the cell cycle. During late G1 and S phase E2F4 is exported out of the nucleus by its nuclear export signal (NES) (Kent *et al.,* 2019; Hsu *et al*., 2016; Gaubatz *et al*., 2001; Verona *et al*., 1997). During G0/1 phase, E2F4 is bound to the hypophosphorylated RB proteins and translocated to the nucleus where it represses transcription by assembling with the DREAM complex (Xanthoulis *et al*., 2013; Tsantoulis *et al*., 2005; Attwooll *et al*., 2004, 1998; Nevins 1998). The DREAM complex consists of numerous proteins, which all work together to repress transcription during the G0/1 phase of the cell cycle (Engeland 2017; Sadasivam *et al*., 2013). The canonical function of E2F4 to

repress genes during G0/1 phase could be observed by numerous working groups (Allmann *et al*., 2020; Roelofs *et al*., 2020; Huang *et al*., 2019; Schade *et al*., 2019; Wiśnik *et al*., 2017). However, apart from this canonical function, there are several new functions of E2F4 described. For example, E2F4 was observed to activate the transcription of target genes, such as genes involved in the development of cilia in multiciliated cells, in the endocytosis as well as in the water channel transport in the testis (Stracker *et al*., 2019; Kim *et al*., 2018; Danielian *et al*., 2016; Hsu *et al*., 2016; Ma *et al*., 2016; Lee *et al*., 2011). Furthermore, E2F4 can promote the proliferation of numerous cell types, like in cardiomyocyte, intestinal, colon cancer, bovine mammary epithelial, mouse embryonic stem, fetal erythroid, colorectal cancer, pancreatic, or acute myeloid leukemia cells (Feng *et al*., 2019; Hong *et al*., 2019; Hsu *et al*., 2019; Zhen *et al*., 2019; Amerongen *et al*., 2010; Gerneau *et al*. 2009; Kinross *et al*., 2006; Deschênes *et al*., 2004).

Apart from manipulating the interaction of Myc with important binding partners, Myc function can be indirectly affected by post-translational modifications such as ubiquitination. The highly conserved ubiquitin protein contains 76 amino acids and can be attached to specific targets typically marking them for proteasome-dependent degradation. To transfer ubiquitin to a protein, an enzymatic cascade is needed. The ubiquitin-activating E1 enzyme activates ubiquitin and transfers it to the ubiquitin-conjugating E2 enzyme. The E3 ubiquitin ligase is interacting at the same time with the E2 enzyme and the substrate to mediate the final ubiquitin transfer to the substrate (Zheng *et al*., 2017; Scheffner *et al*., 1995). The bond between the C-terminal glycine of ubiquitin and a free lysine of the target is thereby covalent (Kliza *et al*., 2020; Pickart, 2001). Ubiquitination is a reversible process as the ubiquitin can be removed by deubiquitinases (DUBs) (Mevissen *et al*., 2017). This large group of proteases cleaves ubiquitin proteins off substrates and thereby stabilizes them (Komander *et al*., 2009; Reyes-Turcu *et al*., 2009). Ubiquitin ligases as well as DUBs are relatively easy druggable proteins because of their distinct enzymatic pockets. Hence, many different small molecule inhibitors were already designed to indirectly manipulate the stability of a specific target protein (Deng *et al*., 2020; Harrigan *et al*., 2018; Bielskiené *et al*., 2015; Farshi *et al*., 2015). Collectively, indirectly manipulating Myc through upstream ubiquitin ligases or DUBs is a promising strategy to treat cancer. In line with this, our working group recently performed a whole genome screen for proteins, which can regulate Myc function, namely Myc-induced apoptosis (Popov *et al*., 2007). One of the best hits was the ubiquitin E3 ligase Trim33.

1.3 Trim33 – a member of the Tripartite motif-containing protein superfamily

Trim33, also known as TIF1γ, RFG7, PTC7 or Ectodermin, belongs to the Tripartite motif-containing (TRIM) protein superfamily, whose members are involved in multiple cellular processes (Yu *et al*., 2019). The TRIM protein superfamily consists out of over 80 members,

whose alterations can lead to developmental disorders, degenerative diseases and tumorigenesis (Hatakeyama 2011; Ozato *et al*., 2008; Short *et al*., 2006; Meroni *et al*., 2005; Stremlau *et al*., 2004; Rhodes *et al*., 2002; Short *et al*., 2002). All TRIM proteins show similar N-terminal and very diverse C-terminal domains (Reymond *et al*., 2001). The conserved N-terminal domain consist of the RING domain, which mediates the E3 ligase activity (Stevens *et al*., 2009), and one or two B-boxes as well as a coiled coil domain, which both facilitate protein-protein interactions (McAvera *et al*., 2020). The diverse C-terminal domains divide the TRIM proteins into 11 defined subgroups (Short *et al*., 2011). Trim33 forms together with Trim24, Trim28 and Trim66 the transcriptional intermediary factor 1 (Tif1) protein family, as they all possess a Plant Homeo Domain (PHD) and a bromodomain at their C-terminus (McAvera *et al*., 2020). PHD domains and bromodomains mediate a direct interaction with modified histone H3. The PHD domain normally interacts with methylated lysines, whereas the bromodomain generally interacts with acetylated lysines (Sanchez *et al*., 2011; Sanchez *et al*., 2009). The Tif1 proteins are all known to be deregulated or mutated in numerous cancer types; however, their role in cancer still needs to be fully understood (McAvera *et al*., 2020). The knowledge of Trim33 is especially interesting, as there are on one hand publications describing Trim33 as a tumor suppressor; and on the other hand, studies which claim that Trim33 has a tumor-promoting activity.

1.3.1 TRIM33 – a stringently regulated gene

The murine TRIM33 gene is 77kb long, localized on chromosome 3F2 and contains 20 exons. The 1142 amino acid long murine protein shows a 96 % identity to the 1120 amino acid long human protein (Yan *et al*., 2004), whose gene is 118 kb long, localized on chromosome 1 and consists out of 21 exons (Venturini *et al*., 1999).

TRIM33 is a tightly regulated gene, which was previously shown by several working groups. For example, SOX2 was shown to transcriptionally repress Trim33 by directly binding to its promoter. Furthermore, it was shown that Trim33 is highly regulated by post-transcriptional mechanisms, such as the binding of different miRNAs and circRNAs (Wang *et al*., 2018; Jingushi *et al*., 2015) or the sumoylation by for example Ad5 E4-ORF3 or Ubc9 (Sohn *et al*., 2016; Fattet *et al.,* 2013; Forrester *et al*., 2012) or the phosphorylation of Tyr-524, -620 and -1048 by the tyrosine kinase c-Abl (Yuki *et al*., 2019). Additionally, its ubiquitin transferring function as well as its binding to protein partners can be opposed by FAM/Usp9, FOXMI or αB-crystallin (Ballaye *et al*., 2014; Xue *et al*., 2014; Dupont *et al.*, 2009). These various ways of regulating Trim33 function demonstrates the importance of balanced Trim33 levels in a cell.

1.3.2 Trim33 – a multi-function protein

Trim33 has numerous cellular functions, such as the regulation of different pathways including TGFβ and Wnt signaling, transcriptional elongation, cell cycle and mitosis, DNA damage, development and differentiation of cells and affects different diseases including cancer (McAvera *et al*., 2020).

1.3.2.1 Trim33 regulates the TGFβ pathway

TGFβ signaling promotes phosphorylation of SMAD proteins, which leads to their translocation to the nucleus and transcriptionally activates TGFβ target genes (Derynck *et al*., 2019; Ikushima *et al*., 2010; Massagué *et al*., 2000). The downstream targets of the TFGβ/SMAD pathway are very broad, explaining its involvement in numerous cellular functions such as the proliferation, apoptosis, differentiation and invasive potential of cells (Derynck *et al*., 2019; Gratchev *et al*., 2017; Massagué, 2012; Wu *et al*., 2009). Additionally, in many cancer types SMAD deletions or mutations could be detected and it is described that TGFβ acts as a tumor suppressor by inhibiting tumor growth and metastasis (Seoane *et al*., 2017; Samanta *et* al., 2012).

Trim33 was shown to have activating as well as repressive effects on the TGFβ/SMAD signaling. On one hand, it has a direct impact on the pathway by ubiquitinating and hence inhibiting SMAD4 (Agricola *et al*., 2011; Dupont *et al*., 2009; Dupont *et al*., 2005). The binding of Trim33 to modified histone H3 by its PHD (H3K9me3) and bromodomain (H3K18ac) is thereby essential for this ubiquitination (Agricola *et al*., 2011; Xi *et al*., 2011; Dupont *et al*., 2009; Dupont *et al*., 2005). This repressive regulation of the TGFβ/SMAD pathway can be opposed by several proteins, such as FAM, FOXM1 and αB-crystallin (Bellaye *et al*., 2014; Xue *et al*., 2014; Dupont *et al*., 2009). On the other hand, Trim33 was shown to interact with SMAD2/3 on chromatin and makes specific Smad2/3 motifs accessible for SMAD4, which results in an enhanced regulation of the TGFβ/SMAD pathway (Xi *et al*., 2011; He *et al*., 2006). These opposing functions of Trim33 remain elusive but were tried to be explained in different ways. It was for example suggested that Trim33 only acts as a repressor of TGFβ/SMAD signaling in cells with high TGFβ threshold (Andrieux *et al*., 2012), or that the function of Trim33 is dependent on the cellular context (Yan *et al*., 2004).

1.3.2.2 The influence of Trim33 on the Wnt/β-catenin signaling

Wnt signaling stabilizes β-catenin by blocking its phosphorylation. Hence, β-catenin can be translocated to the nucleus and activates the expression of Wnt target genes (Harb *et al*., 2019; He *et al*., 2019; Clevers *et al*., 2012). The Wnt/β-catenin pathway was previously described to be involved in numerous cellular processes such as cell proliferation, adhesion, migration, and differentiation (Wang *et al*., 2018; Anastas *et al*., 2013; Kypta *et al*., 2012; Hu *et al*., 2010).

Furthermore, the dysregulation of this pathway leads to tumorigenesis and influences the tumor growth as well as the metastatic potential of tumors (Yao *et al*., 2011; Akiri *et al*., 2009; Holcombe *et al*., 2002; Woo *et al*., 2001).
Trim33 can directly influence this pathway by ubiquitinating β-catenin, leading to its proteasome-dependent degradation in the nucleus (Xia *et al*., 2017; Xue *et al*., 2015). In glioblastoma for example, Trim33-dependent degradation of nuclear β-catenin leads to inhibited cell proliferation and delayed tumorigenesis (Xue *et* al., 2015).

1.3.2.3 Trim33 recruits transcriptional elongation factors

The recruitment of positive elongation factors to erythroid genes is partially Trim33-dependent and leads to an increased transcriptional activity by counteracting RNA polymerase II (Pol II) pausing. Consistent with this, the depletion of Trim33 resulted in defects in transcriptional elongation, and additionally led to defects in erythroids as well as in several other blood compartments (Yu *et al*., 2019; Bai *et al*., 2013; Bai *et al*., 2010).

1.3.2.4 The role of Trim33 during cell cycle and mitosis

It could be shown that Trim33 binds the APC/C holoenzyme (Sedgwick *et al*.; 2013). Trim33 is not a substrate of this ubiquitin ligase, but instead directly regulates its activity. Loss of Trim33 strongly reduces the APC/C ligase activity, leading to the stabilization of APC/C substrates. Those substrates in turn slow down the progression through mitosis from nuclear envelope breakdown to anaphase (McAvera *et al*., 2020). Additionally, cells with a KD of Trim33 failed more often to undergo metaphase-to-anaphase transitions (Sedgwick *et al*., 2013).

1.3.2.5 Efficient DNA damage response is partially dependent on Trim33

Trim33 is required for efficient DNA repair by PARP1 (Yu *et al*., 2019; Hatakeyama *et al*., 2011). It was shown that Trim33 binds to DNA damage sites and that this is dependent on its PHD and bromodomain (Kulkarni *et al*., 2013).

1.3.2.6 Trim33 is necessary for efficient embryonic development

Trim33 was shown to be an indispensable player in embryonic development (Dupont *et al*., 2005; Falk *et al*., 2014). Not only is Trim33 necessary for the early maturation of embryonic bodies (EBs) (Rajderka *et al*., 2017), it also regulates a subset of mesoendodermal genes by binding to H3K18ac marks (Luo *et al*., 2019) and is essential for proper development of precardiogenic mesoderm during late gastrulation (Rajderka *et al*., 2019). Additionally, it was shown that the embryonic depletion of Trim33 leads to death during early somatogenesis (Kim *et al*., 2008), whereas 4-month-old mice with a Trim33 deletion showed an accelerated aging

phenotype (Quéré *et al*., 2014). Finally, Trim33 plays an important role for the specification of the ectoderm (Dupont *et al*., 2005).

1.3.2.7 The differentiation of cells is modulated by Trim33

Trim33 is essential for the differentiation of numerous cell types. For example, it was shown that its depletion leads to severe problems in hematopoiesis in humans as well as in mice (Chrétien *et al*., 2016; Bai *et al*., 2013; He *et al*., 2006; Ransom *et al*., 2004). Furthermore, Trim33-deficient mouse embryonic stem cells (ESCs) remained pluripotent in non-differentiating medium and showed increased apoptosis when the differentiation to EBs was induced (Rajderka *et al*., 2017). Additionally, Trim33 is essential at the end of pregnancy for proper differentiation of alveolar epithelial cells (Hesling *et al*., 2013). Finally, Trim33 is a positive regulator of osteoblast differentiation (Guo *et al*., 2017).

1.3.2.8 Trim33 possesses an antiviral activity

Trim33 was reported to have antiviral activity, by limiting the virus production, as, for example, for the adenovirus or the HIV-1 (Ali *et al*., 2019; Sohn *et al*., 2016; Forrester *et al*., 2011). Consistently, viruses have developed mechanisms to reduce Trim33 protein levels in cells, as for example Ad5 E4-ORF3 can sumyolate Trim33 and subsequently lead to its proteasome-dependent degradation (Sohn *et al*., 2016; Forrester *et al*., 2012).

1.3.2.9 Dermatomyositis (DM) is correlated with anti-Trim33 autoantibodies

Myositis is a disease, which often comes along with cancer and can stay after the cancer got appropriately treated (De Vooght *et al*., 2020; Zahr *et al*., 2011). 60-70 % of myositis patients show myositis specific autoantibodies, such as anti-Trim33 (McHugh *et al*., 2018; Ghirardello *et al*., 2013). Patients with anti-Trim33 autoantibodies show higher risk of cancer and additionally 84 % of anti-Trim33 positive cancer patients develop cancer associated DM (De Vooght *et al*., 2020; Yang, Peng *et al*., 2017; Allenbach *et al*., 2016). Accordingly, anti-Trim33 autoantibodies could function as a marker for the prediction of cancer associated DM (De Vooght *et al*., 2020).

1.3.3 The role of Trim33 in cancer

1.3.3.1 Putative role of Trim33 as a tumor suppressor

Classically, Trim33 is being described as a tumor suppressor. It was for example shown to inhibit metastasis and tumor growth in non-small-cell lung cancer (NSCLC), breast cancer, glioma, clear cell renal cell carcinoma (ccRCC), pancreatic dual adenocarcinoma (PDAC), chronic myelomonocytic leukemia (CMML) and prostate cancer (Xu *et al*., 2020; Qi *et al*., 2019; Chrétien *et al*., 2016; Wang *et al*., 2016; Jingushi *et al*., 2015; Xue *et al*., 2015; Xue *et al*.,

2014; Vincent *et al*., 2012). Additionally, low Trim33 levels are associated with lower OS, poorer prognosis, more aggressive tumors and more advanced pathological stage and grade (Xu *et al*., 2020; Cai *et al*., 2019; Wang *et al*., 2018; Jingushi *et al*., 2015; Pommier *et al*., 2015).

1.3.3.2 Function of Trim33 as an oncoprotein

In contrast to the tumor suppressing functions TRIM33 was shown to also possess oncogenic potential, which has gained increasing scientific interest in recent years (McAvera et al., 2020; Cai *et* al., 2019; Yu et al., 2019). For example, in B lymphoblastic leukemia Trim33 prevents apoptosis of the cancerogenic cells and hence allows them to grow faster (Wang et al., 2015). Additionally, the overexpression of Trim33 leads to a growth benefit of pancreatic cell lines (Ligr *et al*.; 2014) and it is overexpressed in early stage breast cancer (Kassem *et al*.; 2015). Finally, the overexpression of Trim33 was associated with colorectal carcinogenesis and advanced staging (Jain et al., 2011).

1.3.3.3 Contrary function of Trim33 in HCC

Trim33 is known to play opposing roles in HCC. On one hand, Trim33 was described to be reduced in HCC tumors and that its loss promotes HCC, decreases OS and increases the chance of recurrence (Yu *et al*., 2019; Herquel *et al*., 2011). This is in accordance with a study showing that Trim33 acts as a tumor suppressor in advanced stage HCC (Ding *et al*.; 2014). However, on the other hand it was shown that Trim33 can promote HCC development in early stage HCC (McAvera *et al*., 2020; Ding *et al*., 2014).

1.4 Aims of the study

MYC is overexpressed in a variety of tumors, associated with poor prognosis and thereby resembling a promising therapeutic target. However, to date Myc itself is considered to be undruggable. To investigate novel ways of indirectly targeting Myc function is hence an indispensable strategy for designing novel therapeutic options against cancer. Previous data of our working group demonstrated that the E3 ubiquitin ligase Trim33 can regulate Myc-induced apoptosis. The main aim of this study was to understand how Trim33 can influence Myc function, as this remains still unknown.

The first aim was to investigate if Myc is a target of Trim33. As I could disprove this hypothesis, the second aim was to understand how Trim33 can influence Myc function, namely Myc-induces apoptosis. I revealed that Trim33 is not regulating Myc function itself, but rather more generally the response of cells to RS-induction. After I identified E2F4 as a novel Trim33 substrate, which mediates the RS phenotype, the last aim was to analyze how exactly E2F4 can influence the response of cells to RS. I could show that E2F4 most likely recruits RecQL to chromatin and thereby stabilizes replication forks and induces DNA damage repair.

The knowledge gained during this thesis could be the first step to generate novel cancer therapies.

2 Materials and methods

2.1 Materials

2.1.1 Chemicals

Table 1: Utilized Chemicals

Chemical	Company	Cat. Number
2-Propanol	SIGMA	33539
5-Chloro-2'-deoxyuridine	Cayman	18155
5-Ethynyl-2'-deoxyuridine	Cayman	61135-33-9
Acetic acid, glacial	SIGMA	ARK 2183
Agarose Standard	CarlRoth	3810.3
Albumin Fraktion V, NZ Origin	CarlRoth	8076.4
Ampicillin sodium salt	SIGMA	A9518
BIS-TRIS	SIGMA	B9754
Bromphenol blue	SIGMA	B0126
Crystal violet solution	SIGMA	V5265
DAB Substrate Kit	Zytomed Systems	DAB530
DNA Gel Loading Dye (6X)	ThermoFisherScientific	R0611
dNTP-Set 1, 4 x 25 µmol (250 µl), 100 mM	CarlRoth	K039.1
Dulbecco's Modified Eagle's Medium - high glucose	SIGMA	D6429
Duolink™ *In Situ* Mounting Medium with DAPI	SIGMA	DUO82040
Ethanol	CarlRoth	K928.4
Ethidiumbromidlösung 1 %, 10 ml, Glas	CarlRoth	2218.1
Ethylenediaminetetraacetic acid	SIGMA	ED
Fetal Bovine Serum, Research Grade	SIGMA	F0804
Fluoromount™ Aqueous Mounting Medium	SIGMA	F4680
GeneRuler™ 1 kb DNA-Leiter	ThermoFisherScientific	SM0312
Glycine	SIGMA	G7126
GlycoBlue Co-Precipitant	ThermoFisherScientific	AM9516
Hexadimethrine bromide	SIGMA	107689
Hygromycin B Gold	InvivoGen	ant-hg-1
Idoxuridine	Cayman	20222
Imidazole	SIGMA	I0250
Immobilon Western HRP Substrat	Merck Millipore	WBKLS0500
MEM Non-essential Amino Acid Solution (100×)	SIGMA	M7145
Methanol	CarlRoth	8388.6
MG-132	Selleckchem	S2619

MOPS	SIGMA	M1254
N,*N*,*N*′,*N*′-Tetramethylethylenediamine	SIGMA	T9281
Natriumchlorid	CarlRoth	3957.2
Non-fat milk	Hartenstein (ROTH)	CM35 (T145.2)
Opti-MEM™	ThermoFisherScientific	31985062
PageRuler™ Prestained Protein Ladder	ThermoFisherScientific	26617
Paraformaldehyde	SIGMA	P6148
PBS, pH 7.4	ThermoFisherScientific	10010-056
Penicillin-Streptomycin	SIGMA	P4333
Pierce™ Protein A Agarose	ThermoFisherScientific	20333
Polyethylenimin -Lösung	SIGMA	P3143
Potassium chloride	SIGMA	P9333
Potassium phosphate monobasic	SIGMA	P5655
Propidium Iodide Solution	BioLegend	421301
Protein A Magnetic Beads	New England BioLabs	S1425S
Protein G / Agarose	InvivoGen	gel-agg-5
Protein G Magnetic Beads	New England BioLabs	S1430S
PureCube Ni-NTA Agarose	Cube Biotech	31105
Puromycin	InvivoGen	ant-pr-1
Quant-iT™ PicoGreen™ dsDNA-Reagent	ThermoFisherScientific	P7581
ROTI®Phenol/Chloroform/Isoamylalkohol, 250 ml	CarlRoth	A156.1
ROTIPHORESE®Gel 30 (37,5:1)	CarlRoth	3029.1
Salzsäure 5 mol/l (5 N), Titrisol®, Supelco®	VWR Chemicals	1099110001
SDS pellets	CarlRoth	CN30.3
SDS ultra pure	CarlRoth	2326.5
Sodium bisulfite	SIGMA	243973
Sodium phosphate dibasic dihydrate	SIGMA	30435
Streptavidin Magnetic Beads	New England BioLabs	S1420S
tri-Sodium citrate dihydrate	CarlRoth	HN12.2
TritonX100	Amresco	M143
Trizma® base	SIGMA	T1503
Tween 20	SIGMA	P1379
Urea	CarlRoth	7638.1

2.1.2 Plastics

Table 2: Utilized plastics

Plastic	Company	Cat. Number
Amersham™ Hybond® P**,** PVDF membrane	SIGMA	GE10600023
Blottingpapier 0,76 mm, 330 g / m²	Hartenstein	GB33
Deckglas 24x50mm Gr.1; 01-2450/1	Zentrallager	3000302
Deckgläser, rund, duchmesser 10 mm	Hartenstein	DKR0
Nunclon Petrischalen 15cm	ThermoFisherScientific	168381
Nunc™ Zellkultur-Multischalen 12 well	ThermoFisherScientific	150628
Nunc™ Zellkultur-Multischalen 24 well	ThermoFisherScientific	142475
Nunc™ Zellkultur-Multischalen 6 well	ThermoFisherScientific	140675
Pipette grad.m.steril. 10ml	Zentrallager	61341337
Pipette grad.m.steril. 5ml	Zentrallager	3000223
Reaktionsgefäße (Eppi) 1,5ml	Zentrallager	3002923
Reaktionsgefäße (Eppi) 2ml	Zentrallager	3002699
RÖHR. PP 17x120 STERIL SV. 15ml	Zentrallager	3002852
RÖHR. PP 30x115 STERIL SV. 50ml	Zentrallager	3002502
Sarstedt Reagenz- und Zentrifugenröhre, 13 ml	Sarstedt	62.515.006
Sterilfilter millex 0,45 µm SLHA033SS	Zentrallager	61303475
TC-Schale 100	Sarstedt	83.3902
TC-Schale 60	Sarstedt	83.3901
Zellschaber	Sarstedt	83.1832

2.1.3 Enzymes

Thermo enzymes and according buffers (AgeI/EcoRI/XhoI/BamHI/AscI) were utilized.

Table 3: Utilized enzymes

Enzyme	Company	Cat. Number
Blunt/TA Ligase Master Mix	New England BioLabs	M0367L
Exonuclease I (E. coli)	New England BioLabs	M0293S
FastAP	ThermoFisherScientific	EF0651
KAPA HiFi HotStart ReadyMix	Roche	SKU: 7958927001
KAPA2G Robust HotStart ReadyMix	SIGMA	KK5701
Micrococcal Nuclease	New England BioLabs	M0247S
NEBuilder® HiFi DNA Assembly Cloning Kit	New England BioLabs	E5520s
Phosphatase Inhibitor Cocktail 3	SIGMA	P0044
Phusion® High-Fidelity DNA Polymerase	New England BioLabs	M0530 S/ 100 unit

Protease Inhibitor Cocktail	SIGMA	P8340
Proteinase K (rekombinant)	ThermoFisherScientific	EO0491
RNase A, DNase- und proteasefrei	ThermoFisherScientific	EN0531
SYBR® Green JumpStart™ *Taq* ReadyMix™	SIGMA	S4438
T4 DNA-Ligase	ThermoFisherScientific	EL0011
Terminal Transferase	New England BioLabs	M0315L

2.1.4 Standard solutions

Table 4: Utilized Standard solutions

Solution	Recipe	
1 x Running MOPS Buffer	5 %	20 x MOPS
	0.1 M	NaHSO3
1 x TransferBuffer	10 %	10 x TB
	15 %	Methanol
10 x Annealing Buffer	1 M	NaCl
	100 mM	Tris-HCl, pH=7.4
10 x PBS	100 mM	$Na_2HPO_4*2H_2O$
	20 mM	KH_2PO_4
	1.37 mM	NaCl
	27 mM	KCl
10 x Transferbuffer	10 mM	Glycin
	3,67 mM	Tris Base
10 x TBS	500 mM	Tris Base
	1.5 M	NaCl
1 x TBST	10 %	10XTBS
	0.05 %	Tween20
1 x TE	1 mM	EDTA
	10 mM	Tris pH=8.0
20 x Running MOPS Buffer	1 M	MOPS
	1 M	Tris
	2 %	SDS
	20 mM	EDTA
4x Protein sample Buffer	12,5 mL	Tris-HCl pH 6.8
	20 mL	SDS (10 %)
	12,5 mL	glycerol
	0.02 %	bromophenol blue

50 x TAE Buffer	2 M	Tris Base
	1 M	acetic acid
	50 mM	EDTA
B&W ChIP Buffer	10 mM	Tris-HCl pH 8.0
	0.5 mM	EDTA
	1 M	NaCl
	0.02 %	TritonX100
ChIP wash Buffer	10 mM	Tris-HCl ph8.0
	0.02%	TritonX100
Fiber Lysis Buffer	200 mM	Tris pH=7.5
	50 mM	EDTA
	0.5 %	SDS
LB Medium	LB-Medium (Lennox), ROTH, X964.2	
LB Platten	15 g	AgarAgar
	1 L	LB-Medium
	50 mg/mL	Ampicillin
TNT	25 mM	Tris-HCl ph 8.0
	1 %	TritonX100
Urea Buffer	In PBS:	
	8 M	Urea
	10 mM	Imidazole
	1 %	TritonX100

2.1.5 Kits and systems

Table 5: Utilized Kits and systems

Kit/system	Company	Cat. Number
Duolink™ In Situ Detection Reagents Red	SIGMA	DUO92008
Duolink™ In Situ PLA® Probe Anti-Mouse PLUS	SIGMA	DUO92001
Duolink™ In Situ PLA® Probe Anti-Rabbit MINUS	SIGMA	DUO92005
Duolink™ In Situ Wash Buffers, Fluorescence	SIGMA	DUO82049
GenElute™ Gel Extraction Kit	SIGMA	NA1111
GenElute™ HP Plasmid Midiprep Kit	SIGMA	NA0200
Monarch® DNA Gel Extraction Kit	New England BioLabs	T1020S
NEBNext® Ultra™ RNA Library Prep Kit for Illumina®	New England BioLabs	E7530S
RNeasy Mini Kit	Qiagen	74104
Pierce™ BCA Protein Assay Kit	ThermoFisherScientific	23225
Mini-PROTEAN® Tetra Vertical Electrophoresis Cell, 4-gel, for 1.0 mm thick handcast gels	Bio-RAD	**1658001FC**
10x10 cm Elektroblotter für 5 Blots	Biostep	GB33-N1010

2.1.6 Bacteria strains

Table 6: Utilized bacteria strains

Bacteria strain	Company	Cat. Number
NEB® 10-beta Competent E. coli (High Efficiency)	New England BioLabs	C3019I
NEB® 5-alpha Electrocompetent E. coli	New England BioLabs	C2989K

2.1.7 Cell lines

Table 7: Utilized cell lines

Cell line	Source
LentiX	From Lea
$p19^{-/-}$ NRas	From NP
$p19^{-/-}$ NRas c-Myc	From NP
$p19^{-/-}$ NRas c-Myc pLKO_shCtrl	Generated during this thesis
$p19^{-/-}$ NRas c-Myc pLKO_shTrim33_1	Generated during this thesis
$p19^{-/-}$ NRas c-Myc pLKO_shTrim33_2	Generated during this thesis
$p19^{-/-}$ NRas CRISPR/Cas9 KO Ctrl	Generated during this thesis
$p19^{-/-}$ NRas Trim33KO	Generated during this thesis
$p19^{-/-}$ NRas pLKO_shCtrl	Generated during this thesis
$p19^{-/-}$ NRas pLKO_shTrim33_1	Generated during this thesis
$p19^{-/-}$ NRas pLKO_shTrim33_2	Generated during this thesis
PheonixEco	From Lea
U2OS W11	From NP

2.1.8 Plasmids

Table 8: Utilized plasmids

Plasmid	Resistence
His Ubi	
pLKO	Puro
pMD2G	
pPAX2	
pRRL	Hygro
px459	Puro
Retro-Helper	
VSVG	

2.1.9 Antibodies

Table 9: Utilized antibodies

Antibody	Company	Cat.Number
BrdU (Bu20a) Mouse mAb	Cell Signaling	5292 S
Cdc45 (D7G6) Rabbit mAb	Cell Signaling	11881S
Cdc6 (C42F7) Rabbit mAb	Cell Signaling	3387S
Cdk2 Antibody (D-12)	Cell Signaling	sc-6248

E2F4 Polyclonal antibody	Proteintech	10923-1-AP
Histone H3 (96C10)	Cell Signaling	3638 P
Histone H4 (L64C1)	Cell Signaling	2935 P
HA-Tag (6E2) Mouse mAb	Cell Signaling	2367S
HA-Tag (C29F4) Rabbit mAb	Cell Signaling	3724S
Anti-mouse IgG (Alexa Fluor® 488 Conjugate)	Cell Signaling	4408S
Anti-mouse IgG (Alexa Fluor® 555 Conjugate)	Cell Signaling	4409S
Anti-rabbit IgG (Alexa Fluor® 488 Conjugate)	Cell Signaling	4412S
Anti-rabbit IgG (Alexa Fluor® 555 Conjugate)	Cell Signaling	4413S
Anti-rat IgG (H+L), (Alexa Fluor® 488 Conjugate)	Cell Signaling	4416S
MCM2 (D7G11) XP® Rabbit mAb	Cell Signaling	3619
MCM3 Antikörper (E-8)	Santa Cruz	sc-390480
MCM4 (D3H6N) XP® Rabbit mAb	Cell Signaling	12973
Anti-MCM5 antibody	Abcam	ab17967
MCM6 Antikörper (H-8)	Santa Cruz	sc-393618
Mcm7 Antiboy	Bethyl	A302-585A-M
Anti-mouse IgG, HRP-linked Antibody	Cell Signaling	7076
Anti-rabbit IgG, HRP-linked Antibody	Cell Signaling	7074
c-Myc Antikörper (C-33)	Santa Cruz	sc-42
c-Myc (D3N8F) Rabbit mAb	Cell Signaling	13987S
Anti-c-Myc antibody [Y69]	Abcam	ab32072
Phospho-Histone H2A.X (Ser139) (20E3) Rabbit mAb	Cell Signaling	9718T
Anti-TRIM33 antibody produced in rabbit	SIGMA	HPA004345
Monoclonal Anti-TRIM33 antibody	SIGMA	WH0051592M1
Monoclonal Anti-Vinculin antibody produced in mouse	SIGMA	SAB4200080
Anti-BrdU antibody [BU1/75 (ICR1)]	abcam	ab6326I
Anti-E2F-4 Antibody, clone GG22-2A6	MerckMillipore	05-312

2.1.10 Oligonucleotides

Table 10: Utilized oligonucleotides

Oligonucelotide	Sequence
shmTrim33_1 Fw	CCGGTCGATACCAAACTACTATAAACTCGAGTTTATAGTAGTTTG GTATCGATTTTTG
shmTrim33_1 Rev	AATTCAAAAATCGATACCAAACTACTATAAACTCGAGTTTATAGTA GTTTGGTATCGA
shmTrim33_2 Fw	CCGGCGTGTGATAGATTGACGTGTACTCGAGTACACGTCAATCTA TCACACGTTTTTG
shmTrim33_2 Rev	AATTCAAAAACGTGTGATAGATTGACGTGTACTCGAGTACACGTC AATCTATCACACG
E2F4-FL Fw	TGAGTCGGCCGGTGGATCCAATGTACCCTTACGACGTG
E2F4-FL Rev	GGCGGATCCGTCGACACTAGTCAGAGGTTGAGAACAGG
E2F4- ΔC FW	TGAGTCGGCCGGTGGATCCAATGTACCCTTACGACGTG
E2F4- ΔC Rev	GGCGGATCCGTCGACACTAGTCACTCAAAGGAGGTAGAAGGGTT G
E2F4-DB Fw	CTAGCTGTACGCCAGAAGGCAGCAATAGCAGCAATTACCAATGTT TTGGAAG
E2F4-DB Rev	CTTCCAAAACATTGGTAATTGCTGCTATTGCTGCCTTCTGGCGTA CAGCTAG
E2F4-KR Fw	TGAGTCGGCCGGTGGATCCAATGTACCCATACGATGTTCCAGAT TACGCTGCAGAGGCAGGACCGCAAGCT
E2F4-KR Rev	GGCGGATCCGTCGACACTAGTCAAAGGTTGAGGACGGG
RecQL-WT Fw	TGAGTCGGCCGGTGGATCCAATGTACCCTTACGACGTGCCCGAC TACGCCGGGGCGTCCGTTTCAGCTCTAAC
RecQL-WT Rev	GAGGGGCGGATCCGTCGACATCAGGCATCATCGATTTTTCTTTTC
RecQL-K119A Fw	CTACAGGAGGTGGAGCGAGCTTATGTTACCAG
RecQL-K119A Rev	CTGGTAACATAAGCTCGCTCCACCTCCTGTAG
pLKO Seq	GAACGGACGTGAAGAATGTG
pRRL Seq	CTTCTGCTTCCCGAGCTCTA

2.2 Methods

2.2.1 Cell biological techniques

2.2.1.1 Cell cultivation

All used cell lines were cultured in DMEM with additional 10 % FBS, 1 % NEAA and 1 % PenStrep. Cells were counted with the COUNTESSII from Biorad before plating for experiments.

2.2.1.2 Polyethylenimine (PEI) Transfection

400 µL plain DMEM containing 6 µg target DNA were prepared. 12 µL PEI solution (1 mg/mL) were added, the mixture was vortexed and incubated for 20 min at RT. Subsequently, the solution was added carefully to the target cells. 12 h post transfection, the medium was changed and 48 h after transfection the cells were harvested for the according experiment.

2.2.1.3 Freezing cells

A 80 % confluent 10 cm dish was harvested and spun down at 4500 rpm for 5 min. The cell pellet was resuspended in 3 mL full DMEM containing additional 10 % FBS and 10 % DMSO. The suspension was divided in three cryo vials and frozen at – 80 °C.

2.2.1.4 Lentiviral Transduction

For the stable expression of shRNAs (pLKO) or cDNAs (pRRL), Lenti-Viruses were produced to infect target cells. Therefore, Lenti-X cells were plated on a 10 cm dish (4x10^6) and transfected 24 h later. After a 5 min incubation of 700 µL OptiMEM containing 30 µL PEI, this mixture was added to another 700 µL OptiMEM PEI containing 11.1 µg of the shRNA or cDNA plasmid, 2.8 µg pPAX2 and 1.4 µg pMD2G/VSVG. The final mix was incubated for another 20 min and then carefully added on the Lenti-X cells. The medium was changed 24 h after transfection by discarding the medium, carefully washing the cells with PBS and adding 5 mL of fresh Medium. Additionally, the target cells were seeded in low density in 6 cm dishes. 48 h after transfection, the target cells were infected with the Virus produced by the Lenti-X cells. Therefore, the medium on the target cells was discarded and after a PBS wash, 1 mL complete DMEM containing 6 µL Polybrene solution (8 mg/mL) was added. Afterwards, the 5 mL of medium on the Lenti-X cells containing the virus was filtered (0.45 µm) and added to the target cells. The target cells were incubated with the Virus for 72 h before selection was initiated by the addition of Puromycin or Hygromycin.

2.2.1.5 CRISPR-Cas9

To generate CRISPR-Cas9 mediated Knock-Out (KO) cell lines, sgRNAs in the px459 plasmid were transfected with PEI to the target cells. After selection with Puromycin, the pools of cells were analyzed by Western blotting (2.2.2.3.8). If the sgRNA pools showed a good knock-down (KD), cells were plated in low density on a 15 cm dish. After one to two weeks, the formed single cell colonies were picked and transferred to a 24-well plate. After the wells were about 80-90 % confluent, the cells were harvested for a test Western Blot. All colonies, which looked promising in the test blot were plated in the same cell number together with control transfected cells and parental cells. These were harvested 24 h after plating and analyzed by Western Blotting. Correct cell lines were frozen and used for subsequent analysis.

2.2.1.6 Growth analysis

2.2.1.6.1 Cumulative growth curve

1 x 10^5 cells were seeded in a 6 cm dish in triplicates. After three days, the cells were harvested by washing once with PBS, adding 500 µL Trypsin-EDTA, incubating for 3 min and adding 1 mL of full medium on top. The cells were counted with the Countess from BioRAD and 1 x 10^5 cells were plated again on 6 cm dishes. Every three days the cells were collected, counted and plated again as 1 x 10^5 cells per 6 cm dish. The counted cell numbers were additively calculated as shown in the example. In this way; one can measure the exponential growth of the cells, imitating unlimited area.

Example:

1x10^5 cells were seeded on day 0; on day 3 they were collected and counted. The corresponding counted cell number can be seen in table11 as “counted cells”. To calculate the fold increase in cell number, the value of day 3 (3x10^5) has to be divided by the starting cell number (1x10^5). By additively calculating the cell number, the “adjusted cell number” was received (see table11):

- The adjusted cell number of day 3 is being calculated by multiplying the day 0 cell number with the day 3 fold increase
- The adjusted cell number of day 6 is calculated by multiplying the day 3 adjusted cell number with the day 6 fold increase
- The adjusted cell number of day 9 is calculated by multiplying the day 6 adjusted cell number with the day 9 fold increase
- …

Table11: Example of calculating cumulative growth curves.

	Day 0	Day 3	Day 6	Day 9
Counted cells	1 x 10^5	3 x 10^5	3.3 x 10^5	3.2 x 10^5
Fold increase		(day3/1x10^5) = 3	(day6/1x10^5) = 3.3	(Day9/10^5) = 3.2
Adjusted cell number		3*day1 = 3x10^5	3.3*day3 = 9.9x10^5	3.2*day6 = 3.2 x 10^5

2.2.1.6.2 Crystal Violet staining

Cells were cultured in a 6-well dish and treated as needed. After the cells reached the preferred confluency, they were washed once with PBS and then air dried. Subsequently, 1 mL Crystal Violet solution was added to each well and incubated on a one-dimensional shaker for 20 min at RT. The cells were washed three times with ddH_2O by shaking each 5 min on the one-dimensional shaker before being air dried. The plates were documented by scanning them. To quantify the intensity of the staining, 2 mL of 0.5 % SDS solution were added to each well and the plate was incubated for 20 min at RT on a one-dimensional shaker. Finally, the 6-well plates were measured with the Tecan Reader at 590 nm, with 7x7 measurements per well, with a border of 750 µm and a number of flashes of 10.

2.2.1.7 FACS

Cells were cultured on 10 cm dishes and used when they reached 80 % confluency. After the cells were harvested, the pellet was resuspended in 200 µL PBS and 80 µL 100 % EtOH were added dropwise while vortexing for a final concentration of 80 % EtOH. This mix was incubated ON at 4 °C before it was spun for 5 min at 2000 rpm and washed once with PBS. Subsequently, the pellet was resuspended in 200 µL PBS containing 0.5 µL RNAseA and incubated for 20 min on the rotating wheel at RT. Finally, 10 µL of 1 mg/mL PI were added, the mix was incubated for another 30 min on the rotating wheel at RT in the dark and the samples were measured at the FACS facility

2.2.1.8 Scratch

Cell culture inserts for 6-well plates from ibidi (804466) were used to analyze the migration of cells. The chamber was put in a plate and around it the well was filled with PBS to avoid drying out. In the 4 parts of the chamber each 200 µL containing 1000 cells were pipetted. 24 h after seeding, the chamber was carefully removed and the 0 h timepoint was imaged. Subsequently, pictures of the wound were made at different time points.

2.2.1.9 Invasion

10 cm dishes were prepared by filling them with 5 mL ddH_2O. Drops of 5000 cells per 25 µL were then pipette on the inside of the lid of the 10 cm plate and put the lid on the plate. The drops were incubated upside down for two days. Meanwhile a 96 well plate was coated with 40 µL Matrigel solution (1.53 mg/mLMatrigel + 1.8 % FBS + 136 mM HEPES in DMEM) and polymerized for 60 min at 37 °C. 60 µL of collagen gel were added on the precoated plate and transfer one spheroid from the lid of the 10 cm plate with a pipette set to 0.5 µL to the collagen plate. After a polymerization of 60 min at 37 °C, the 0 h timepoint was imaged. Subsequently, pictures of the spheroid were made at different time points.

2.2.2 Molecular biological methods

2.2.2.1 Cloning

2.2.2.1.1 Polymerase Chain Reaction

For amplifying DNA the Phusion Polymerase from NEB was used. The mix was assembled according to the manufacturer protocol:

10 µL	5x Phusion HF or GC Buffer
1 µL	10 mM dNTPs
2.5 µL	10mM forward primer
2.5 µL	10 mM reverse primer
0.5 µL	Phusion DNA Polymerase

The mixture was incubated in a thermocycler with the following protocol:

98 °C	30 sec	
98 °C	10 sec	┐
55 °C	30 sec	├ 29 cycles
72 °C	30 sec per kb	┘
72 °C	10 min	
4 °C	Hold	

2.2.2.1.2 Annealing Oligonucleotides

11.25 µL	forward primer
11.25 µL	reverse primer
2.5 µL	10 x Annealing Buffer

The mixture was incubated for 5 min at 95 °C before the heating block was removed and allowed to chill to RT. For further use, the annealed oligonucleotides were diluted 1:400 in 0.5 x Annealing Buffer (10xAnnealing Buffer: 1 M NaCl / 100 mM Tris-HCl, pH=7.4).

2.2.2.1.3 Plasmid digestion and dephosphorylation

3 µg	plasmid
1 µL	Thermo Fisher Buffer
0.5 µL	Thermo Fisher restriction enzyme
Ad 10 µL	ddH_2O

The mixture was incubated ON at 37 °C. Plasmids, which should be cloned by HiFi cloning were directly gel purified (2.2.2.1.4), plasmids, which should be cloned by ligation were dephosphorylated by adding 1 µL FastAP (Thermo Fisher) and incubating the mixture for another hour at 37 °C before gel purification.

2.2.2.1.4 Agarose gel and gel purification

1 % or 2 % Agarose were mixed in 1 x TAE buffer and heated in a microwave. When all Agarose was dissolved, the mixture was allowed to chill for 1 min before Ehtidium Bromid was added. The mixture was poured in a Biometra compact system (analytic jena) and left for 20 min to allow polymerization. The digested plasmids or PCR fragments were mixed with 6x DNA loading Dye (Thermo Fisher) and loaded on the gel. After 30 min at 130 V, the DNA signals were visualized by UV Light. If necessary, the corresponding DNA fragments were cutted out of the gel and purified with the GenElute™ Gel Extraction Kit from SIGMA according to the manual.

2.2.2.1.5 HiFi reaction

For the HiFi reaction, plasmids were not dephosphorylated before gel purification. The concentration of the plasmid and insert DNA fragments were determined by Nanodrop measurement. Subsequently, the pmols were calculated using this formula:

pmols = (weight in ng) x 1,000 / (base pairs x 650 daltons)

Finally, the mixture was assembled as following:

0.067 pmols	digested and gel purified plasmid
0.133 pmols	insert
5 µL	NEBuilder HiFi DNA Assembly Master Mix
Ad 10 µL	ddH_2O

After an incubation of 15 min at 50°C, the mix was allowed to chill down before transforming 1 µL of it into bacteria (2.2.2.1.7).

2.2.2.1.6 Ligation

For the ligation reaction, plasmids were dephosphorylated before gel purification. The concentration of the plasmid and insert DNA fragments were determined by Nanodrop measurement. Subsequently, the pmols were calculated using this formula:

pmols = (weight in ng) x 1,000 / (base pairs x 650 daltons)

Subsequently, the following mix was pipetted:

0.020 pmols	digested and dephosphorylated plasmid
0.060 pmols	insert
2 µL	T4 Ligase Buffer
1 µL	T4 Ligase
Ad 20 µL	ddH_2O

The ligation mixture was incubated ON at 16 °C before 1 µL of this mix was transformed into bacteria (2.2.2.1.7).

2.2.2.1.7 Bacteria transformation

Plasmids were either transformed in 5-α or in 10-β bacteria purchased from NEB, depending on the kind of plasmid. In both cases, bacteria were taken out of the - 80 °C freezer and allowed to thaw on ice for 5 min. Subsequently, 1 µL of the HiFi or the ligation mix were added to the bacteria and incubated for 30 min on ice. After a 30 sec heatshock at 42 °C, the samples were put back on ice for another 5 min. Prewarmed 200 µL LB medium (5-α) or special 10-β medium (10-β) were added and samples were incubated 1 h shaking at 37 °C. Subsequently, samples were either plated on LB-Agar plates or putted in flasks with LB medium each containing a final concentration of 50 µg/mL Ampicillin and incubated ON at 37 °C.

2.2.2.1.8 DNA preparation

Plasmids were transformed in bacteria and cultured ON at 37 °C in fluid cultures. For Mini-Preps a culture of 2 mL, for Midi-Preps 200 mL were used. These cultures were spun down at 4000 rpm at 4 °C for 15 min and subsequently the DNA was isolated according to the protocol of either the GenElute™ Plasmid Miniprep Kit or the GenElute™ HP Plasmid Midiprep Kit.

2.2.2.1.9 Plasmid sequencing

1 µg	DNA
3 µL	10 µM Primer
Ad 12 µL	ddH_2O

The prepared sequencing mix was sent to the MycroSynth laboratory.
(https://srvweb.microsynth.ch/)

2.2.2.1.10 Cloning strategies

2.2.2.1.10.1 pLKO

The Oligonucleotides were annealed and diluted 1:400 in 0.5 x Annealing Buffer. Meanwhile, the pLKO plasmid was ON digested with AgeI and EcoRI and dephosphorylated with FastAP for 1 h at 37 °C. The diluted annealed Oligonucleotides were then ligated in the gel purified digested and dephosphorylated vector by T4 ligaseON at 16 °C. 1 µL of the ligation mix was transformed in 5-alpha bacteria according to the manufacture protocol. After ON incubation at 37 °C, colonies were picked, Mini-Preps were performed and the ON test digested with XhoI. On a 1 % agarose gel one can observe 1 signal at 200 bp for the empty plasmid and two closely migrating signals, one at 200 bp and one above, for a pLKO vector with an inserted shRNA. Positively digested plasmids were sent for Sequencing with the pLKO Seq primer.

2.2.2.1.10.2 pRRL

The RecQL and E2F4 genes and all mutants were amplified using their specific Oligonucleotides (E2F4-FL/E2F4-336/E2F4-DB/E2F4-KR/RecQL; each Fw and Rev). The PCR product was gel extracted and HiFi cloned in the AgeI and SpeI digested pRRL_Hygro vector, which was as well gel purified. Subsequently, the HiFi reaction was transformed in 10 -β bacteria, plated on LB+Amp plates, Minis were picked and ON test digested with EcoRI. All test digestions, which looked promising were sent for sequencing with the pRRL Seq primer.

2.2.2.2 RNA

2.2.2.2.1 RNA isolation

The RNA was isolated with the RNeasy Kit from Qiagen according to the manufacturer protocol.

2.2.2.2.2 Library preparation

For the purpose of sequencing the total RNA of cells, the RNA was isolated using the RNAeasy Kit and subsequently processed after the manufacture protocol of the NEBNext® Ultra™ RNA Library Prep Kit for Illumina® (E7530) and with the NEBNext® Multiplex Oligos for Illumina® (Dual Index Primer Set 1) (E7600). Finally, the amount of DNA was measured by PicoGreen (2.2.2.2.3).

2.2.2.2.3 PicoGreen measurement

1 µL of the DNA samples was diluted in 99 µL 1x TE buffer and an additional 100 µL of 1X TE buffer containing 1:200 PicoGreen reagent (Thermo, P7581) were mixed. After an incubation of 7 min at RT in the dark, the samples were measured with the Tecan (in duplicates) with the following settings:
Excitation: 480 nm
Emission: 520 nm
Subsequently the measured values were calculated into ng/µL using a calibration curve.

2.2.2.3 Protein biochemistry

2.2.2.3.1 Protein isolation

Cells were harvested when they reached about 80 % confluency. After spinning the samples for 5 min at 4500 rpm and 4 °C, they were washed once with PBS. The pellet was lysed by resuspending it in different lysis buffers dependent on the type of experiment. For normal preparation of protein samples for Acrylamid gel and following Western Blot analysis (2.2.2.3.8), cells were lysed in PBS containing 1 % TritonX100. After a 30 min incubation on ice, the sample concentration was measured (2.2.2.3.2). Same concentrations were prepared, mixed with loading buffer and loaded on an Acrylamid gel (2.2.2.3.8).

2.2.2.3.2 Concentration measurement

The lysed cells were measured in duplicates by the Pierce™ BSA Protein Assay Kit (Thermo, 23225). 5 µL of lysate were mixed with 100 µL Solution (A:B – 1:50). After 7 min incubation at RT, the absorbance of the samples was measured at 562 nm wavelength with a Bandwidth of 9 nm and 20 flashes with the Tecan. The concentration was calculated with an according calibration curve.

2.2.2.3.3 Immunoprecipitation (IP)

Cells were harvested and washed with PBS before they were lysed in 1 mL of TNT buffer containing 100-300 mM NaCl, depending on the used antibody, and incubated 30 min on ice. After a 10 min spin at 13000 rpm and 4 °C, 100 µL of the supernatant was kept as input. The remaining 900 µL were separated in tubes containing 2 µg of either the according isotype control or the specific antibody. This mix was incubated ON at 4 °C on a rotating wheel. On the next day, 30 µL of agarose beads (per sample) were washed with the according lysis buffer and added to the samples. After another rotating step at 4 °C for 4 h, samples were washed twice with lysis buffer (10 min, rotating wheel, 4 °C). Subsequently, loading buffer was added, samples were heated at 95 °C for 10 min and loaded on an Acrylamid gel (2.2.2.3.8).

2.2.2.3.4 Cell fractionation

Cells were cultured on a 6-well plate and harvested when they reached about 80 % confluency. After a PBS wash, the pellets were resuspended in 100 µL PBS containing 0.5 % TritonX100, Protease and Phosphatase inhibitors. The samples were incubated 30 min on ice before 50 µL were kept as total fraction. The remaining 50 µL were spun down at 3.2 rpm for 3 min at 4 °C. The supernatant was kept as soluble fraction and the pellet was resuspended in 50 µL PBS containing 0.5 % TritonX100, Protease and Phosphatase inhibitors. After another 30 min on ice, loading buffer was added to all samples and they were boiled at 95 °C for 30 min before loading on an Acrylamid gel (2.2.2.3.8).

2.2.2.3.5 Mass Spectrometry

Cells were cultured on 15 cm dishes. When they reached about 80 % confluency, cells were washed once with PBS and then scraped in PBS. Subsequently, an IP was performed until the final washing steps as described in 2.2.2.3.3 with TNT250 as the lysis buffer. After two washes with TNT250, the samples were washed once with 1xTBS. Finally, the pellets were resuspended in 250 µL 1xTBS. 50 µL were mixed with loading buffer and loaded on an Acrylamid gel (2.2.2.3.8) to validate good pulldown of the protein. The remaining 200 µL were sent to the Core Facility Flow Cytometry Berg (university clinicum Tübingen), which performed the mass spectrometry experiment.

2.2.2.3.6 His-Ubiquitin assay

Cells were transfected like described in 2.2.1.2 with 2 µg FLAG tagged Trim33, 3.5 µg HA tagged substrate (E2F4/Myc) and 3.5 µg His tagged ubiquitin. 24 h after medium change, the cells were harvested, washed once with PBS and then resuspended in 100 µL PBS. 5 µL of this mix were kept as input and directly mixed with 50 µL loading buffer. The remaining 95 µL were mixed with 1 mL Urea Buffer and rotated for 15 min at RT. After a 10 min spin at 13000 rpm at RT, the supernatant was transferred in a new tube and 50 µL pre-washed Ni-NTA beads were added. Subsequently, the samples were rotated on a wheel at RT ON before they were washed twice with Urea buffer. Finally, 50 µL of loading buffer were added to the beed pellets, samples were boiled and loaded on an Acrylamid gel (2.2.2.3.8).

2.2.2.3.7 Cycloheximide assay

Cycloheximide is a chemical blocking overall protein synthesis and allowing the analysis of protein degradation over time (Jimenez, 1976; Liu *et al.*, 2021). During this study, 100 µg/ml Cycloheximide were added to the cells for different timepoints. Subsequently, the cells were harvested and analyzed using Western Blot (2.2.2.3.8).

2.2.2.3.8 Acrylamid gels and Western Blot

To separate proteins according to their size they were loaded on an Acrylamid gel, transferred to a PVDF membrane and stained with specific antibodies.

2.2.2.3.8.1 Preparing Acrylamid gels

4 gels were generated at the same time according to the following protocols for 12 % gels:

Table 12: Recipe of 12 % acrylamide gels

	Separating gel	Stacking gel
30 % Acrylamid	7 mL	1.3 mL
ddH_2O	8 mL	4.3 mL
Bis-Tris	5.5 mL	2.3 mL
10 % APS	200 µL	100 µL
TEMED	15 µL	2.5 µL

The Separating gel was poured in the casting chambers from BioRAD in glasses with a 1 mm spacer and covered with 200 µL Isopropanol. After 20 min the separating gel was polymerized and the alcohol was removed. Subsequently, the Stacking gel was poured on top of the Separating gel and 15 spot combs were inserted. The polymerization was done after another 20 min and the gels were used further as described in 2.2.2.3.8.2 – 2.2.2.3.8.4.

2.2.2.3.8.2 Running Acrylamid gels

The ready gels were put in the running chamber and covered with 1 x MOPS buffer. All samples were mixed with loading buffer, heated up for at least for 10 min at 95 °C and allowed to chill down to RT before loading together with the PAGE Ruler (Thermo, 26617). The gels run at 80 V for 10 min before the voltage was increased to 130 V.

2.2.2.3.8.3 Western Blot

The gels were incubated in 1 x transfer buffer for 5 min before assembling the blot. The PVDF membranes were activated in methanol, washed with ddH_2O and subsequently put in 1x transfer buffer. Subsequently, the blot was assembled in a semi dry chamber as following:

Two Whatman paper

PVDF membrane

Acrylamid gel

Two Whatman paper

The semi dry blot was plugged in a power supply and ran at 25 V and constant 250 mA for 2 h.

2.2.2.3.8.4 Detecting proteins

The blot was disassembled and the membranes were directly put in 5 % milk in TBST for 1 h. Subsequently, the membranes were washed with TBST, cut as needed and incubated ON in primary antibody diluted in TBST at 4 °C on a roller. On the next day, the membranes were washed three times 5 min in TBST on a one-dimensional shaker before they were incubated in secondary antibody diluted in TBST for 2 h at RT. After another three washes for each 15 min on a one-dimensional shaker, the blots were developed in the ChemiDoc Imaging System from BioRAD with the Immobilon Wesern HRP Substrate from Millipore (WBKLS0500). The scan was performed with the Chemi High Resolution settings of the ImageLab software belonging to the machine.

2.2.2.3.9 Chromatin IP (ChIP) – Sequencing

2.2.2.3.9.1 Chromatin pulldown

Cells were cultured on 15 cm dishes and used when they reached 80 % confluency. After a wash with PBS, the cells were fixed with 10 mL of 1 % PFA in PBS for 3 min at RT before the reaction was quenched with 1 mL of 2 M Glycine for 1 min. Subsequently, the dishes were washed two times with PBS, the cells were scraped in PBS and spun down. The cell pellet was resuspended in 200 µL TNT buffer containing 200 mM NaCl as well as protease and phosphatase inhibitors. After 30 min on ice, 1 µL MNase was added to the mix and incubated for 3 min at 37 °C and 1500 rpm. Immediately afterwards, 20 µL of 0.5 M EDTA were added and samples were kept on ice. 800 µL of TNT-300 + 0.1 % SDS were added to the samples and they were sonicated (3 times 2 min at 30 % power and 100 amplitude). After a spin at 13000 rpm and 4 °C for 10 min, 20 µL of the supernatant were kept as Input sample. The rest was split in two tubes containing either isotype control or the E2F4 antibody. This mix was incubated ON at 4 °C on a rotating wheel.

On the next day, magnetic beads were washed in the according lysis buffer, added to the samples and put back on the rotating wheel at 4 °C for another 4 h. Subsequently, the samples were washed twice with TNT-300 + 0.1 % SDS and then dissolved in 200 µL 1xTE buffer containing 0.5 % SDS, 250 mM NaCl and 1 µL RNAsA (inputs as well). The samples were incubated for 2 h at 37 °C before another 200 µL 1xTE was added, containing 0.5 % SDS, 250 mM NaCl and 2 µL ProteinaseK. This mix was incubated for another 2 h at 50 °C before the temperature was increased to 65 °C for an ON incubation with a shaking of 20 sec 1500 rpm every 10 min.

On the next day, the magnetic beads were removed from the samples using a magnetic rac and 1 volume ROTI®Phenol/Chloroform/Isoamylalcohol was added. After 30 sec of vortexing, the samples were spun for 10 min at 13000 rpm and the upper phase was transferred to a new

tube. To this new tube, 2.5 V EtOH and 2 µL GlycoBlue were added before they were incubated ON at -20 °C.
On the next day, samples were spun at 13000 rpm for 30 min, washed once with 75 % EtOH, dried and resuspended in 10 mM Tris pH=8.0 (Inputs: 100 µL / IgG and IP samples: 25 µL).

2.2.2.3.9.2 Library preparation

The DNA concentration of the samples was determined by PicoGreen measurement. The same amount of DNA of each sample was diluted in 9 µL ddH_2O (10-2000 ng) and 0.35 µL 10x EXTaq Buffer and 0.35 µL rSAP were added. This mix was incubated for 1 h at 37 °C and for 10 min at 65 °C. Subsequently, 0.35 µL of 1 mM dCTP was added, the mix was incubated for 5 min at 95 °C and for 5 min on ice, before 0.35 µL terminal deaxynucleotidyl transferase was added and the samples were incubated for 35 min at 37 °C. After the transferase was heat inactivated for 20 min at 75 °C, 0.5 µL of 10 µM biotin-labeled anchor primer and 10 µL of Kapa robust mastermix were added. This mix was put in the thermo cycler with the following protocol:

95 °C	3 min	
47 °C	1 min	⎫ 16 cycles
68 °C	2 min	⎭
72 °C	10 min	
4 °C	Hold	

Subsequently, the primer was removed by a 1 h incubation at 37 °C with Exonuclease I. The samples were transferred to 1.5 mL Eppendorf tubes and filled up to 500 µL with B&W Buffer before 10 µL of washed magnetic streptavidin C1 beads were added. This mix was incubated for 2 h at 23 °C with 10 sec shaking with 14000 rpm and 10 sec pause. Then, samples were washes once with 300 µL B&W Buffer, three times with 300 µL of 10 mM Tris-HCl pH08.0 containing 0.02 % Triton X-100 and resuspended in 4 µL 10 mM Tris-HcL ph=8.0. These 4 µL were mixed with 0.5 µL of the annealed Adapter, 0.5 µL ddH_2O and 5 µL Blunt/TA Ligase Master Mix. After an ON ligation at 16 °C with a 20 min shake at 1400 rpm every 10 min, the samples were washed once with 300 µL B&W buffer and 2 times with 10 mM Tris-HCl pH=8.0 containing 0.02 % TritonX-100 before they were resuspended in 10 µL 10 mM Tris-HCl pH=8.0. For the final PCR, 2.5 µL of this resuspended beads were mixed with 0.5 µL of 10 µM Index primer 5, 0.5 µL of 10 µM Index primer 7, 6.5 µL ddH_2O and 10 µL ready HiFi Hot Start Mix. The PCR was performed in a thermo cycler with the following protocol:

95 °C	3 min	
98 °C	20 sec	20-25 cycles
65 °C	15 sec	
72 °C	1 min	
72 °C	7 min	
4 °C	Hold	

After running the samples on a 2 % Agarose gel, the DNA was cutted out from 250 bp signal up to the 1 kb signal and gel extracted using the GelExtraction Kit from Qiagen. The exact amount of the final DNA library was measured by PicoGreen. Furthermore, a pool of 5 nM was sent to the sequencing facility and results were analyzed by Prof. Dr. Nikita Popov.

2.2.3 Immunofluorescence

Cells were cultured on 10 mm x 10 mm round glass slides in a 6-well dish and treated as needed. When cells reached 80 % confluency, they were washed once with PBS and fixed either by PFA or Methanol depending on the antibody used. To fix cells with PFA, they were incubated with 1 % PFA in PBS for 10 min at RT. To fix cells with Methanol, they were incubated in pre-chilled 100 % Methanol for 10 min at - 20 °C. In both fixing methods, slides were washed 3 times with PBS before they were stored in PBS at 4 °C.

The glass slides were transferred in a dark box and 100 µL 1xTBS containing 0.3 % Triton X-100 were added and incubated on them for 5 min to permeabilize the cells. After one wash with PBS, 100 µL 5 % BSA in TBST were added and an incubation step of 30 min at RT was performed to block the slides.

Subsequently, 25 µL of the primary antibody solution was added, incubated for 2 h at RT (1:20-1:1000 diluted in 5 % BSA in TBST) and washed three times with 100 µL PBS (each 5 min at RT). Secondary antibodies were diluted in 5 % BSA in TBST (1:200) and incubated 2 h at RT before slides were washed three times with 100 µL PBS (each 5 min at RT). Finally, the slides were dried for 5 min at RT and mounted on coverslips.

2.2.3.1.1 Proximity Ligation Assay (PLA)

For the PLA assay, the Duolink® In Situ PLA® Probes (anti-rabbit minus and anti-mouse plus), the Duolink™ In Situ Wash Buffers Fluorescence and the Duolink® In Situ Detection Reagents Red Kit containing the ligase, the polymerase and the according buffers were used from SIGMA.

Cells were fixed in PFA, permeabilized, blocked, incubated with primary antibody solution and washed in PBS as described under 2.2.3. Meanwhile, the PLA probes were diluted 1:10 in 5 % BSA in TBST and incubated 20 min at RT before 25 µl of this mix was added to each slide and incubated for 1 h at 37 °C. Subsequently, the slides were washed twice with 100 µL Wash

Buffer A (each 5 min at RT on a one-dimensional shaker), the 5x ligation stock solution was diluted 1:5 in dH_2O and ligase was added (1:40). 25 µL of the ligation mix were added to each slide and incubated 1 h at 37 °C before the slides were washed again twice with 100 µL PLA wash buffer A (each 2 min at RT on a one-dimensional shaker). Meanwhile, the 5x amplification stock solution was diluted 1:5 in ddH_2O and polymerase was added (1:80). This mix was incubated on the slides for 2 h at 37 °C (25 µL each). Finally, the slides were washed twice with 100 µL Wash Buffer B (each 10 min at RT on a one-dimensional shaker) and once with 100 µL of 0.01 x PLA Wash Buffer B diluted in ddH_2O (1 min at RT on a one-dimensional shaker). The slides were dried and mounted on coverslips.

2.2.3.1.2 DNA Fiber Assay

Cells were cultured in a 6-well dish and treated as needed. After treatment, cells were washed once with PBS before 1 mL of fresh medium containing 25 µM IdU was added and cells were incubated for 20 min at 37 °C. Subsequently, the cells were washed with PBS and 1 mL fresh medium containing 250 µM CldU was added and cells were incubated for 20 min at 37 °C. After another PBS wash, the cells were harvested and the pellet was resuspended in 50-200 µL PBS, depending on the cell number and the cell line. 2 µL of these resuspended cells were put as a drop on a coverslip and allowed to dry at RT for 5 min. Subsequently, 7 µL Fiber Lysis Buffer was added and incubated for another 2 min before the slides were tilt in a 45 ° angle to allow DNA to flow down the coverslip. After air drying the DNA completely, the coverslips were incubated for 10 min at RT in prechilled Methanol:AceticAcid (3:1) solution (-20 °C). The coverslips were washed in ddH_2O before incubating them in 2.5 M HCl for 60-120 min, depending on the cell line. After three washes in PBS, each 5 min at RT, the coverslips were blocked in 5 % BSA in PBS for 20 min at RT before they were incubated for 2 h at RT with the primary antibodies diluted in 5 % BSA in PBS (anti-BrdU mouse 1:25 / anti-BrdU rat 1:300). Subsequently, the coverslips were washed again three times in PBS (each 5 min at RT), before they were incubated for 1 h at RT with the secondary antibodies diluted in 5 % BSA in PBS (anti-mouse Alexa555 and anti-rat Alexa 488 each 1:200). After the final three washes in PBS (each 5 min at RT), the coverslips were dried and mounted.

3 Results

3.1 Trim33 regulates Myc-induced apoptosis

To reduce Myc protein levels in cancer patients is the goal of scientists all over the world, as it is transcriptionally overexpressed in 50 % of all tumors and associated with poor clinical outcome (Schaub *et al*., 2018). So far, no efficient small molecule inhibitors directly targeting Myc could be developed for cancer therapy. An alternative way is to target upstream regulators to indirectly modulate Myc levels. Previous work of our group focused on the identification of such regulators, which are important for Myc function. For this, Myc was fused with the hormone binding domain of the estrogen receptor (ER). The ER acts as a repressive regulatory domain and is inhibited by 4-hydroxytamoxifen (4-OHT) treatment (Whitfield *et al*., 2015). U2OS cells expressing the Myc-ER fusion protein were used to additionally express a whole genome library of sgRNAs. 4-OHT treatment triggered Myc-induced apoptosis and cells which could rescue this effect, due to the accordingly expressed shRNAs, were analyzed subsequently (Popov *et al*., 2007; Fig 1A). One of the best hits found by our working group was the ubiquitin E3 ligase Trim33, which was validated by two independent shRNAs (Fig 1B). As it can be seen in Figure 1C, the apoptosis of cells increased strongly upon Myc induction, as measured by propidiumiodid (PI) and Annexin-V (AV) staining. This effect was strongly decreased in Trim33 depleted cells (Fig 1C). As Trim33 is a ubiquitin E3 ligase, which ubiquitinates and thereby marks their substrates for proteasome-dependent degradation (Yu *et al*., 2019), Myc might be a substrate of Trim33. I used ubiquitination assays during this thesis to test this hypothesis and could show that the overexpression of Trim33 did not increase ubiquitination of the Myc protein (Fig 1D). Furthermore, cells were treated with cycloheximide, which prevents protein translation. Hence protein degradation over time can be measured using Western Blot analysis. It could be seen that the Myc protein was not stabilized in Trim33KO cells compared to control cells (Fig 1E).

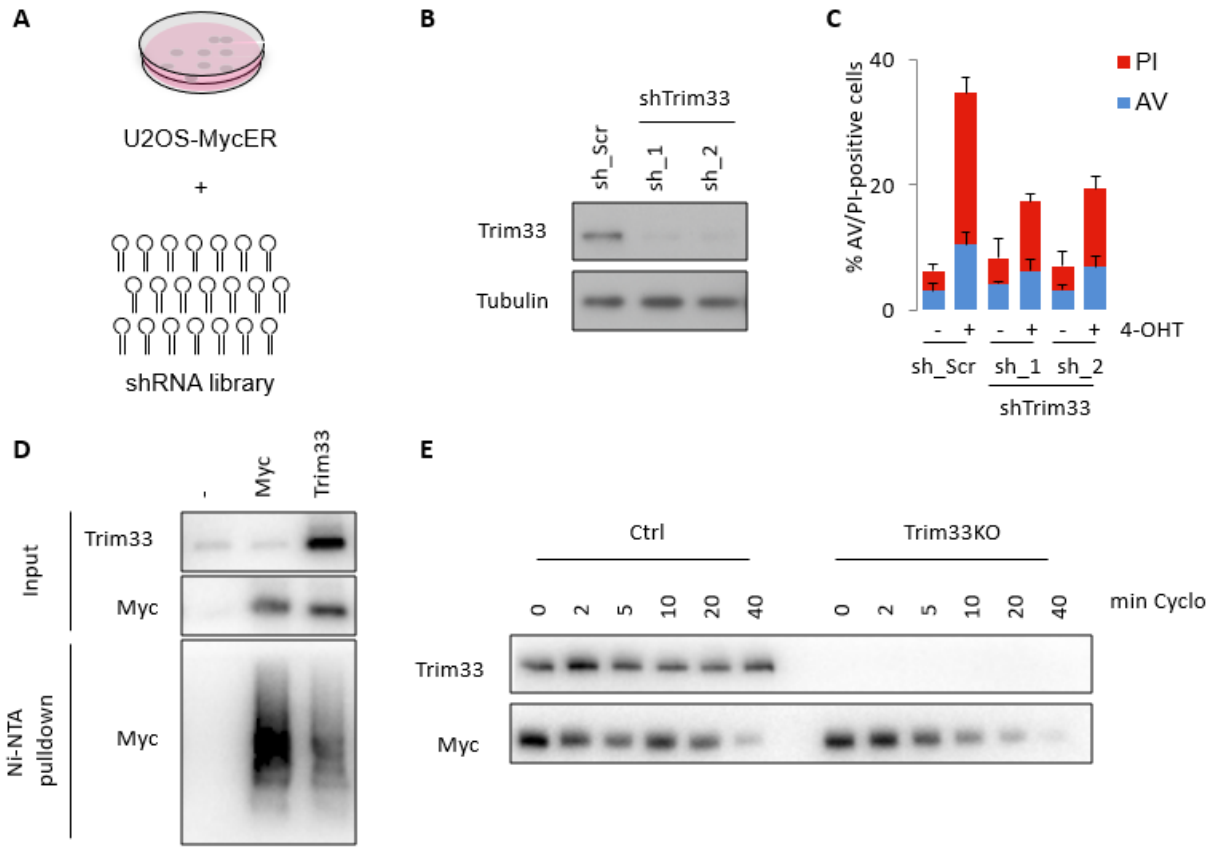

Figure 1: Screen against genes, which regulate Myc-induced apoptosis
A) Scheme of the shRNA-screen performed by Popov *et al.,* 2007. **B)** Western Blot of shTrim33 expressing U2OS cells. **C)** PI and AV experiments of shTrim33 expressing U2OS cells (Popov *et al*., 2007). 4 days treatment with 200 nM 4-OHT induced Myc OE. **D)** His-Ubiquitin assay of Myc-HA and Trim33-FLAG overexpressing $p19^{-/-}$Nras cells. **E)** Cycloheximide assay of $p19^{-/-}$Nras control and Trim33KO cells. Blotted are cells treated for 0, 2, 5, 10, 20 or 40 min.

Taken together, I could disprove the hypothesis that Myc is a substrate of Trim33 and that this is how Trim33 can influence the Myc-induced apoptosis in murine liver cancer cells.

3.2 Trim33KO does not influence growth, migration or invasion of cells

Trim33 is known to have a direct influence on two important signaling pathways, the TGFβ and the Wnt signaling, regulating various basic cellular processes such as proliferation, migration and invasion of cells (Xue *et al*., 2015; Clevers *et al*., 2012; Massagué *et al*., 2012; Dupont *et al*., 2005). Trim33KO cells could dysregulate these basic cellular functions and thereby provide a general survival benefit leading to reduced Myc-induced apoptosis. To analyze this hypothesis, I generated Trim33KO p19$^{-/-}$Nras liver cancer cells (Fig 2A). A cumulative growth curve could prove that there is no significant difference regarding the growth of Trim33KO compared to control cells (Fig 2B). Additionally, the migratory potential of the cells was not significantly different, shown using a wound healing assay (Fig 2C). Likewise, Trim33KO cells invaded in Matrigel to the same extent as control cells (Fig 2D).

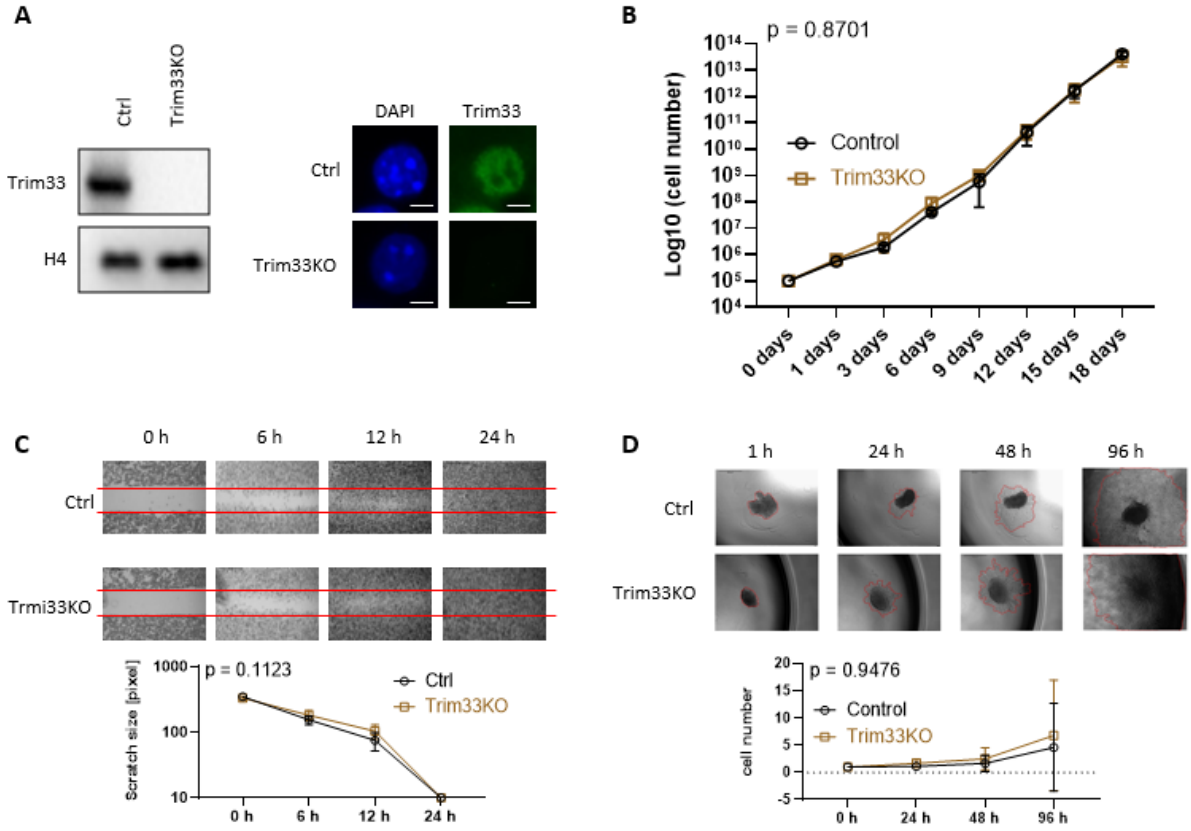

Figure 2: Proliferative, migratory and invasive potential upon Trim33KO
Shown are p19$^{-/-}$Nras control (Ctrl) and Trim33KO cells under normal growth conditions. **A)** Immunoblot and Immunofluorescence of Trim33 with representative pictures. The scale bar corresponds to 2 µm. **B)** Growth curve between 0 and 18 days. **C)** Scratch assay after 0, 6, 12 and 24 h. **D)** Invasion assay at the timepoints 1, 24, 48 and 96 h.

In summary, the hypothesis that Trim33KO cells are less sensitive to Myc-induced apoptosis because they provide a general survival benefit by increasing the growth or the aggressiveness of the cells could not be proven.

3.3 Trim33 influences the growth of cells exposed to RS

How exactly Myc induces apoptosis is still not fully understood. One theory is that Myc induces RS, which leads to DSBs and initiates the controlled cell death (Chen *et al*., 2018; Zheng *et al*., 2017; Gabay *et al*., 2014). This induction of DSBs can be assessed by analyzing the DSB marker protein pH2AX (Collins *et al*., 2020) upon increasing Myc levels. The more Myc is expressed in U2OS cells with Doxycycline (Dox)-inducable Myc, the higher were the pH2AX levels (Fig 3B). Trim33 might influence the Myc-induced apoptosis by regulating the sensitivity of cells to RS. To test this hypothesis, I analyzed the replication process itself in closer detail using the fiber assay. The fork rate did not differ under normal growth conditions (Mock) when Trim33 was depleted (Fig 3C). However, when RS was induced by the overexpression of Myc, the replication speed strongly decreased in control cells while this effect was significantly less prominent in Trim33KD cells (Fig 3C, left panel). Furthermore, Trim33KO cells showed significantly weaker effects on the fork rate compared to control cells when RS was induced by the treatment with the RS-inducing drugs HU (Fig 3C, middle panel) and Etop (Fig 3C, right panel), (Gómez-Herreros 2019; Liew *et al*., 2016, Koç *et al*., 2004; Burden *et al* 1998).

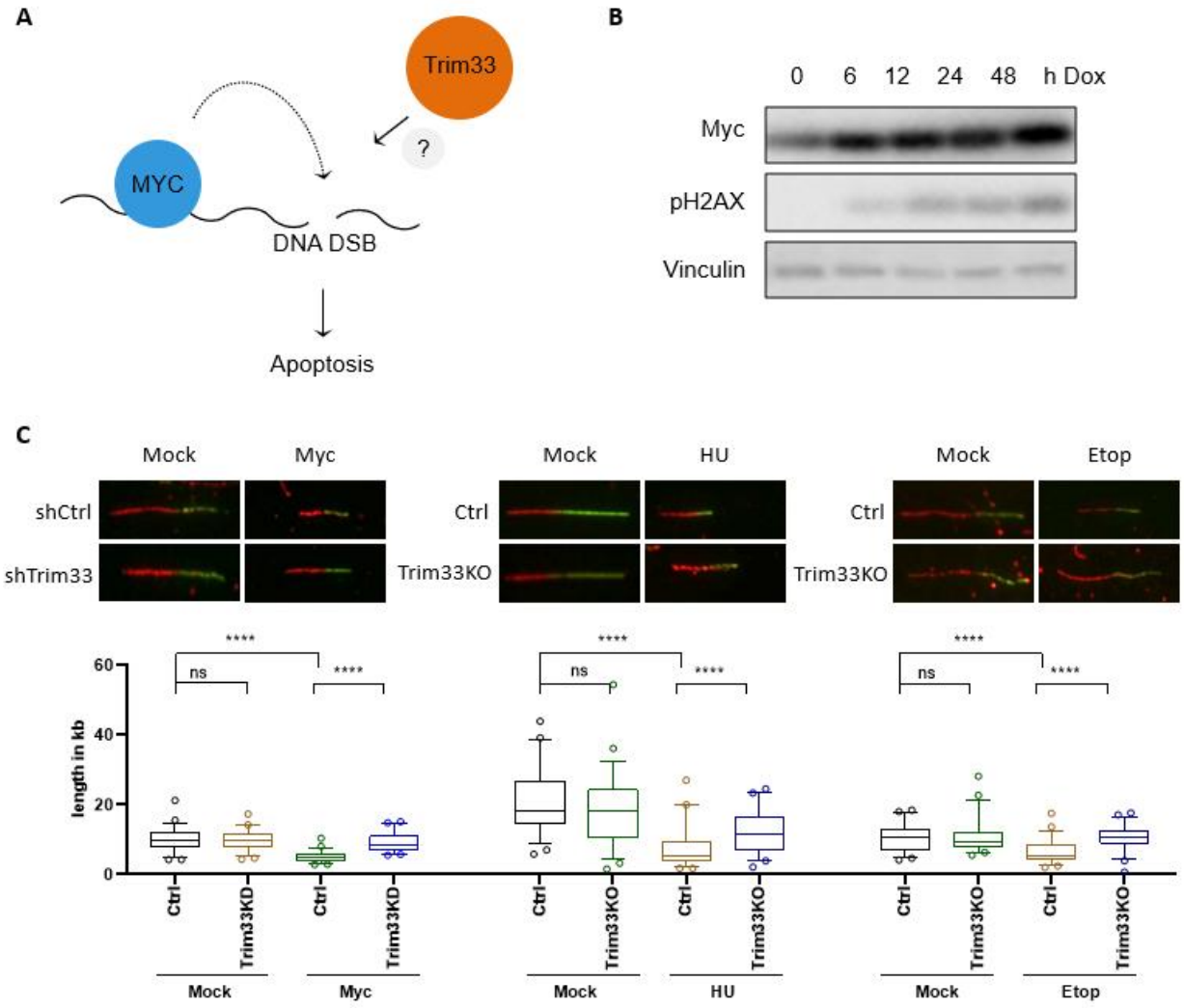

Figure 3: Replication analysis upon Trim33KO under RS
A) Scheme of induction of DSBs by Myc. **B)** Western Blot of U2OS cells with increasing Myc levels. Treatment with 10 µg/mL Dox induces Myc overexpression. **C)** Fiber assay of p19$^{-/-}$Nras control (Ctrl) and Trim33KO cells upon Myc overexpression, 4 h HU treatment (1 mM) or 4 h Etop treatment (5 µM).

All in all, the hypothesis that Trim33 might influence the sensitivity of cells against RS is strongly supported by our experiments for the induction of RS by Myc overexpression and HU or Etop treatment.

3.4 Trim33 inhibits DNA replication and cell cycle progression under RS

I showed in Figure 3 that Trim33KO cells can start replication more efficiently after exposure to RS compared to control cells. These faster replicating cells might as well reenter cell cycle faster and proliferate more efficiently upon RS. To analyze this hypothesis, I first investigated how Trim33KO cells undergo cell cycle. A flow cytometry (FACS) experiment, in which cells were treated 12 h with HU before they were released in medium containing nocodazole (Noc) was performed (Fig 4A). After the 12 h HU treatment, all cells were arrested in S phase due to the lack of dNTPs (Liew *et al*., 2016; Koç *et al*., 2004). When released from HU, cells continue cell cycle and were directly arrested in G2/M phase by Noc due to the blockage of microtubule polymerization (Warren *et al*., 2020; Eilers *et al*., 1989). With this experimental setup, all cells, which reenter cell cycle after RS-induced S phase arrest by HU, are directly arrested in the next G2/M phase and can be quantified. As shown in Figure 4B and C, the S phase arrest was efficient in Trim33KO as well as in control cells. After releasing the cells in medium containing Noc, it can be observed that more cells continued to G2/M phase upon Trim33KO (Fig 4B; D). Furthermore, a growth curve of cells exposed for 48 h to HU before they were released in fresh medium showed that Trim33KO cells proliferated more efficiently compared to control cells (Fig 4E). Crystal violet assays additionally proved that cells grew better upon Trim33KO under RS induced by the overexpression of Myc (Fig 4F, left panel), HU (Fig 4F, middle panel) or Etop treatment (Fig 4F; right panel).

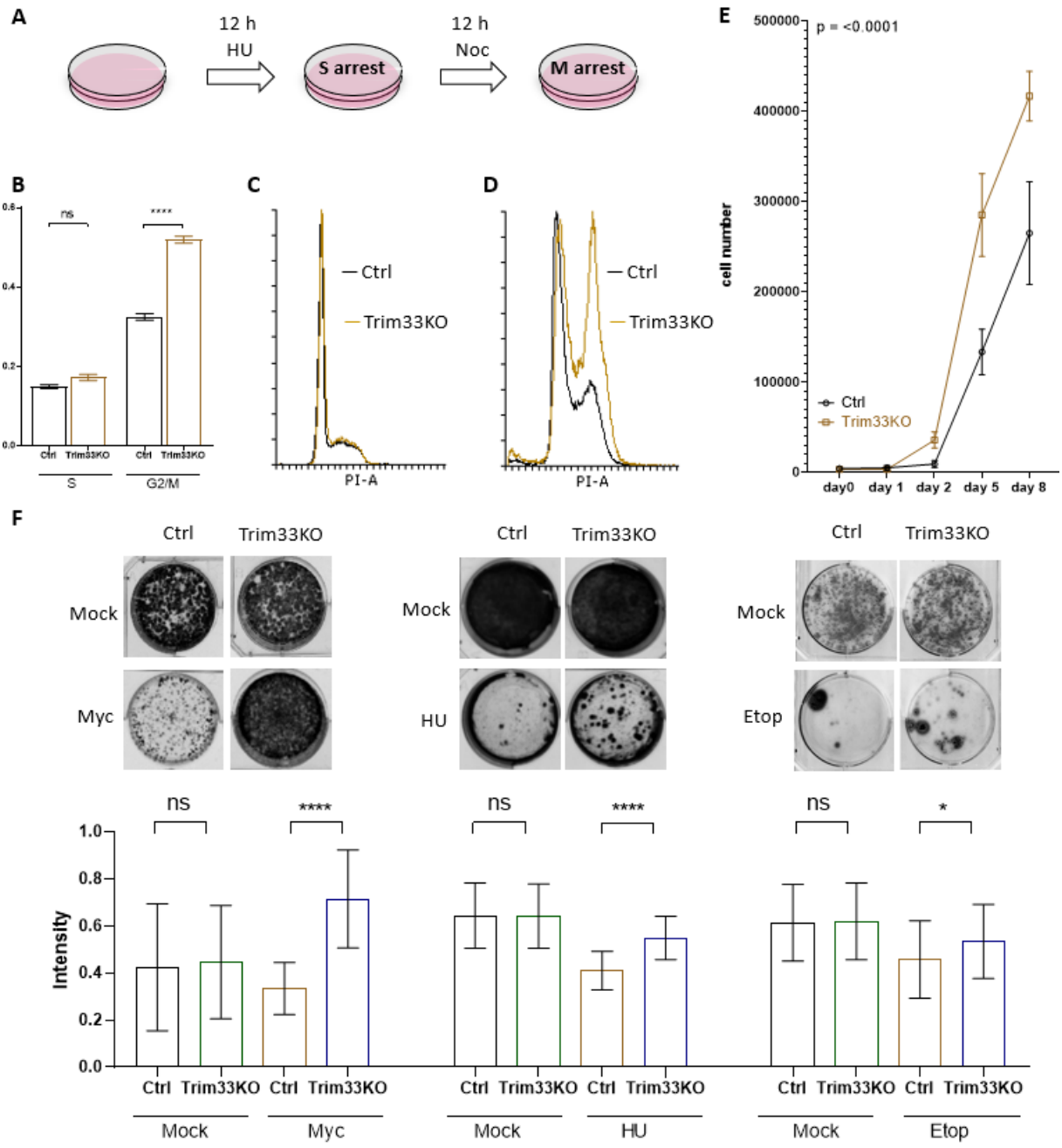

Figure 4: FACS and growth analysis of Trim33KO cells upon RS induction
Shown are p19$^{-/-}$Nras control (Ctrl) and Trim33KO cells. **A)** Scheme of the performed FACS experiment. **B)** Quantification of the FACS analysis shown in A. **C)** Example histogram of 12 h HU (1 mM) treated cells. **D)** Example histogram of 12 h HU (1 mM) treated and subsequently 12 h Noc (100 ng/mL) treated cells. **E)** Growth curve after 24 h HU treatment HU (1 mM). **F)** Crystal Violet assay of cells upon overexpression of Myc, HU treatment (1 mM; 24 h) or Etop treatment (5 µM; 24 h).

Taken together, I could verify the hypothesis that Trim33KO cells go through the cell cycle faster and proliferate more efficiently under RS compared to control cells.

3.5 Trim33KO cells show delayed induction of H2AX phosphorylation

When cells are exposed to RS over a longer time, DSBs will accumulate (Gadgil *et al*., 2020; Fig 5A). If Trim33KO cells proliferate faster compared to control cells under RS, they might induce less DSBs or repair them more efficiently. To evaluate this hypothesis, I analyzed pH2AX under RS. As shown in Figure 5B, the pH2AX levels increased strongly after 4 h HU treatment in control cells. This effect was significantly less pronounced in Trim33KO cells. After 12 h HU treatment the levels of pH2AX were equal in Trim33KO and control cells (Fig 5B). To analyze their potential to repair DSBs, cells were treated 12 h with HU and subsequently released in fresh medium for different time points. The pH2AX levels decreased faster in Trim33KO cells compared to control cells (Fig 5 C). After treating cells for 12 h with Etop, the pH2AX levels decreased faster in Trim33KO cells compared to control cells as well (Fig 5D).

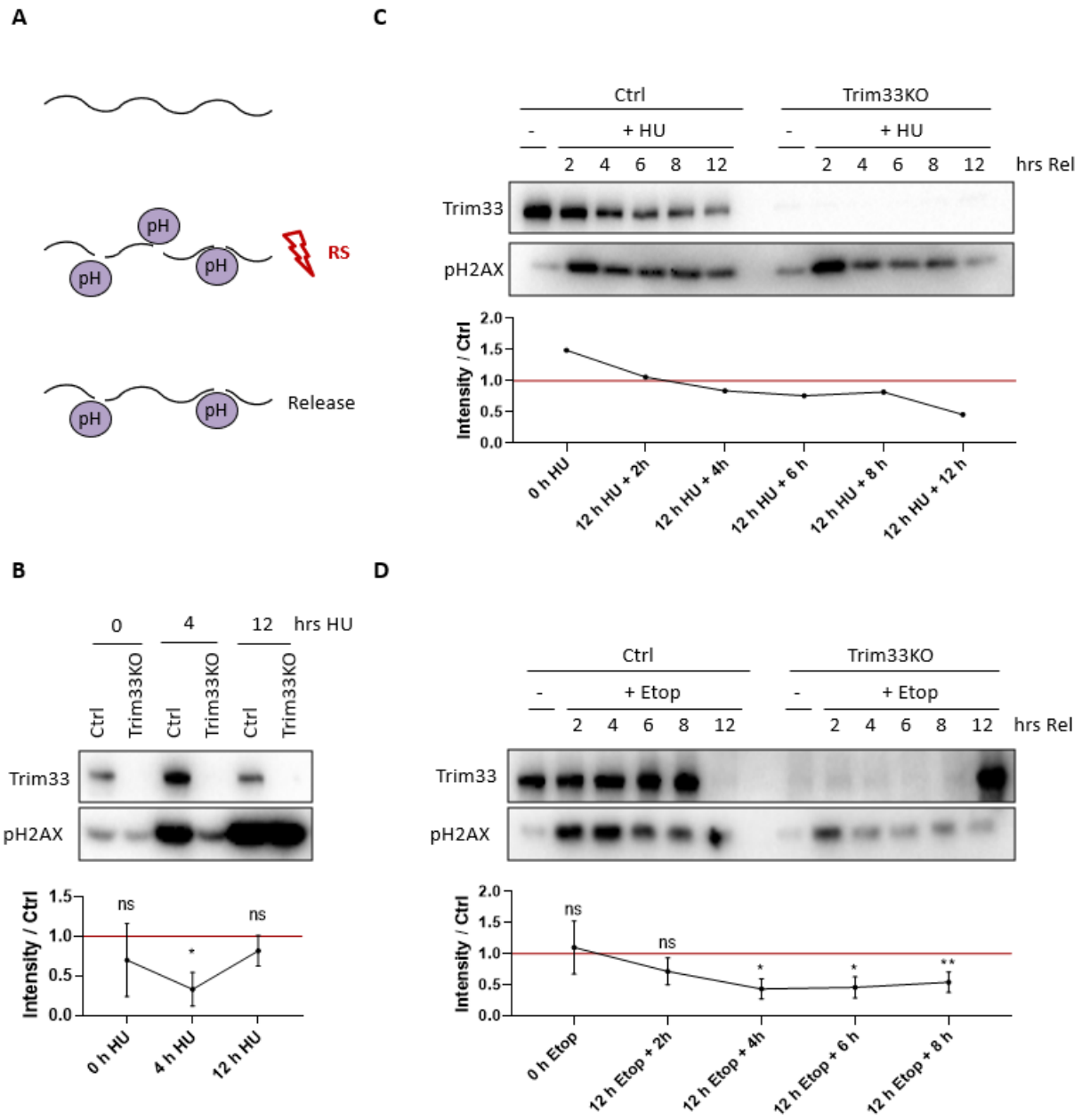

Figure 5: Immunoblots for the DSB marker protein pH2AX
A) Scheme of the induction of DSBs, the recruitment of pH2AX (pH) and its release. **B-D** Shown are Western Blot analyses and quantification of p19$^{-/-}$Nras control (Ctrl) and Trim33KO cells. **B)** 4 and 12 h HU treatment (1 mM). **C)** 12 h HU treatment (1 mM) and subsequent release in normal medium for 2, 4, 6, 8 and 12 h. **D)** 12 h Etop treatment (5 µM) and subsequent release in normal medium for 2, 4, 6, 8 and 12 h.

Summarizing, I could demonstrate that Trim33KO cells induce the phosphorylation of H2AX later and repair DSBs more efficiently.

3.6 E2F4 is a novel substrate of Trim33

To understand how Trim33 can mediate the RS phenotype, we sequenced the mRNA of Trim33KO and control cells (Fig 6A). The deregulated genes were analyzed by a gene set enrichment analysis (GESA) with the Enrichr website (https://maayanlab.cloud/Enrichr/). According to the WikiPathways 2019 dataset, the most deregulated pathways in Trim33KO cells were DNA replication followed by closely related pathways such as cell cycle or mRNA processing (Fig 6B), consistent with the results from Figure 3C. Additionally, the deregulated genes were previously shown by the ENCODE TF ChIP-Seq 2015 dataset to be bound by E2F4 (Fig 6C).

The canonical function of E2F4 is to repress the expression of target genes during the G0/1 phase of the cell cycle (Allmann *et al*., 2020; Xanthoulis *et al*., 2013; Tsantoulis *et al*., 2005). Recent studies show that E2F4 has additionally important transcription-activating and pro-proliferative effects (Feng *et al*., 2019; Stracker *et al*., 2019; Kim *et al*., 2018; Amerongen *et al*., 2010). Furthermore, its overexpression could be observed in numerous cancer types, such as acute myeloid leukemia, breast, skin, gastric or colorectal cancer (Feng *et al*., 2019; Manicum *et al*., 2018; Ongen *et al*., 2014; Rakha *et al*., 2004; Mady *et al.,* 2002; Wang *et al*., 2001). High E2F4 levels are thereby correlated with poor prognosis and reduced OS (Feng *et al*., 2019; Rakha *et al*., 2004; Bankovic *et al*., 2010; Parisi *et al*., 2009; Lee *et al*., 2002). Finally, E2F4 is known to be a key TF in HCC (Wang *et al*., 2018), whereas its exact function in the tumor progression is not fully understood yet.

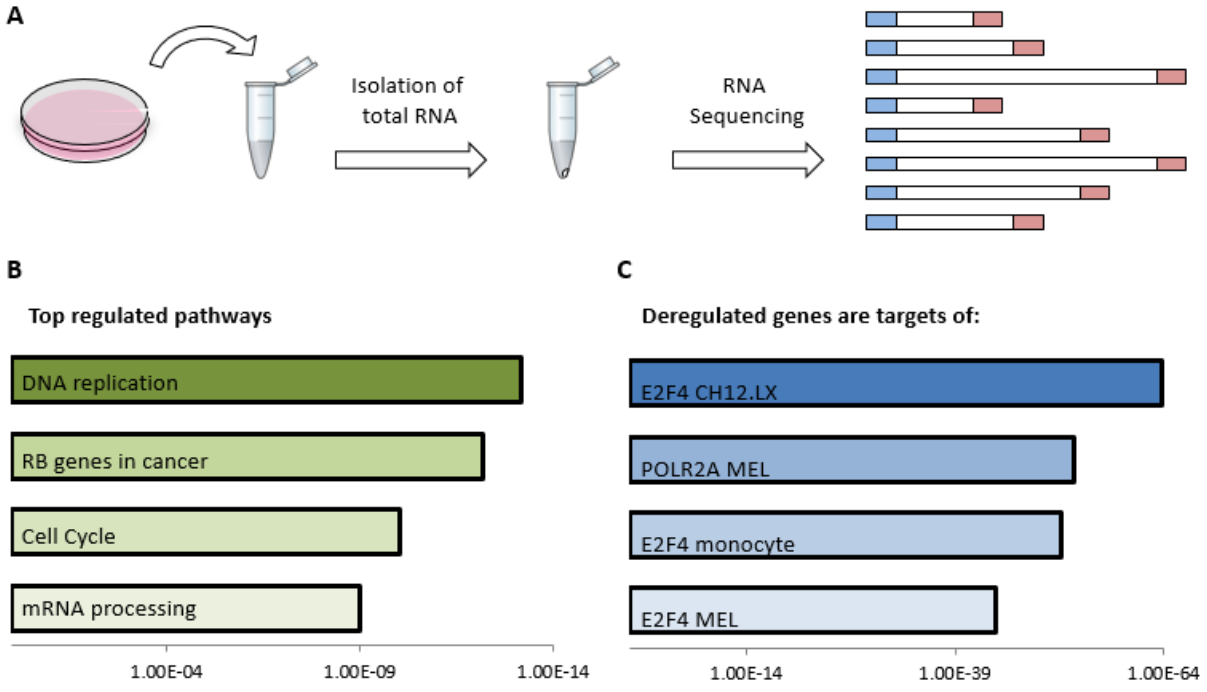

Figure 6: RNA Seq analysis upon Trim33KO.
Shown are p19$^{-/-}$Nras control (Ctrl) and Trim33KO cells. **A)** Schematic overview of the RNA Seq experiment. **B)** Deregulated pathways upon Trim33KO. **C)** Deregulated genes upon Trim33KO are targets of E2F4.

As Trim33 is a ubiquitin E3 ligase, it may ubiquitinate and thereby mark E2F4 for proteasome-dependent degradation. To validate this hypothesis, I performed IP experiments of endogenous proteins, which demonstrated that E2F4 and Trim33 interact with each other (Fig 7A). This result could be enhanced when transiently overexpressing Trim33-FLAG and E2F4-HA (Fig 7B). Additionally, a PLA assay showed that endogenous E2F4 and Trim33 proteins interact with each other under the treatment with the proteasome inhibitor MG132 (Fig 7C). When substrates are interacting with their ubiquitin ligases, they are typically degraded by the proteasome. This degradation can be quite fast, so the interaction is easier detectable under the treatment with proteasome inhibitors. The Trim33KO cell line served as a negative control, in which the signal did not increase upon MG132 treatment (Fig 7C). Moreover, the ubiquitination of E2F4 increased when co-expressed with Trim33 (Fig 7D). Finally, the stability of the E2F4 protein was enhanced upon Trim33KO, shown using a cycloheximide assay (Fig 7E).

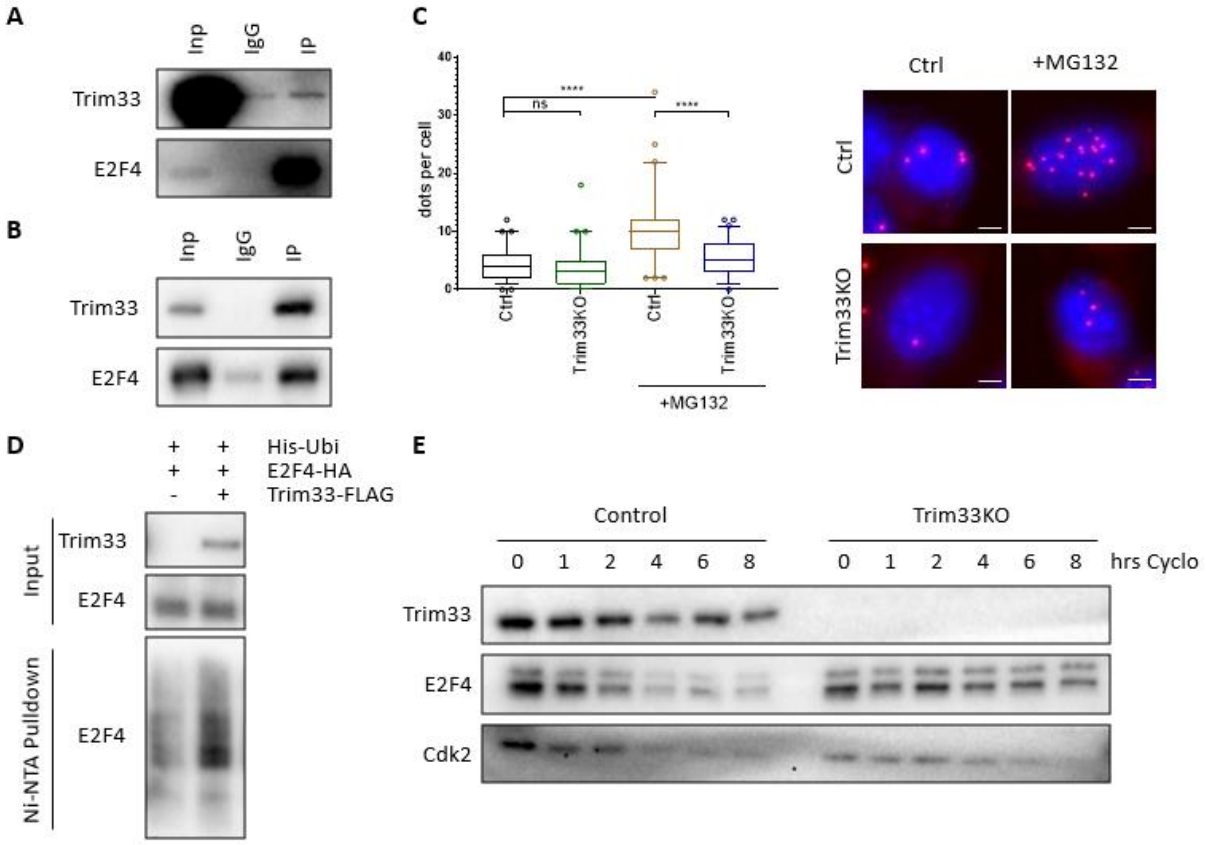

Figure 7: Validation of E2F4 as a Trim33 substrate
Shown are p19$^{-/-}$Nras control (Ctrl) and Trim33KO cells. **A)** Western Blot of an IP experiment. Inp = Input; IgG = Isotype control; IP = E2F4 pulldown **B)** Western Blot of an IP experiment of E2F4-HA and Trim33-FLAG overexpressing control cells. Inp = Input; IgG = Isotype control; IP = HA pulldown **C)** PLA of Trim33 and E2F4 in 0 or 4 h treated cells with the proteasome inhibitor MG132 (10 µM; 4 h). Shown are quantifications and representative pictures. The scale bar corresponds to 2 µm. **D)** His-Ubiquitin assay of E2F4-HA and Trim33-FLAG overexpressing control cells. **F)** Cycloheximide experiment after 0, 1, 2, 4, 6 and 8 h.

With these experiments, the hypothesis that E2F4 is a novel substrate of the E3 ubiquitin ligase Trim33 is strongly supported.

3.7 A functional E2F4 protein is needed to mediate the RS phenotype

E2F proteins possess different functional domains. Typical activator E2Fs (E2F1-E2F3) contain the transactivation domain, a DNA binding domain, a dimerization domain, a CyclinA regulatory domain and a nuclear localization signal (NLS) (Kent *et al*., 2019; Morgunova *et al*., 2015; Nevins 1998). During the G1-S phase of the cell cycle they are not bound to the repressive Rb family members and activate the expression of target genes. E2F4 on the other hand, belongs to the typical repressors, lacks the CyclinA regulatory domain and the NLS, but has two NES sequences (Kent *et al*., 2019; Morgunova *et al*., 2015). During the G1-S phase of the cell cycle the NES leads to the Crm1 dependent nuclear export of E2F4 (Kent *et al*., 2019; Hsu *et al*., 2016). This limits the function of E2F4 to the G0/1 phase when it is bound to the Rb family members, which translocates E2F4 to the nucleus (Xanthoulis *et al*., 2013; Tsantoulis *et al*., 2005). Nuclear E2F4 associates with the DREAM complex to repress the expression of target genes (Engeland *et al*., 2017; Sadasivam *et al*., 2013). However, a publication reported that E2F4 is cytoplasmic as well as partially nuclear in cycling cells, suggesting additional functions of E2F4 (Kent *et al*., 2019), such as the transcriptional activation or the promotion of proliferation (Hong *et al*., 2019; Danielian *et al*., 2016; Ma *et al*., 2016; Kinross *et al*., 2006).

E2F4 is a novel substrate of Trim33 (Fig 7) and might mediate the RS phenotype seen in Trim33KO cells, which might be dependent on different domains of E2F4. To test this hypothesis, I cloned three E2F4 mutants; the E2F4-ΔC, which lacks a part of the C-terminus containing the transactivation domain, the E2F4-DB, which cannot bind to DNA and the E2F4-KR, which cannot be ubiquitinated as all lysines are mutated to arginines (Fig 8A). These three mutants and the wildtype full length E2F4 protein (E2F4-FL) were expressed in control and Trim33KO cells (Fig 8B). As shown in the growth analysis, no difference could be observed under normal growth conditions (Fig 8C; left panel). However, when RS was induced by HU treatment, several effects could be seen (Fig 8D; right panel). First, cells infected with a control plasmid containing the mCherry fluorescent protein (mCh) survived better in Trim33KO cells compared to control cells expressing mCh, which was previously shown in Figure 4F (middle panel). The same effect could be seen when overexpressing E2F4-FL in control cells, mimicking the effect of the Trim33KO. The E2F4 mutants ΔC and DB could not enhance the proliferation of control cells after induction of RS. The E2F4-KR expressing control cells showed similar effects compared to E2F4-FL expressing control cells. In Trim33KO cells, the higher proliferation after HU treatment was strongly reduced when E2F4-ΔC and E2F4-DB were expressed. The E2F4-FL and E2F4-KR expressing Trim33KO cells showed enhanced proliferation compared to mCh expressing Trim33KO cells.

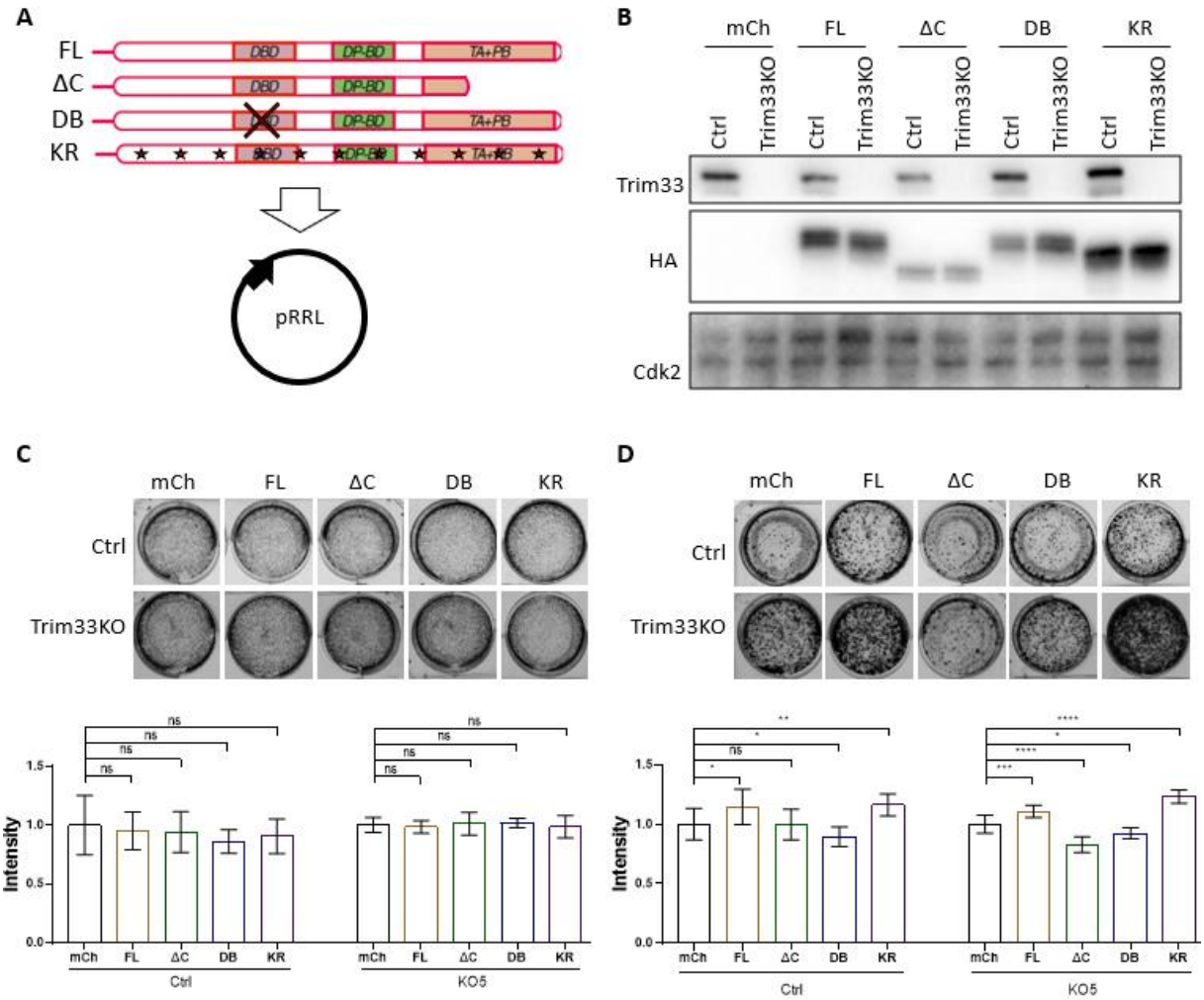

Figure 8: Growth analysis of E2F4 full length and mutant overexpressing Trim33KO cells.
Shown are p19$^{-/-}$Nras control (Ctrl) and Trim33KO cells overexpressing E2F4 mutants. **A)** Schematic overview of cloned E2F4 mutants. E2F4 full length (FL), a mutant which cannot transcriptionally activate and bind partner proteins (ΔC), a mutant which cannot bind DNA (DB) and a mutant which cannot be ubiquitinated (KR). **B)** Western Blot analysis of E2F4 overexpressing cells. **C)** Crystal Violet staining and quantification of E2F4 overexpressing cells under normal growth conditions. **D)** Crystal Violet staining and quantification of E2F4 overexpressing cells after 24 h HU treatment (1 mM).

Furthermore, the KO of Trim33 led to increased fork rate in mCh expressing cells upon RS induction by HU treatment (Fig 9B), which was already seen in Figure 3C (middle panel). Expression of E2F4-FL and -KR in control cells mimicked the effect of the Trim33KO cells, while the expression of E2F4-ΔC and -DB decreased replication speed significantly (Fig 9B). The expression of E2F4-FL or -KR in Trim33KO cells did not significantly change the replication speed, while the expression of E2F4-ΔC and -DB decreased it (Fig 9A-B).

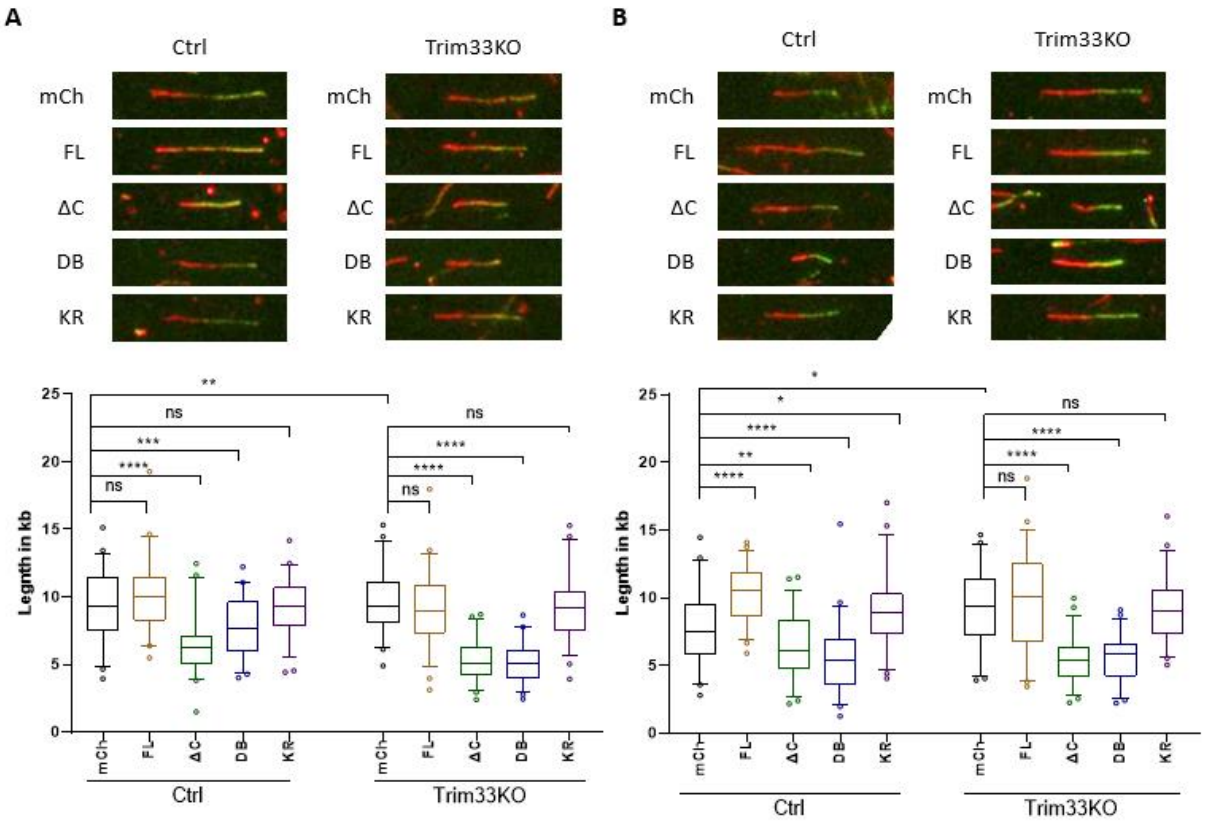

Figure 9: Replication analysis of E2F4 full length and mutant overexpressing Trim33KO cells.
Shown are p19$^{-/-}$Nras control (Ctrl) and Trim33KO cells overexpressing E2F4 mutants (FL/ΔC/DB/KR). **A)** Fiber assay of E2F4 overexpressing cells under normal growth conditions. **B)** Fiber assay of E2F4 overexpressing cells after 4 h HU treatment (1 mM).

All in all, I could demonstrate the E2F4 dependency of the mechanism. Additionally, I could show that E2F4 needs its C-terminus as well as its ability to bind to DNA to mediate the RS phenotype.

3.8 Overall E2F4 binding to chromatin is increased upon Trim33KO

The TF E2F4 is stabilized in Trim33KO cells (Fig 7E), hence it might be localized more efficiently on chromatin upon Trim33KO leading to the differential expression of target genes. To evaluate this hypothesis, I analyzed chromatin binding of E2F4 using ChIP-Seq. In this experiment, E2F4 was pulled down in crosslinked cells, before the proteins were digested and the remaining DNA pieces, which E2F4 was bound to, were sequenced (Fig 10A). As it is shown in Figure 10B, the overall binding of E2F4 to chromatin strongly increased upon Trim33KO. For example, the binding of E2F4 to the promoter of the Rnd1 gene increased strongly upon Trim33KO, while the mRNA expression of the gene was reduced (Fig 10C), in agreement with the canonical transcriptional-repressive function of E2F4 (Kent *et al*., 2019). However, some genes were bound stronger by E2F4, while their mRNA expression was enhanced as shown for claspin (Fig 10D). These results are corresponding with recent publications, in which the transcriptional-activating function of E2F4 is documented (Stracker *et al*., 2019). Many genes, whose mRNA was upregulated upon stronger binding of E2F4 in Trim33KO cells are directly involved in DNA replication, such as Mcm3 or Cdc6 (Fig 10E-F).

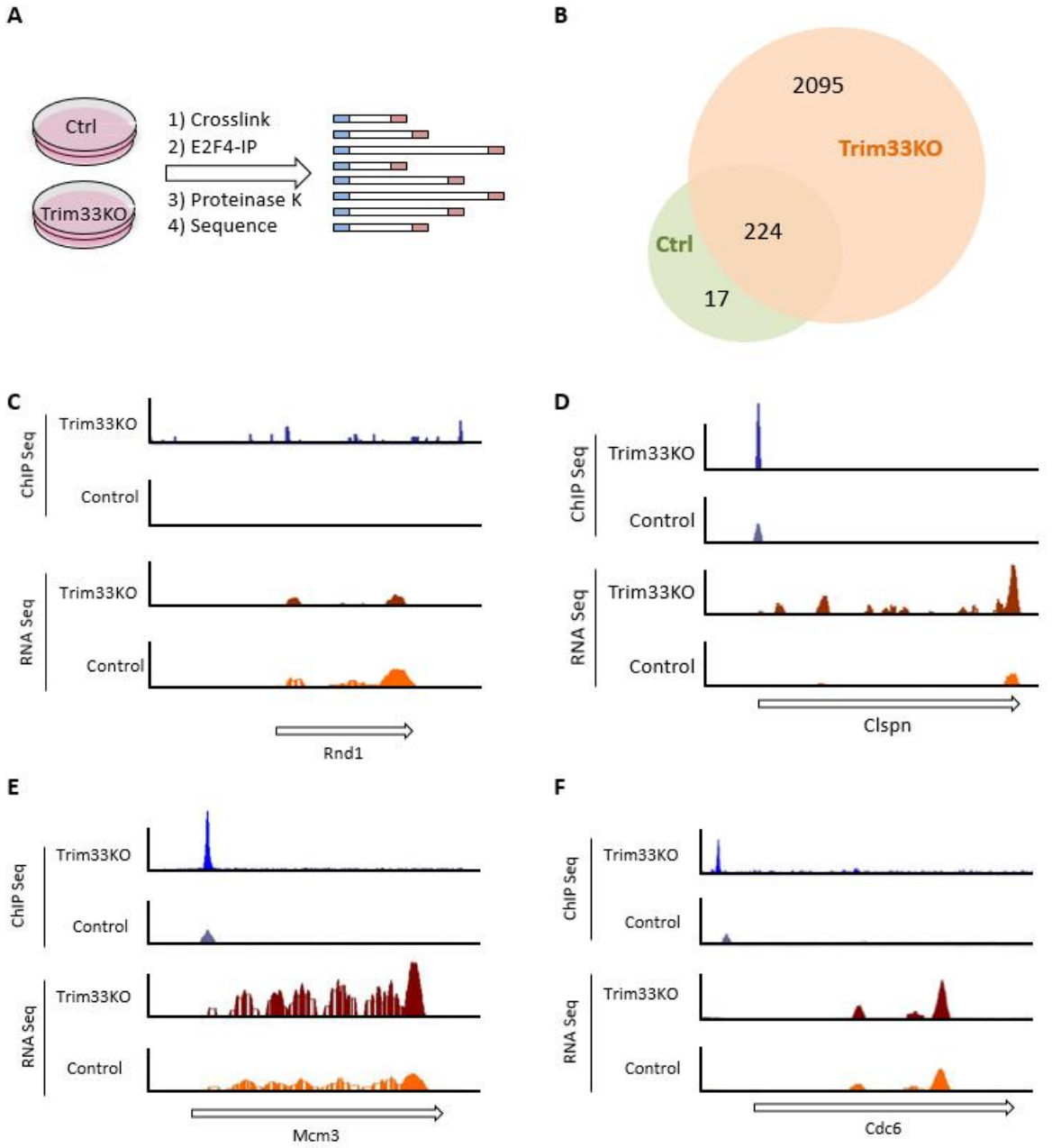

Figure 10: ChIP Seq analysis of E2F4 upon Trim33KO
A) Schematic overview of the performed ChIP Seq of E2F4 in p19$^{-/-}$Nras control (Ctrl) and Trim33KO cells. **B)** Overall binding of E2F4 to chromatin shown in a Venn Diagram. **C-F)** Example genes. Shown are peaks of the E2F4 ChIP Seq experiments as well as peaks of the RNA Seq analysis shown in Figure 6.

Summarizing, we could verify the hypothesis that E2F4 localizes more on chromatin upon Trim33KO. Furthermore, I observed that E2F4 might activate the transcription of DNA replication-related genes.

3.9 E2F4 is not upregulating DNA replication related genes on protein level

For efficient replication, Mcm complexes, which work as helicases, are being recruited to origins of replication (orc) by Cdc6 and Cdt1 (Fig 11A). The more Mcm complexes are recruited to chromatin, the more locations are available to initiate the replication process by binding of Cdc45 (Bell *et al*, 1992; Chem *et al*., 2007; Speck *et al*, 2005; Köhler *et al*, 2016). In the ChIP and RNA Seq experiments we observed that the genes of Mcm complex members as well as Cdc6 and Cdc45 were bound stronger by E2F4 and were transcriptionally upregulated in Trim33KO compared to control cells (Fig 10E-F). E2F4 might increase the transcription of these genes leading to more Mcm complexes localized on chromatin and hence giving cells more options to restart replication after RS. To investigate this hypothesis, I analyzed the protein levels and presence of the Mcm family members, as well as Cdc6 and Cdc45 on chromatin. However, the protein levels were either unchanged or downregulated upon Trim33KO (Fig 11B). Additionally, the amount of protein on chromatin (Chr) was downregulated or unchanged for the mentioned candidates as shown by fractionation assays (Fig 11C) as well as by PLA assays with Mcm2 and H3 antibodies (Fig 11D).

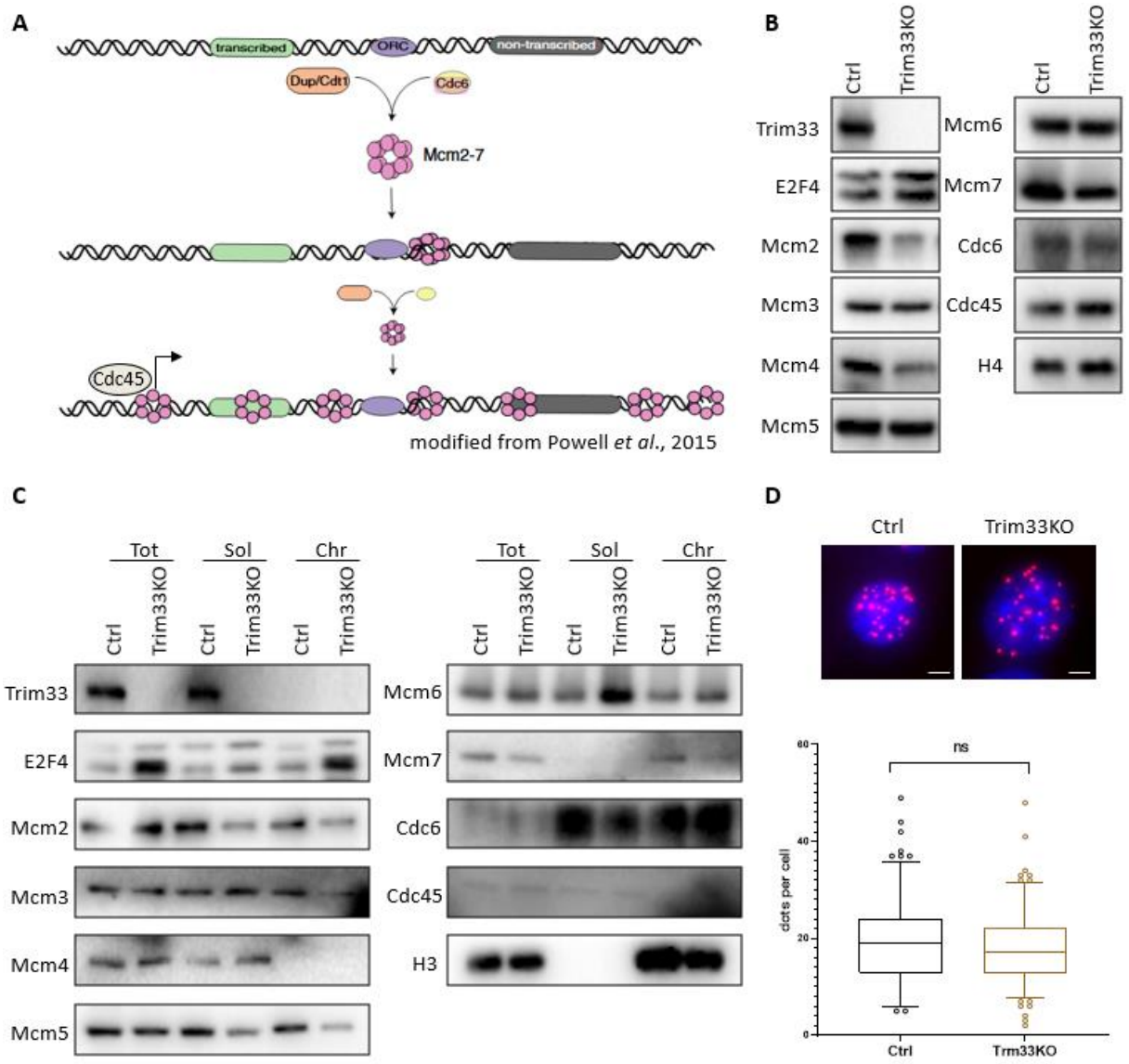

Figure 11: Protein levels and chromatin binding of candidates found in the ChIP Seq experiment
Shown are p19$^{-/-}$Nras control (Ctrl) and Trim33KO cells. **A)** Schematic overview of the replication initiation after Powell *et al.* 2015. **B)** Western Blot analysis of ChIP Seq candidates. **C)** Fractionation experiment of the ChIP-Seq candidates. Tot = total; Sol = soluble; Chr= chromatin fraction. **D)** PLA of Mcm2 and Histone H3 with representartve picturs. The scale bar corresponds to 2 µm.

Taken together, I could disprove the hypothesis that E2F4 might mediate the RS phenotype by enhancing the amount of Mcm complexes on chromatin.

3.10 E2F4 recruits RecQL to chromatin

As E2F4 function is known to be dependent on many interaction partners (Hsu *et al*., 2016), it might facilitate the RS phenotype by differentially binding to specific partners upon Trim33KO. To validate this hypothesis, I analyzed the interactome of E2F4 in Trim33KO and control cells (Fig 12A). For the proteomic analysis, E2F4 was pulled down under native conditions in Trim33KO as well as control cells and all co-precipitated proteins were subsequently analyzed by mass spectrometry. The experiment revealed several already known E2F4 interactors, which are components of the DREAM complex such as TFDP1, TFDP2, Rbl1, Rbl2, RBBP4, Lin9 and Lin54 (Hsu *et al*., 2016) (Fig 12B, light red). However, most of them showed no difference in binding E2F4 between Trim33KO and control cells. Looking at the candidates, which were bound stronger to E2F4 in Trim33KO cells compared to control cells, several proteins could be found, which are involved in DNA repair pathways or directly in the DNA replication (Fig 12B, dark red). The ones involved in repair pathways were on one hand ERCC4 (XPF), which forms a complex with ERRC1 involved in the nucleotide excision repair (Manandhar *et al*., 2015). On the other hand, SMARCB1 (Ini1) and SMARCE1, components of the Swi/Snf complex, were found. This nucleotide remodeling complex is involved in the DNA damage response (Ribeiro-Silva *et al*., 2019). However, the stronger interaction observed in the proteomic analysis of E2F4 to those two complexes could not be validated using PLA assays (Fig 12C). However, another candidate was the helicase RecQL, whose stronger interaction with E2F4 upon Trim33KO could be validated in PLA (Fig 12C).

RecQL is a helicase executing several functions during the replication process (Chen *et al*., 2013). It is known to bind origins of replication and promote the DNA replication (Lu *et al*., 2013; Thangavel *et al*., 2010). Additionally, RecQL has important roles under RS, as it accumulates on fragile sites on chromatin, which are at risk to collapse and generate a DSB, it stabilizes the according replication forks and it allows them to restart more efficiently after stress release (Qiu *et al.,* 2021; Viziteu *et al*., 2017 Bertie *et al*., 2013; Lu *et al*., 2013; Popuri *et al*., 2012). Moreover, RecQL was described to be involved in the repair of DSBs (Parvathaneni *et al*., 2013), as DNA damage and chromosomal instability accumulate upon its depletion (Mendoza-Maldonado *et al*., 2011; Bohr *et al*., 2008; Sharma and Stumpo *et al*., 2007; Viziteu *et al*., 2017; Popuri *et al*., 2012; Banerjee *et al*., 2015). Furthermore, cells with RecQL-depletion are described to possess enhanced sensitivities to different anti-cancer therapies targeting DNA as for example γ-radiation, HU, camptothecin or gemcitabine (Parvathaneni *et al*., 2019; Popuri *et al*., 2012; Sharma and Brosh, 2007). Finally, the RecQL gene is overexpressed or amplified in many different cancer types, for example in glioblastomas, ovarian cancer, head and neck squamous cell carcinoma, multiple myeloma, and HCC (Viziteu *et al*, 2017; Sanada *et al*., 2013; Arai *et al*., 2011; Matsushita *et al.,* 2011; Mendoza-Maldonado *et al*., 2011; Futami *et al*., 2010).

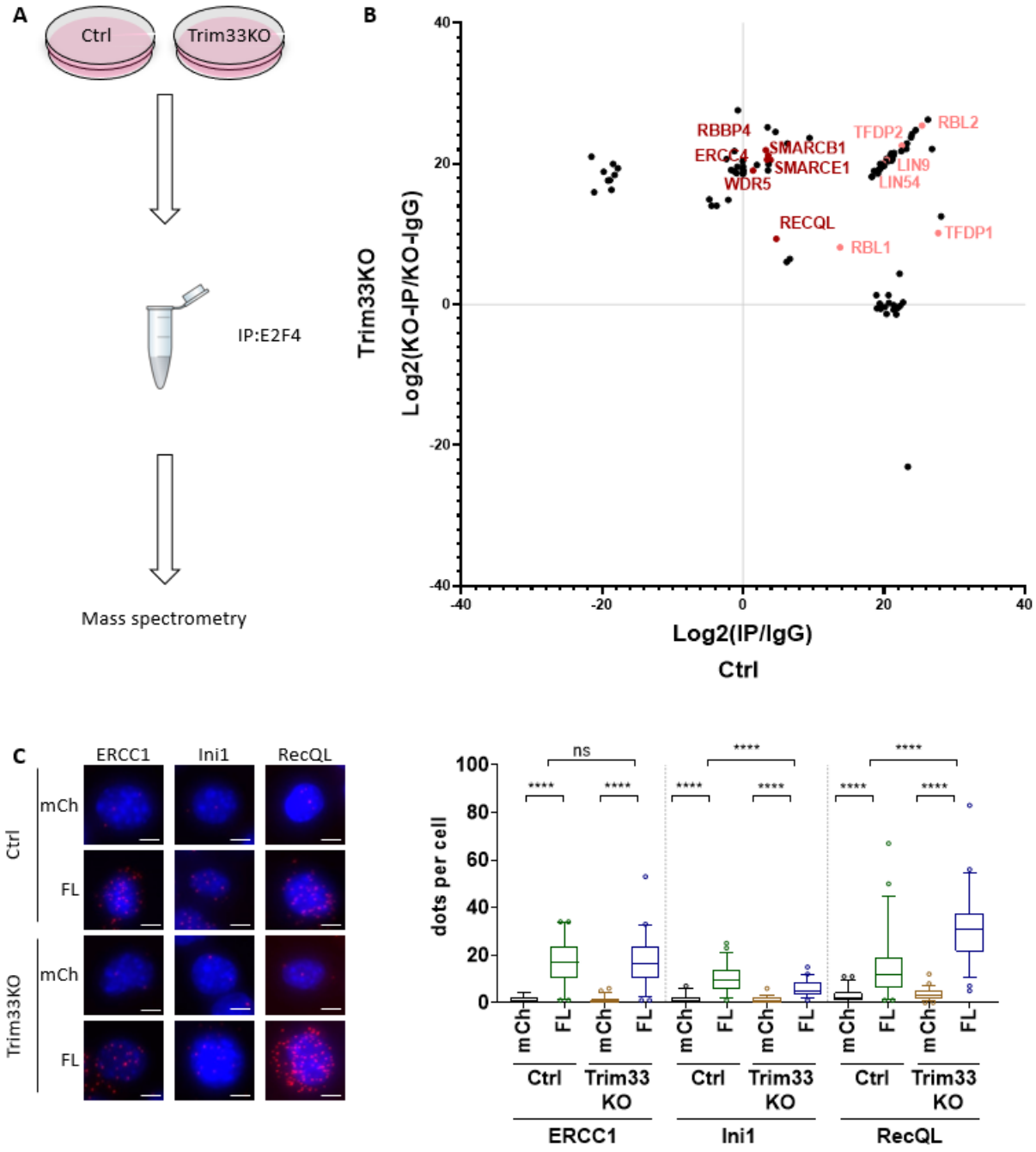

Figure 12: Proteomic analysis of E2F4 upon Trim33KO and its validation.
Shown are p19$^{-/-}$Nras control (Ctrl) and Trim33KO cells. **A)** Schematic overview of the performed mass spectrometry experiment. **B)** Results of the mass spectrometry experiment. Highlighted in light red are components of the DREAM complex; highlighted in dark red are proteins directly involved in DNA repair or DNA replication. **C)** PLA assays of E2F4 with ERCC1, Ini1 or RecQL with representative pictures. The scale bar corresponds to 2 µm.

E2F4 might mediate the RS phenotype by recruiting RecQL to chromatin where it stabilizes replication forks and helps to repair occurring DSBs. I tested this hypothesis first by analyzing RecQL binding to E2F4 mutants. RecQL could bind to E2F4-FL, E2F4-DB and E2F4-KR proteins while its binding to the E2F4-ΔC mutant was significantly decreased (Fig 13A). Additionally, I could show that RecQL binding to chromatin increased in control cells upon RS-induction by HU treatment, shown by a PLA assay with pH2AX and RecQL antibodies (Fig 13B). In Trim33KO cells on the other hand, the binding of RecQL to chromatin was already higher in unstressed cells compared to control cells and remained unchanged when cells were treated with HU (Fig 13B). Finally, fiber assays revealed that the effect of enhanced DNA replication upon RS exposure observed in Trim33KO cells compared to control cells (Fig 3C), could be mimicked by the overexpression of wildtype RecQL in control cells (RecQL). Expression of a RecQL mutant (K119A), which lacks helicase activity (Doherty *et al*., 2005), reduced the fork speed in control cells under exposure to RS. In Trim33KO cells, the expression of RecQL did not change the fork rate, while the expression of K119A significantly decreased it (Fig 13C).

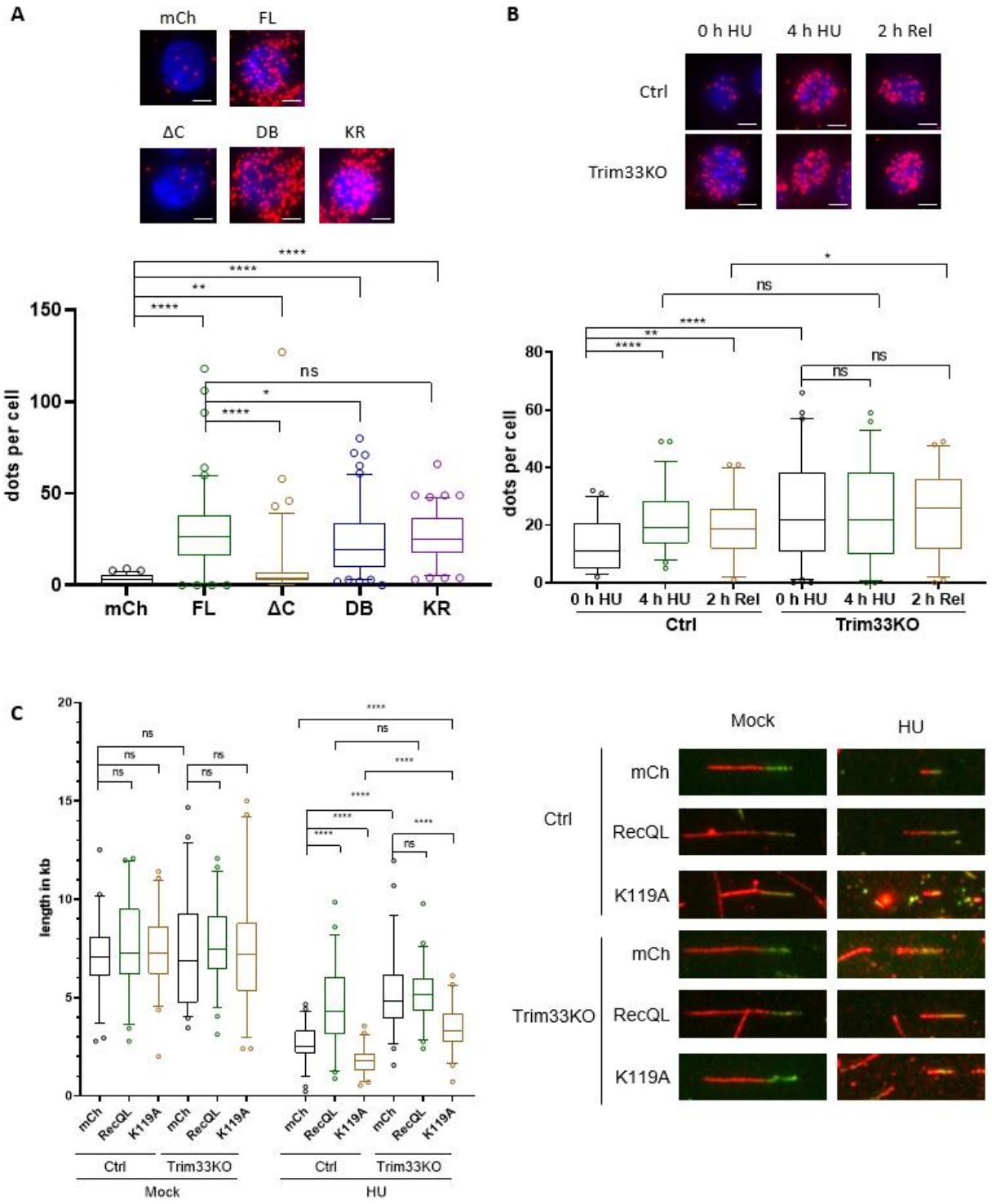

Figure 13: Binding analysis of RecQL.
A) PLA of RecQL and E2F4-FL or mutants (DB/ΔC/KR) in control cells with representative pictures. The scale bar corresponds to 2 µm. **B)** PLA of RecQL and pH2AX in cells treated for 4 h with 1 mM HU (4 h HU) and cells, which were released after the 4 h treatment (4 h) for 2 h in normal medium (2 h Rel) with representative pictures. The scale bar corresponds to 2 µm. **C)** Fiber assay of RecQL overexpressing p19$^{-/-}$Nras control (Ctrl) and Trim33KO cells under normal growth conditions (Mock) and after 4 h HU treatment (1 mM).

Taken together, I could show that the binding of E2F4 to RecQL is increased as well as RecQL binding to chromatin is enhanced upon Trim33KO. Additionally, the replication fork phenotype seen in Trim33KO cells upon RS can be mimicked by RecQL overexpression, strongly suggesting the RecQL-dependency of the mechanism.

4 Discussion

Cancer is one of the most severe and frequent diseases worldwide as every third person develops it in their life and due to insufficient treatment options, it causes millions of deaths annually (Pucci *et al*., 2019; Charkraborty *et al*., 2012). This is due to the fact that tumors are very heterogenic and show a huge complexity of altered genes, keeping reliable treatment options rare. Additionally, they develop drug resistances, which makes it a big task to develop novel therapeutic strategies (Zugazagoitia *et al*., 2016; Charkraborty *et al*., 2012). One gene, which is altered in nearly all human tumors and has been the focus of studies for several decades is the master TF Myc (Wang *et al*., 2021; Dang *et al*., 2012).

Myc is known to regulate growth as well as metastasis and drug resistance development of multiple tumors (Allen-Petersen *et al*., 2019; Chen *et al*., 2018). Targeting Myc with small molecule inhibitors would be a very promising strategy to treat cancer patients. However, Myc is known to have a mainly unstructured surface and it is considered to be a disordered protein, raising several structural and functional difficulties in the attempt to develop such inhibitors (Madden *et al*., 2019). Typically, enzymatic or defined binding pockets are targeted by small molecule inhibitors. Myc lacks this kind of pockets and is additionally localized in the nucleus making it not easily accessible (Madden *et al*., 2019). Hence, different strategies to indirectly interfere with Myc function were developed (Allen-Petersen *et al*., 2019; Chen *et al*., 2018; Dang *et al*., 2012).

One such strategy is to inhibit its expression by stabilizing transcriptional repressors or targeting proteins, which activate its expression. Another alternative approach to regulate Myc function is to inhibit its interaction with important partner proteins, such as MAX, which are necessary for Myc to execute its functions. In addition, targeting Myc-mediated downstream processes is considered to be a promising strategy. For example, when Myc is inducing growth factors, which lead to enhanced proliferation of the tumor, these factors could be targeted. Finally, the manipulation of proteins, which are involved in the post-translational regulation of Myc, such as members of the ubiquitin system, is considered as a good way to indirectly regulate Myc (Allen-Petersen *et al*., 2019; Chen *et al*., 2018; Dang *et al*., 2012).

Previous work of our group focused on the identification of novel proteins, which regulate Myc function, namely Myc-induced apoptosis (Popov *et al*., 2007). The experiments revealed the ubiquitin E3 ligase Trim33 as one of the top hits in regulating Myc-induced apoptosis (Fig 1A-C). Trim33 is a known ubiquitin E3 ligase, hence it is adding ubiquitin proteins to substrates, marking them for proteasome-dependent degradation (McAvera *et al*., 2020). This post-translational modification is mediated by an enzymatic cascade, in which the E3 enzyme executes the last step of ligating the ubiquitin protein to the substrate (Zheng *et al*., 2017; Scheffner *et al*., 1995). To perform this function, the E3 enzyme has to directly bind to the according substrate.

Interestingly, an interactome study found that Trim33 binds to Myc (Kalkat *et al*., 2018), suggesting that Myc might be a substrate of Trim33. During this study, my first aim was to investigate if Trim33 is regulating Myc function by limiting its protein levels due to ubiquitination and followed proteasome-dependent degradation. I could show that Myc is not ubiquitinated by Trim33 and its stability is not enhanced in Trim33KO cells (Fig 1D-E). Hence, Myc is not a Trim33 substrate in murine liver cancer cells ($p19^{-/-}$Nras) and Trim33 does not regulate Myc-induced apoptosis by destabilizing the protein, but rather indirectly. As the interactome study, in which Trim33 was found to bind to Myc, was performed in human fetal kidney cells and the experiments of this thesis were performed in murine liver cancer cells, I suggest tissue specific differences. To clarify this facet of the project, Myc stability upon Trim33KO should be analyzed in several different tissues.

The theory that Trim33 is regulating Myc indirectly is consistent with published data about other Trim family members, such as Trim11, Trim15, Trim26, Trim44 and Trim59, which were all shown to not directly, but indirectly regulate Myc levels. Their overexpression led to increased expression of β-Catenin, which is regulating numerous basic cellular processes, such as proliferation, migration or invasion of cells, through its high number of downstream targets, such as Myc (Harb *et al*., 2019; Wang *et al*., 2018; Rennoll *et al*., 2015). The increased expression of β-Catenin thereby leads to enhanced Myc protein levels. In agreement with these known functions of β-Catenin signaling, the overexpression of the mentioned Trim proteins increased proliferation, migration and invasion of different types of cancer cells (Lan *et al*., 2021; Xie *et al*., 2021; Zhang *et al*., 2021; Chen, Chen, Ye *et al*., 2019; Zhou *et al*., 2017).

I investigated in this thesis, if Trim33 indirectly manipulates Myc function by influencing signaling pathways, which are involved in basic cellular functions. In line with this hypothesis, Trim33 is known to influence two major pathways regulating these basic processes, the Wnt and the TGFβ signaling. The main mediator of the Wnt signaling is considered to be β-Catenin while Smad proteins are considered to be the main mediators of the TGFβ signaling (He *et al*., 2019; Seoane *et al*., 2017). Smad4 as well as β-Catenin are both known Trim33 substrates showing the direct influence of Trim33 on both pathways (Xue *et al*., 2015; Dupont *et al*., 2005). In line with this, I investigated if Trim33 can influence basic cellular functions via one of these pathways, and if Trim33KO cells thereby possess a general survival benefit. Myc-induced apoptosis could be less severe in cells, which provide a general survival benefit. However, I could not detect any difference in growth, migration or invasion of Trim33KO cells compared to control cells (Fig 2). These results indicate that Trim33 is not regulating Myc function by inducing the proliferation or aggressiveness of cells.

At first glance, these results contradict the published data shown for other Trim proteins, which indirectly regulate Myc by increasing its expression through the Wnt signaling. Here, I show

that Trim33 is not regulating Myc function by manipulating its protein levels as other Trim proteins do. Additionally, it was shown that the KD of Trim33 leads to spontaneous hepatocarcinogenesis. Hence, Trim33 has an obvious effect on the growth of liver cancer cells, contradicting the experiments performed (Herquel *et al.*, 2011). However, it was further shown that Trim33 only promotes the proliferation of HCC in early stage liver cancer (Ding *et al*., 2014). In advanced stages, Trim33 is not involved in the growth of cells anymore and the reduced expression of Trim33 in HCC correlates with poor prognosis (Ding *et al*., 2014). To understand if Trim33 has different functions in early and late stages of HCC, Trim33 should be knocked out in cell lines derived from different stages of HCC in further experiments and possible differences should be compared. However, in reality, liver cancer is mainly diagnosed in late stages, which makes it more promising to investigate the mechanisms of advanced liver cancer cells for developing novel therapeutic strategies (Yang *et al*., 2019). The experiments shown in this thesis were performed in cells derived from late stage HCC. Hence, the published data support the finding that Trim33KO does not influence the growth of cells and is thereby not giving cells a general survival benefit by increasing the proliferation of aggressiveness of cells.

To understand how else Trim33 can influence Myc-induced apoptosis, I investigated through what kind of mechanisms Myc can induce cell death. One widely accepted and well-studied theory is that the Myc protein manipulates the expression of members of the BCL2 or p53 signaling pathways. Both are pathways, which regulate the pro-survival or pro-apoptotic signaling in cells (Aubrey *et al*., 2018; Siddiqui *et al*., 2015; McMahon 2014; Levine *et al*., 2009). The p53/Arf signaling can indirectly be manipulated by Myc as it enhances the expression of the upstream regulator protein Arf, leading to repression of p53 (Yu *et al*., 2019; Hoffman *et al*., 2008). Myc can interfere with the BCL2 signaling by inducing the expression of pro-apoptotic members, such as BIM, Bax or Bak, as well as by inhibiting the expression of anti-apoptotic proteins, such as Bcl-2 or Bcl-xl (Opferman *et al.*, 2018; McMahon 2014; Muthalagu *et al*., 2014; Westphal *et al*., 2014; Hoffman *et al*., 2008; Jiang *et al*., 2007). However, another broadly accepted theory is that Myc induces apoptosis by enhancing overall replication, RS and DSBs, which finally leads to the activation of pathways inducing programmed cell death, namely the apoptosis (Chen *et al*., 2018; Zheng *et al*., 2017; Gabay *et al*., 2014).

RS occurs when cancer cells are not able to perform efficient DNA replication, which is required to maintain genome stability. If this process is in some way defective, DNA damage will occur, which is normally either repaired or leads to the induction of apoptosis (Curti *et al*., 2021). RS can be induced by several sources which interfere with normal replication, such as inadequate firing of origins of replication, increased number of reactive oxygen species (ROS), a lack of dNTPs, accumulation of DNA damage or uncontrolled proliferation (Primo *et al*., 2019).

Myc was shown to play a role in each of the above-mentioned replication errors. For instance, Myc binds to origins of replication and modulates their activity (Curti *et al*., 2021; Chen *et al*., 2018; Srinivasan *et al*., 2013). For example, in *Xenopus laevis* extracts the depletion of Myc leads to a strong decrease in active replicons (Dominguez-Sola *et al*., 2007). Moreover, it is well-known that Myc can induce ROS, which in turn can create RS and DNA damage (Curti *et al*., 2021; Zheng *et al*., 2017; Rohban *et al*., 2015). Furthermore, Myc regulates the expression of nearly all genes, which are involved in the biosynthesis of dNTPs (Curti *et al.*, 2021). A lack of dNTPs leads to RS as replication forks stall and hence are at higher risk to collapse and generate DNA damage (Primo *et al*., 2019). Additionally, Myc is well-known to induce DNA damage, as the levels of DNA damage markers increase when Myc is overexpressed (Zheng *et al*., 2017; Rohban *et al*., 2015; Dominguez-Sola *et al*, 2013; Srinivasan *et al*., 2013). Recent publications suggest that Myc induces DSBs by inducing overall origin firing and subsequent RS resulting in DNA damage (Rohban *et al*., 2015; Dominguez-Sola *et al*., 2013; Srinivasan *et al*., 2013). For example, the elevated levels of the DSB marker pH2AX could only be observed in replicating cells and not in cells where the DNA synthesis was blocked by geminin (Dominguez-Sola *et al*., 2013). These results suggest that the induction of DNA damage by Myc is replication dependent. Finally, Myc strongly enhances the proliferation of cells increasing the risk of RS, as replication errors accumulate as well as the DNA repair gets inefficient (Zheng *et al*., 2017; Karlsson *et al*., 2003). For example, the overexpression of Myc in hepatocytes showed a 50 % higher proliferation rate compared to control cells (Zheng *et al*., 2017; Muakkassah-Kelly *et al*., 1988). Taken together, there are numerous ways how Myc induces RS, leading to genome instability, which is a known hallmark of cancer (Curti *et al*, 2021) and can possibly induce tumor development. Hence, enhancing the RS in Myc-driven tumors could be a promising therapeutic strategy.

In this thesis, I wanted to understand if Trim33 has an effect on the Myc-induced RS. Indeed, I could show that Trim33KO cells could replicate DNA more efficiently, reenter cell cycle faster and show increased proliferation after the induction of RS by Myc overexpression (Fig3-4). These data suggest that the replication forks are either more stable or freshly assembled more efficiently after RS, leading to simplified replication and subsequent proliferation. The same effects could be seen when RS was induced by HU or Etop treatment (Fig 3-4) (Gómez-Herreros 2019; Liew *et al*., 2016, Koç *et al*., 2004; Burden *et al* 1998). Hence, Trim33 does not only simplify the handling of Myc-induced RS, but also of chemically-induced RS. These results strongly suggest that Trim33 is regulating the Myc-induced apoptosis by helping cells to deal with RS. Hence, Trim33 possesses a broader function then expected. Not only is it important for Myc-induced apoptosis, but in general for cells exposed to RS. As RS leads to genome instability, which is a hallmark of cancer (Curti *et al*., 2021), the stabilization of Trim33 might be an important therapeutic strategy in numerous cancer types.

Cells exposed to RS will primarily pause their replication by stalling replication forks. If these forks cannot be stabilized enough and the RS holds on, the replication forks will collapse. This leads to incomplete replication and to generation of DNA damage, such as DSBs (Primo *et al*., 2019; Alexander *et al*., 2016; Cortez *et al*., 2016). DSBs are marked by a specific protein, pH2AX. The H2AX histone is generally important for the stabilization of DNA and only gets phosphorylated upon DSBs (Stope *et al*., 2021). The phosphorylation at serine 139 is the initial signal to identify DSBs in a range of up to 1.7 mega base pairs around the break (Stope *et al*., 2021; Collins *et al*., 2020). Subsequently, pH2AX recruits other factors to start the repair pathway, such as checkpoint and repair proteins (Stope *et al*., 2021; Collins *et al*., 2020; Podhrecka *et al*., 2010). Cells exposed to RS will accumulate collapsed replication forks and hence have enhanced numbers of DSBs.

As Trim33KO cells can replicate more efficiently upon RS, I hypothezied that these cells may also accumulate less DSBs. The analysis of pH2AX in Trim33KO cells revealed that they indeed induce the phosphorylation of H2AX later and additionally release pH2AX levels more efficiently after release from RS compared to control cells (Fig 5). These data are in line with the hypothesis that Trim33KO cells may have more stable replication forks. Stabilized replication forks would collapse less or later and lead to less DSBs. Additionally, the faster release of pH2AX levels suggests that occurring DSBs are repaired more efficiently in Trim33KO cells compared to control cells (Fig 5C-D). The detection of DSBs by a cell can be the first step in initiating the programmed cell death. Hence, the result that Trim33KO cells have less DSBs and repair occurring breaks faster, corresponds with a reduced induction of apoptosis upon RS.

As apoptosis is mostly repressed in tumor cells, either through genetic alterations or development of drug resistances, most cancer therapies include the activation of an apoptotic pathway to induce the elimination of the tumor cells (Pfeffer *et al*., 2018; Bold *et al*., 1997). Numerous signaling pathways can initiate the controlled cell death, which can be triggered by different stress signals such as DNA damage or RS (Carneiro *e al*., 2020; Bold *et al*., 1997). In most cancer cells, cellular checkpoints are deregulated and cells accumulate RS. Hence, making tumor cells more sensitive to RS is a very promising strategy for cancer treatment (Zhu *et al*., 2020; Ubhi *et al*., 2019; Zhang *et al*., 2016). Our data suggest that enhancing the stability of Trim33 can sensitize tumor cells to controlled cell death. This could be a general mechanism of Trim33 and the therapeutic potential would thereby not be limited to liver cancer or Myc overexpressing tumors, but could additionally be applied in numerous other types of tumors. To validate this hypothesis, the Trim33 effect upon RS should be analyzed in several different tumor entities in further experiments.

Collectively, I could demonstrate that Trim33 influences the effects of RS in cells, perhaps by stabilizing replication forks. Subsequently, the second aim of this thesis was to investigate how

Trim33 can provide the reduced sensitivity against RS. Hence, an RNA Sequencing analysis was performed to identify differentially expressed genes upon Trim33KO, which might be able to mediate the RS phenotype. The experiment revealed that the most deregulated pathways were DNA replication, Rb genes in cancer and cell cycle upon Trim33KO (Fig 6A-B). These Data are consistent with the already shown data that Trim33KO cells can replicate and grow better under RS (Fig 3-4). Additionally, the target genes of E2F4 are upregulated in Trim33KO cells compared to control cells (Fig 6C).

E2F4 is a well-known TF whose canonical function is to transcriptionally repress the expression of cell cycle genes during the G0/1 phase (Chen *et al*., 2009; Attwooll *et al*., 2004). However, E2F4 was as well described to have pro-proliferative and transcription-activating functions (Zhen *et al*., 2019; Kim *et al*., 2018; Hsu *et al*., 2016). A pro-proliferative effect can for example be seen in a study showing that E2F4 induces the tumor development of Myc-induced lymphomagenesis (Rempel *et al*., 2009). Additionally, its abnormal expression is correlated with Myc overexpression in squamous cell carcinoma as well as the survival of patients with overexpressed Myc reduced from 7.5 months to 1 month if they have additional altered E2F4 (Dai *et al*., 2019). It was already shown for E2F1, which generally has opposing functions to E2F4 (Kent *et al*., 2019), that it enhances the ability of Myc to induce apoptosis (Leone *et al*., 2001). Finally, human cancer cells overexpressing Myc significantly induced apoptosis stronger when a constitutively active pRb protein was expressed (Santoni-Rugiu *et al*., 2002). pRB blocks the transcription activation domain of activator E2Fs, such as E2F1, and meanwhile translocates typical repressor E2Fs, such as E2F4, to the nucleus where it can execute its different functions (Kent *et al*., 2019). These data suggest that high E2F4 expression might reduce the sensitivity of cells to Myc induced apoptosis. Not only is E2F4 linked to pro-proliferative functions and to Myc, but as well to apoptosis. For instance, it was described that E2F4 can reduce hypoxia-induced apoptosis in ventricular cardiomyocytes (Dingar *et al*., 2012). Furthermore, the KD of E2F4 leads to enhanced sensitivity against apoptosis-inducing drugs in several human cancer cells as well as E2F4 deficient mice show an increased number of apoptotic cells (Rempel *et al*., 2009; Ma *et al*., 2004). These data demonstrate a function of E2F4 in proliferation, in Myc function as well as in apoptosis.
I demonstrated that Trim33KO cells are less sensitive to Myc-induced RS and followed apoptosis by possibly stabilizing replication forks. Additionally, I showed enhanced expression of E2F4 target genes upon Trim33KO, which is known to be important for Myc function as well as for apoptosis. All in all, this suggests a E2F4 dependency of the mechanism.

During this thesis I could show that E2F4 indeed is a novel substrate of the ubiquitin E3 ligase Trim33, being ubiquitinated and thereby marked for proteasome-dependent degradation by Trim33 (Fig 7A-E). Additionally, the overexpression of E2F4-FL protein in control cells mimicked the effects seen in Trim33KO cells to replicate DNA more efficiently and proliferate

faster after the induction of RS (Fig 8-9). These data demonstrate that the RS phenotype observed upon Trim33KO is E2F4 dependent. Hence, upon Trim33KO, E2F4 protein is stabilized and its increased levels mediate the simplified replication as well as proliferation after RS exposure. Furthermore, to investigate which domains of E2F4 are necessary to mediate the RS phenotype, I analyzed different E2F4 mutants. I could demonstrate that the C-terminus of E2F4 as well as its DNA binding domain are indispensable to mediate the reduced sensitivity against RS (Fig 8-9). As E2F4 needs to bind to DNA to execute its transcription-repressive or -activating functions, I hypothesized that target genes of E2F4 might execute the effects of reduced sensitivity against RS or directly stabilize replication forks.

Hence, I subsequently analyzed the chromatin binding of E2F4 in Trim33KO and control cells. We could show by a ChIP-Seq experiment that the overall E2F4 binding to chromatin increased significantly upon Trim33KO (Fig 10B). These results are consistent with the fact that E2F4 is stabilized and its levels are strongly increased in Trim33KO cells (Fig 7E; 11B). Moreover, E2F4 binding was increased at several promoters and the transcription of the according gene was enhanced, in agreement with recent publications suggesting transcriptional-activating functions of E2F4 (Hsu *et al.*, 2019; Fig 10D). Many of these upregulated genes in our analysis are involved in the DNA replication, such as members of the Mcm complex or Cdcs. During the replication process, Mcm complexes are recruited to chromatin and start replication when initiated, while Cdcs finetune this process (Bell *et al*, 1992; Chem *et al*., 2007; Speck *et al*, 2005; Köhler *et al*, 2016). The more Mcm complexes are bound to chromatin, the more efficient is the restart of replication after the induction of RS. Summarizing, if more Mcm complexes are localized on chromatin in Trim33KO cells, this could make cells less sensitive against RS.

Interestingly, E2F proteins were already described to regulate the expression of replication dependent genes (Bracken *et al*., 2004; Ohtani *et al*., 1999). For example, E2Fs are shown to regulate the expression of all Mcm complex members (Mcm2-7) (Bracken *et al*., 2004; Polager *et al*., 2002; Leone *et al*., 1999; Othani *et al*., 1999). Furthermore, the expression of Cdc6 and Cdc45 are shown to be highly E2F dependent (Bracken *et al*., 2004; Polager *et al*., 2002; Hateboer *et al*., 1998; Leone *et al*., 1998; Yan *et al*., 1998). However, the experiments performed during this study clearly showed that although the mRNA expression of these proteins is slightly upregulated, the protein levels and their presence on chromatin remained unchanged upon Trim33KO (Fig 11). These data suggest that the RS phenotype, which E2F4 mediates, is not executed by transcriptionally enhancing the expression of replication-dependent genes. During this thesis, all promising genes at whose promoter E2F4 binding was increased were analyzed. However, unobvious candidates also have the potential to be involved in the mechanism. To get certitude about this facet of the project, a whole genome library of sgRNAs should be cloned for all differentially bound genes upon Trim33KO

in further experiments. Screening cells which were infected with this library for their sensitivity against RS could identify additional possible candidates.

Anyhow, it was previously described that E2F4 has additional non-transcriptional functions, such as recruiting different proteins to chromatin where they can execute their functions. For example, it was shown that Multicilin and Gemc1, which both lack a DNA binding site, are dependent on E2f4 or E2F5 to be recruited to chromatin where they in turn activate the transcription of target genes (Kim *et al*., 2018; Ma *et al*., 2014). This recruiting function was as well described for E2F1. For example, it was shown to recruit the pontin/reptin ATPase complex to DNA, opening the chromatin structure and to recruit the histone acetyl transferase Tip60, modifying histones (Tarangelo *et al*., 2015; Taubert *et al*., 2004). Finally, repressor E2Fs were described to recruit the corepressor mSin3B to chromatin, which in turn can execute its functions (Rayman *et al*., 2002). All in all, E2F4 seems to have important protein recruiting functions. Hence, I investigated if E2F4 differentially binds to a partner protein upon Trim33 and thereby facilitates the RS phenotype.

I performed a proteomic analysis of E2F4 in Trim33KO and control cells (Fig 12). The experiment revealed members of two pathways well described to be involved in the DNA repair to be bound stronger to E2F4 in Trim33KO cells compared to control cells. The ERCC1/XPF complex, which is important for the nucleotide excision repair as well as the nucleotide remodeling complex Swi/Snf, which is important for the DNA damage response (Ribeiro-Silva *et al*., 2019; Manandhar *et al*., 2015) were found. Both complexes could help repair occurring DNA damage faster, thereby stabilizing the genome and making cells less sensitive to RS. However, the stronger binding to E2F4 upon Trim33KO observed in the mass spectrometry experiment, could not be validated using PLA assays (Fig 12 C). Additionally, the helicase RecQL was found to bind stronger to E2F4 upon Trim33KO while this result could be verified by PLA assays (Fig 12C). E2F4 might recruit RecQL to chromatin allowing it to execute its functions.

RecQL is a very promising candidate as it could strongly simplify the handling of RS for cells. It stabilizes unstable sites on chromatin and stalled replication forks. Hence, the fork collapse is significantly delayed, allowing cells to withstand RS and restart replication more efficiently (Qiu *et al.,* 2021; Viziteu *et al*., 2017 Bertie *et al*., 2013; Lu *et al*., 2013; Popuri *et al*., 2012). Additionally, it is known that DNA damage and chromosomal instability accumulate strongly in RecQL depleted cells, demonstrating its role in the repair of DSBs (Parvathaneni *et al*., 2013; Mendoza-Maldonado *et al*., 2011; Bohr *et al*., 2008; Sharma and Stumpo *et al*., 2007; Viziteu *et al*., 2017; Popuri *et al*., 2012; Banerjee *et al*., 2015). Furthermore, the depletion of RecQL was already shown to enhance the sensitivity against HU (Popuri *et al*., 2012) and to be overexpressed in HCC (Futami *et al*., 2010). Taken together, if E2F4 recruits RecQL more efficiently to chromatin upon Trim33KO, it would be able to simplify the handling of RS for cells

massively. Hence, the stabilization of Trim33 would be a promising therapeutic strategy, as it would destabilize E2F4, leading to less RecQL localized on chromatin and making cells more sensitive to RS-induced apoptosis, including Myc-induced apoptosis.

To investigate this hypothesis, I analyzed RecQL in more detail. Not only could I show that E2F4 bound stronger to chromatin (Fig 10B), also the binding of RecQL to chromatin was enhanced upon Trim33KO (Fig13B). These results are in line with the theory that E2F4 is recruiting RecQL to chromatin. Additionally, only E2F4-FL, E2F4-DB and E2F4-KR proteins were able to bind to RecQL, while E2F4- ΔC could not (Fig 13A). E2F4-FL and E2F4-KR can mimic the effect of Trim33KO cells when overexpressed in control cells (Fig 3-4). As they can also bind to RecQL (Fig 13A), these data support the model of E2F4 recruiting RecQL to chromatin. Furthermore, the fact that the E2F4-DB mutant, which is not able to bind to DNA and cannot mimic the effect (Fig 3-4), perfectly supports the model. Even though it can bind to RecQL (Fig 13A), it cannot bind to DNA, hence it cannot recruit RecQL to chromatin. Moreover, the E2F4-ΔC mutant cannot mediate the phenotype (Fig 3-4). This mutant lacks the transcription-activating domain as well as a part of the protein, which is important for partner protein binding (Liban *et al*., 2016; Morgunova *et al*., 2015; Xanthoulis *et al*., 2013; Balog *et al*., 2011; Tsantoulis *et al*., 2005; Ginsberg *et al*., 1994). The need of the C-terminus for partner protein binding is in line with the finding that RecQL cannot bind to this protein (Fig13A). Due to the missing interaction between RecQL and E2F4- ΔC, it cannot be recruited to chromatin and hence, E2F4-ΔC cannot mediate the RS phenotype. To better understand this facet of the project, a crystal structure analysis of E2F4 bound to RecQL could be performed in further studies. Subsequently, several more point mutations should be performed within the C-terminus to narrow down the exact site of interaction. Additionally, ChIP-Seq experiments should be performed in further experiments to identify shared E2F4 and RecQL binding sites on chromatin upon Trim33KO.

For subsequent analysis, I expressed wildtype and a mutant (K119A) RecQL, which lacks its helicase activity (Doherty *et al*., 2005), in Trim33KO and control cells. The overexpression of wildtype RecQL (RecQL) in control cells could mimic the enhanced fork rate seen in Trim33KO cells (Fig 13C), demonstrating the RecQL-dependancy of the mechanism. The K119A mutant decreased fork rates in control as well as in Trim33KO cells (Fig 13C). The helicase activity of RecQL is hence indispensable to facilitate the RS phenotype seen upon Trim33KO. All of these data strongly suggest that E2F4 recruits RecQL to chromatin, where it in turn stabilizes replication forks as well as initiates DSB repair, giving cells a general survival benefit against RS (Fig 14). To get certitude about this facet of the Trim33-E2F4-RecQL project, shRNA mediated KDs of RecQL should be performed in Trim33KO cells in further analysis. However, many more candidates were found in the proteomic analysis, which were not analyzed yet. All

of these candidates should be cloned in a sgRNA library and screened for their ability to reduce sensitivity against RS in further studies.

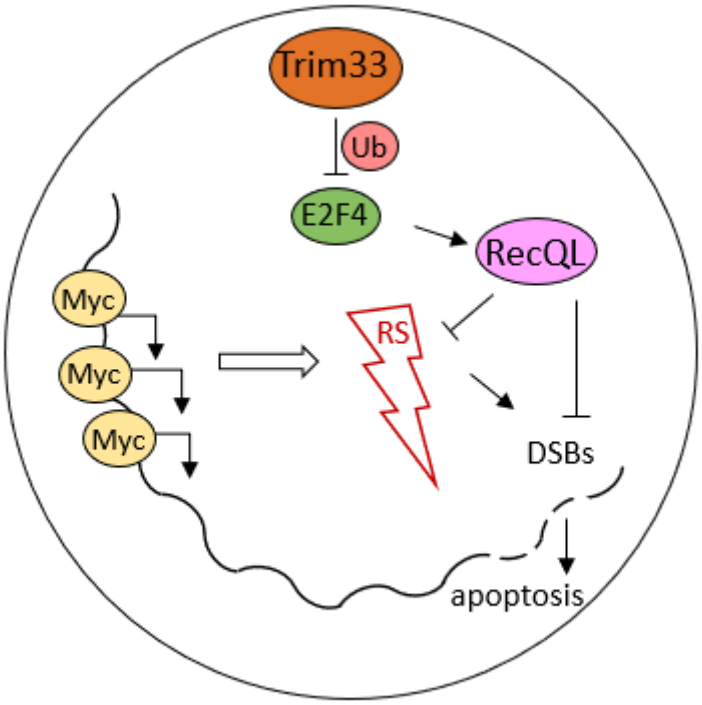

Figure 14: Suggested model of how Trim33 can provide cells a general survival benefit under RS
In Trim33KO cells, E2F4 is not ubiquitinated by Trim33 and its protein levels are accumulating. Subsequently, it is recruiting RecQL to chromatin, which in turn stabilizes replication forks, delays the induction of DSBs and helps repair occurring DNA damage.

Finally, Trim33 function on RS should be further analyzed *in vivo* to understand if novel putative curative therapeutic strategies require stabilization of Trim33. *In vivo* experiments were already started during this thesis and are still ongoing.

5 Acknowledges

First of all, I want to thank Prof. Dr. Nikita Popov for the opportunity to work on this interesting project. His constant guidance and advice were essential for my work. I will miss our scientific discussions and am very glad for all the skills Nikita was teaching me over the years, thank you.

Further, I would like to express my gratitude and appreciation for the support of Prof. Dr. Tassula Proikas-Cezanne. Thank you for being a great primary supervisor. I thank Prof. Dr. Jennifer Ewald and Prof. Dr. Boris Maček for being members of my thesis committee and thereby giving me the opportunity to present and discuss my thesis.

Without the members of AG Popov, AG Zender, AG Leibold, AG Feucht and AG Dauch Iabs I would have not made it. Thank you all for your continuous technical support and good working atmosphere. Especially, I have to thank Ravi Babu Kollampally, Stefan Zwirner, Melanie Henning and Aylin Heinrich for all the fruitful discussions, for their patients and their friendship.

Finally, I have to thank my family and friends. Particularly, my parents Andrea Rousseau with her boyfriend Kurt(i) Sonntag and Thierry Rousseau with his wife Mirela Pietrar were always supporting me when the stress threatened to overwhelm me. Thank you for all the long phone calls and the always opened doors. Additionally, I have to thank my grandparents Gerda and Horst Eberle who were always ready to raise my mood with great food and a round of “Mensch-ärgere-dich-nicht!”. I am thanking my big brother Fabian and his daughter Luna Rousseau who always gave me the feeling of being a careless child again. I really enjoyed all the great holidays we spent with each other. My little brother Marcel and his wife Jasmin Pause were helping me a lot with delicious food and formatting guidance, thank you. I am thankful for the many evenings with romanian liquor and card games I spent with my newest brothers Richard and Ticyan Igaz. Most importantly, I have to thank my boyfriend Marc Votteler for listening to all my fears and to always calm me down as well as showing me how great and easy life can be, thank you. The whole family Votteler was irreplaceable as well, inviting me to all their family parties and taking me up in their family in a very friendly and uncomplicated way, thank you all. My best friends Daniela and her husband Joshua Hellwig as well as Vivien Siegmund and her boyfriend Fabian Lipperoth were additionally giving me all the support needed, professionally as well as in the shape of some good drinks mixed with a lot of sweets, thank you.

I know that I missed a few family events due to unusual working hours. I am very glad that none of my family members ever blamed me for being absent, physical as well as mental. Thank you for all your help, your understanding, your patience and your love. I could have never made it without you!

6 Danksagung

Zu allererst möchte ich Herrn Prof. Dr. Nikita Popov für die Möglichkeit danken, an diesem interessanten Projekt arbeiten zu können. Seine kontinuierliche Anleitung und sein Rat waren essentiell für meine Arbeit. Ich werde unsere wissenschaftlichen Diskussionen vermissen und bin sehr dankbar für all die Skills die mir Nikita über die Jahre beigebracht hat, Dankeschön.
Des Weiteren möchte ich meine Dankbarkeit und Wertschätzung für die Unterstützung von Frau Prof. Dr. Tassula Proikas-Cezanne zum Ausdruck bringen. Sie waren eine tolle primäre Betreuerin, vielen Dank.
Ich danke Prof. Dr. Jennifer Ewald and Prof. Dr. Boris Maček dafür, dass sie sich bereit erklärt haben, Mitglieder meines Prüfungskomitees zu sein und mir dadurch die Möglichkeit gegeben zu haben meine Arbeit vorzutragen und zu diskutieren.
Ohne die Mitglieder der AG Popov, AG Zender, AG Leibold, AG Feucht und AG Dauch Labs hätte ich es nicht geschafft. Danke für all eure kontinuierliche technische Unterstützung und die gute Arbeitsatmosphäre. Insbesondere muss ich Ravi Babu Kollampally, Stefan Zwirner, Melanie Henning und Aylin Heinrich danken, für all die Diskussionen, für ihre Geduld und ihre Freundschaft.
Schließlich danke ich meiner gesamten Familie und meinen Freunden. Vor allem meine Eltern Andrea Rousseau mit ihrem Freund Kurt(i) Sonntag und Thierry Rousseau mit seiner Frau Mirela Pietrar haben mich immer unterstützt, wenn der Stress mich zu übermannen drohte. Vielen Dank für die langen Telefonate und die Türen, die mir immer offen standen. Zusätzlich möchte ich meinen Großeltern Gerda und Horst Eberle danken, welche immer gerne bereit waren, meine Laune mit guten Essen und einer Partie „Mensch-ärgere-dich-nicht!“ zu heben. Ich danke meinem großen Bruder Fabian und seiner Tochter Luna Rousseau, die mir immer das Gefühl gaben, wieder ein sorgloses Kind zu sein. Ich habe all die Urlaube, die wir zusammen verbracht haben wirklich sehr genossen. Mein kleiner Bruder Marcel und seine Frau Jasmin Pause haben mir immer gerne geholfen, mit köstlichem Essen und Formatierungs-Beratung, Dankeschön. Ich bin dankbar für die vielen Abende mit rumänischem Schnaps und Kartenspielen, welche ich mit meinen neusten Brüdern Richard und Ticyan Igaz verbracht habe. Am wichtigsten ist es mir, meinem Freund Marc Votteler dafür zu danken, dass er sich immer all meine Sorgen angehört hat, mich beruhigt hat und mir gezeigt hat, wie schön und einfach das Leben sein kann, Dankeschön. Die gesamte Familie Votteler war unersetzlich, mit all den Einladungen zu Familienfeiern und ihrer herzlichen und unkomplizierten Aufnahme in ihre Familie, danke euch allen! Meine besten Freundinnen Daniela und ihr Mann Joshua Hellwig wie auch Vivien Siegmund und ihr Freund Fabian Lipperoth gaben mir zusätzlich jede nötige Unterstützung, sowohl professionell als auch in Form von guten Drinks gepaart mit vielen Süßigkeiten, Dankeschön.

Ich weiß, dass ich einige Familien Events dank meiner ungewöhnlichen Arbeitszeiten verpasst habe. Ich bin sehr dankbar dafür, dass kein einziges Familienmitglied mir je einen Vorwurf gemacht hat hinsichtlich meiner körperlichen und teilweise auch geistigen Abwesenheit. Danke euch allen für eure Hilfe, euer Verständnis, eure Geduld und eure Liebe. Ohne euch hätte ich es niemals geschafft!

7 References

G.K. **Abou-Alfa**, T. Meyer, A.-L. Cheng, A.B. El-Khoueiry, L. Rimassa, B.-Y. Ryoo, I. Cicin, P. Merle, Y.H. Chen, J.-W. Park, J.-F. Blanc, L. Bolondi, H.-J. Klümpen, S.L. Chan, V. Zagonel, T. Pressiani, M.-H. Ryu, A.P. Venook, C. Hessel, A.E. Borgman-Hagey, G. Schwab, R.K. Kelley (2018): Cabozantinib in Patients with Advanced and Progressing Hepatocellular Carcinoma. In: *N Engl J Med*, 379(1), 54-63

E. **Agricola**, R.A Randall, T. Gaarenstroom, S. Dupont, C.S. Hill (2011): Recruitment of TIF1γ to chromatin via its PHD finger-bromodomain activates its ubiquitin ligase and transcriptional repressor activities. *Mol Cell*, 43 (1), 85-96

G. **Akiri**, M.M. Cherian, S. Vijayakumar, G. Liu, A. Bafico, S.A. Aaronson (2009): Wnt pathway aberrations including autocrine Wnt activation occur at high frequency in human non-small-cell lung carcinoma. In: *Oncogene*, 28(21), 2163-72

J.L. **Alexander**, T.L. Orr-Weaver (2016): Replication fork instability and the consequences of fork collisions from rereplication. In: *Genes Dev*, 30(20), 2241-2252

H. **Ali**, M. Mano, L. Braga, A. Naseem, B. Marini, D. My Vu, C. Collesi, G. Meroni, M. Lusic, M. Giacca (2019): Cellular TRIM33 restrains HIV-1 infection by targeting viral integrase for proteasomal degradation. In: *Nat Commun*, 10(1):926

B.L. **Allen-Petersen**, R.C. Sears (2019): Mission Possible: Advances in MYC Therapeutic Targeting in Cancer. In: *BioDrugs*, 33(5), 539-553

Y**.** **Allenbach**, J**.** Keraen, A**.**-M**.** Bouvier, V**.** Jooste, N**.** Champtiaux, B**.** Hervie**r**, Y**.** Schoindre, A**.** Rigolet, L**.** Gilardin, L**.** Musset**,** J.-L**.** Charuel, O**.** Boyer, F**.** Jouen, L**.** Drouot, J**.** Martinet, T**.** Stojkovic, B**.** Eymard, P**.** Laforêt, A**.** Behin, E**.** Salort-Campana, O**.** Fain, A**.** Meyer, N**.** Schleinitz, K. Mariampillai, A**.** Grados, O. Benveniste (2016): High risk of cancer in autoimmune necrotizing myopathies: usefulness of myositis specific antibody. In: *Brain*, 139(Pt 8), 2131-5

S. **Allmann**, L. Mayer, J. Olma, B. Kaina, T.G. Hofmann, M.T. Tomicic, M. Christmann (2020): Benzo[a]pyrene represses DNA repair through altered E2F1/E2F4 function marking an early event in DNA damage-induced cellular senescence. In: *Nucleic Acids Res*, 48(21), 12085-12101

S.F. **Altekruse**, K.A. McGlynn, M.E. Reichman (2009): Hepatocellular carcinoma incidence, mortality, and survival trends in the United States from 1975 to 2005. In: *J Clin Oncol*, 27(9), 1485-91

J.N. **Anastas**, R.T. Moon (2013): WNT signalling pathways as therapeutic targets in cancer. In: *Nat Rev Cancer*, 13(1), 11-26

G. **Andrieux**, L. Fattet, M. Le Borgne, R. Rimokh, N. Théret (2012): Dynamic Regulation of Tgf-B Signaling by Tif1γ: A Computational Approach. In: *PLoS One.*, 7(3): e33761

A. **Arai**, T. Chano, K. Futami, Y. Furuichi, K. Ikebuchi, T. Inui, H. Tameno, Y. Ochi, T. Shimada, Y. Hisa, H. Okabe (2011): RECQL1 and WRN proteins are potential therapeutic targets in head and neck squamous cell carcinoma. In: *Cancer Res,* 71(13), 4598-607

V.M. **Arlt**, M. Stiborova, H.H. Schmeiser (2002): Aristolochic acid as a probable human cancer hazard in herbal remedies: a review. In: *Mutagenesis*, 17(4), 265-77

C. **Attwooll**, E. Lazzerini Denchi, K. Helin (2004): The E2F family: specific functions and overlapping interests. In: *EMBO J.*, 23(24), 4709—4716

B.J. **Aubrey**, G.L. Kelly, A. Janic, M.J. Herold, A. Strasser (2018): How does p53 induce apoptosis and how does this relate to p53-mediated tumour suppression? In: *Cell Death Differ*, 25(1), 104-113

R. **Aucagne**, N. Droin, J. Paggetti, B. Lagrange, A. Largeot, A. Hammann, A. Bataille, L. Martin, K.-P. Yan, P. Fenaux, R. Losson, E. Solary, J.-N. Bastie, L. Delva (2011): Transcription intermediary factor 1γ is a tumor suppressor in mouse and human chronic myelomonocytic leukemia. *J Clin Invest*, 121 (6), 2360-71

P. **Awasthi**, M. Foiani, A. Kumar (2015): ATM and ATR signaling at a glance. In: *J Cell Sci*, 128(23), 4255-62

C.Z. **Bachrati**, I.D. Hickson (2008): RecQ helicases: guardian angels of the DNA replication fork. In: *Chromosoma*, 117(3), 219-33

X. **Bai**, J. Kim, Z. Yang, M.J. Jurynec, T.E. Akie, J. Lee, J. LeBlanc, A. Sessa, H. Jiang, A. DiBiase, Y. Zhou, D.J. Grunwald, S. Lin, A.B. Cantor, S.H. Orkin, L.I. Zon (2010): TIF1γ controls erythroid cell fate by regulating transcription elongation. *Cell*, 142 (1), 133-43

X. **Bai**, J.J. Trowbridge, E. Riley, J.A. Lee, A. DiBiase, V.M. Kaartinen, S.H. Orkin, L.I. Zon (2013): TiF1-gamma plays an essential role in murine hematopoiesis and regulates transcriptional elongation of erythroid genes. In: *Dev Biol*, 373(2), 422-30

E. **Balciunaite**, A. Spektor, N.H. Lents, H. Cam, H. te Riele, A. Scime, M.A. Rudnicki, R. Young, B.D. Dynlacht (2005): Pocket Protein Complexes Are Recruited to Distinct Targets in Quiescent and Proliferating Cells. In: *Mol Cell Biol.*, 25(18), 8166–8178

C. **Balsano**, M.L. Avantaggiati, G. Natoli, E. De Marzio, H. Will, M. Perricaudet, M. Levrero (1991): Full-length and truncated versions of the hepatitis B virus (HBV) X protein (pX) transactivate the cmyc protooncogene at the transcriptional level. In: *Biochem Biophys Res Commun*, 176(3), 985-92

E.R.M. **Balog**, J.R. Burke, G.L. Hura, S.M. Rubin (2011): Crystal Structure of the Unliganded Retinoblastoma Protein Pocket Domain. In: *Proteins.*, 79(6), 2010–2014

T. **Banerjee**, J.A. Sommers, J. Huang, M.M. Seidman, R.M. Brosh Jr (2015): Catalytic strand separation by RECQ1 is required for RPA-mediated response to replication stress. In: *Curr Biol*, 25(21), 2830-2838

J. **Bankovic**, J. Stojsic, D. Jovanovic, T. Andjelkovic, V. Milinkovic, S. Ruzdijic, N. Tanic (2010): Identification of genes associated with non-small-cell lung cancer promotion and progression. In: *Lung Cancer*, 67(2), 151-9

S.P. **Bell**, B. Stillman (1992): ATP-dependent recognition of eukaryotic origins of DNA replication by a multiprotein complex. In: *Nature*, 357(6374), 128-34

P.-S. **Bellaye**, G. Wettstein, O. Burgy, V. Besnard, A. Joannes, J. Colas, S. Causse, J. Marchal-Somme, A. Fabre, B. Crestani, M. Kolb, J. Gauldie, P. Camus, C. Garrido, P. Bonniaud (2014): The small heat-shock protein αB-crystallin is essential for the nuclear localization of Smad4: impact on pulmonary fibrosis. In: *J Pathol*, 232(4), 458-72

B. **Benedict**, M.A.E. van Bueren, F.P.A. van Gemert, C. Lieftink, S.G. Llobet, M.A.T.M. van Vugt, R.L. Beijersbergen, H. te Riele (2020): The RECQL helicase prevents replication fork collapse during replication stress. In: *Life Sci Alliance.*, 3(10): e202000668

L.L. **Bernet**, M.A. Lewis, K.E. Rieger, L. Casciola-Rosen, D.F. Fiorentino (2016): Ovoid Palatal Patch in Dermatomyositis: A Novel Finding Associated With Anti-TIF1γ (p155) Antibodies. In: *JAMA Dermatol,* 152(9), 1049-51

M. **Berti**, A.R. Chaudhuri, S. Thangavel, S. Gomathinayagam, S. Kenig, M. Vujanovic, F. Odreman, T. Glatter, S. Gaziano, R. Mendoza-Maldonado, F. Marino, B. Lucic, V. Biasin, M. Gstaiger, R. Aebersold, J.M. Sidorova, R.J. Monnat Jr, M. Lopes, A. Vindigni (2013): Human RECQ1 promotes restart of replication forks reversed by DNA topoisomerase I inhibition. In: *Nat Struct Mol Biol*, 20(3), 347-54

C. **Bertoli**, J.M. Skotheim, R.A.M. de Bruin (2013): Control of cell cycle transcription during G1 and S phases. In: *Nat. Rev. Mol. Cell Biol.*, 14(8), 518–28

K. **Bhawe**, D. Roy (2018): Interplay between NRF1, E2F4 and MYC transcription factors regulating common target genes contributes to cancer development and progression. In: *Cell Oncol (Dordr)*, 41(5), 465-484

K. **Bielskienė**, L. Bagdonienė, J. Mozūraitienė, B. Kazbarienė, E. Janulionis (2015): E3 ubiquitin ligases as drug targets and prognostic biomarkers in melanoma. In: *Medicina (Kaunas)*, 51(1), 1-9

V.A. **Bohr** (2008): Rising from the RecQ-age: the role of human RecQ helicases in genome maintenance. In: *Trends Biochem Sci*, 33(12), 609-20

R.J. **Bold**, P.M. Termuhlen, D.J. McConkey (1997): Apoptosis, cancer and cancer therapy. In: *Surg Oncol,* 6(3), 133-42

C. **Bouchard**, S. Lee, V. Paulus-Hock, C. Loddenkemper, M. Eilers, C.A. Schmitt (2007): FoxO transcription factors suppress Myc-driven lymphomagenesis via direct activation of Arf. In: *Genes Dev*, 21(21), 2775-87

A.P. **Bracken**, M. Ciro, A. Cocito, K. Helin (2004): E2F target genes: unraveling the biology. In: *Trends Biochem Sci*, 29(8), 409-17

J. **Bruix**, S. Qin, P. Merle, A. Granito, Y.-H. Huang, G. Bodoky, M. Pracht, O. Yokosuka, O. Rosmorduc, V. Breder, R. Gerolami, G. Masi, P.J. Ross, T. Song, J.-P. Bronowicki, I. Ollivier-Hourmand, M. Kudo, A.-L. Cheng, J.M. Llovet, R.S. Finn, M.-A. LeBerre, A. Baumhauer, G. Meinhardt, G. Han, RESORCE Investigators (2017): Regorafenib for patients with hepatocellular carcinoma who progressed on sorafenib treatment (RESORCE): a randomised, double-blind, placebo-controlled, phase 3 trial. In: *Lancet*, 389(10064), 56-66

F. **Cai**, L. Cai, Z. Zhou, X. Pan, M. Wang, S. Chen, M.A.F. Luis, C. Cen, E. Biskup (2019): Prognostic role of Tif1γ expression and circulating tumor cells in patients with breast cancer. In: *Mol Med Rep*, 19(5), 3685-369

D. **Caracciolo**, F. Scionti, G. Juli, E. Altomare, G. Golino, K. Todoerti, K. Grillone, C. Riillo, M. Arbitrio, M. Iannone, E. Morelli, N. Amodio, M.T. Di Martino, M. Rossi, A. Neri, P. Tagliaferri, P. Tassone (2021): Exploiting MYC-induced PARPness to target genomic instability in multiple myeloma. In: *Haematologica*, 106(1), 185-195

B.A. **Carneiro**, W.S. El-Deiry (2020): Targeting apoptosis in cancer therapy. In: *Nat Rev Clin Oncol*, 17(7), 395-417

S. **Chakraborty**, T. Rahman (2012): The difficulties in cancer treatment. In: *Ecancermedicalscience.*, 6: ed16

G. **Chen**, W. Chen, M. Ye, W. Tan, B. Jia (2019): TRIM59 knockdown inhibits cell proliferation by down-regulating the Wnt/β-catenin signaling pathway in neuroblastoma. In: *Biosci Rep*, 39(1):BSR20181277

Y.-Y. **Chen**, Y. Chen, W.-C. Wang, Q. Tang, R. Wu, W.-H. Zhu, D. Li, L.-L. Liao (2019): Cyclin D1 regulates osteoarthritis chondrocyte apoptosis *via* WNT3/β-catenin signaling. In: *Artif Cells Nanomed Biotechnol*, 47(1), 1971-1977

S. **Chen**, M.A. de Vries, S.P. Bell (2007): Orc6 is required for dynamic recruitment of Cdt1 during repeated Mcm2-7 loading. In: *Genes Dev*, 21(22), 2897-907

J. **Chen**, C. Ding, Y. Chen, W. Hu, Y. Lu, W. Wu, Y. Zhang, B. Yang, H. Wu, C. Peng, H. Xie, L. Zhou, J. Wu, S. Zheng (2020): ACSL4 promotes hepatocellular carcinoma progression via c-Myc stability mediated by ERK/FBW7/c-Myc axis. In: *Oncogenesis*, 9(4), 42

H. **Chen**, H. Liu, G. Qing (2018): Targeting oncogenic Myc as a strategy for cancer treatment. In*: Signal Transduct Target Ther*., 3, 5

H.-Z. **Chen**, S.-Y. Tsai, G. Leone (2009): Emerging roles of E2Fs in cancer: an exit from cell cycle control. In: *Nat Rev Cancer*, 9(11), 785-97

A.-L. **Cheng**, Y.-K. Kang, Z. Chen, C.-J. Tsao, S. Qin, J.S. Kim, R. Luo, J. Feng, S. Ye, T.-S. Yang, J. Xu, Y. Sun, H. Liang, J. Liu, J. Wang, W.Y. Tak, H. Pan, K. Burock, J. Zou, D. Voliotis, Z. Guan (2009): Efficacy and safety of sorafenib in patients in the Asia-Pacific region with advanced hepatocellular carcinoma: a phase III randomised, double-blind, placebo-controlled trial. In: *Lancet Oncol*, 10(1), 25-34

M. **Chrétien**, C. Legouge, R.Z. Martin, A. Hammann, M. Trad, R. Aucagne, A. Largeot, J. Bastie, L. Delva, R. Quéré (2016): Trim33/Tif1γ is involved in late stages of granulomonopoiesis in mice. In: *Exp Hematol*, 44(8), 727-739

W.K. **Chu**, I.D. Hickson (2009): RecQ helicases: multifunctional genome caretakers. In: *Nat Rev Cancer*, 9(9), 644-54

H. **Clevers**, R. Nusse (2012): Wnt/β-catenin signaling and disease. In: *Cell*, 149(6), 1192-205

P.L. **Collins**, C. Purman, S.I. Porter, V. Nganga, A. Saini, K.E. Hayer, G.L. Gurewitz, B.P. Sleckman, J.J. Bednarski, C.H. Bassing, E.M. Oltz (2020): DNA double-strand breaks induce H2Ax phosphorylation domains in a contact-dependent manner. In: *Nat Commun*, 11(1), 3158

D. **Cortez** (2016): Preventing Replication Fork Collapse to Maintain Genome Integrity. In: *DNA Repair (Amst).*, 32, 149–157

A. **Cucchetti**, F. Piscaglia, M.Cescon, A. Colecchia, G. Ercolani, L. Bolondi, A.D. Pinna (2013): Cost-effectiveness of hepatic resection versus percutaneous radiofrequency ablation for early hepatocellular carcinoma. In: *J Hepatol.*, 59(2), 300-7

S. **Cui**, R. Klima, A. Ochem, D. Arosio, A. Falaschi, A. Vindigni (2003): Characterization of the DNA-unwinding activity of human RECQ1, a helicase specifically stimulated by human replication protein A. In: *J Biol Chem*, 278(3), 1424-32

L. **Curti,** S. Campaner (2021): MYC-Induced Replicative Stress: A Double-Edged Sword forCancer Development and Treatment. In: *Int J Mol Sci*, 22, 6168

Y, **Dai**, Y. Li, R. Cheng, J. Gao, Y. Li, C. Lou (2018): TRIM37 inhibits PDGF-BB-induced proliferation and migration of airway smooth muscle cells. In: *Biomed Pharmacother,* 101, 24-29

R. **Dalla-Favera**, M. Bregni, J. Erikson, D. Patterson, R.C. Gallo, C.M. Croce (1982): Human c-myc onc gene is located on the region of chromosome 8 that is translocated in Burkitt lymphoma cells. In: *Proc Natl Acad Sci U S A*, 79(24), 7824-7

C.V. **Dang** (1999): c-Myc Target Genes Involved in Cell Growth, Apoptosis, and Metabolism. In: *Mol Cell Biol.*, 19(1), 1–11

C.V. **Dang** (2012): MYC on the path to cancer. In: *Cell*, 149(1), 22-35

C.V. **Dang**, K.A. O'Donnell, K.I. Zeller, T. Nguyen, R.C. Osthus, F. Li (2006): The c-Myc target gene network. In: *Semin Cancer Biol*, 16(4), 253-64

P.S. **Danielian**, L.B. Friesenhahn, A.M. Faust, J.C. West, A.M. Caron, R.T. Bronson, J.A. Lees (2008): E2f3a and E2f3b make overlapping but different contributions to total E2f3 activity. In: *Oncogene*, 27(51), 6561–6570

P.S. **Danielian**, R.A. Hess, J.A. Lees (2016): E2f4 and E2f5 are essential for the development of the male reproductive system. In: *Cell Cycle*, 15(2), 250-60

C.M. **D'Cruz**, E.J. Gunther, R.B. Boxer, J.L. Hartman, L. Sintasath, S.E. Moody, J.D. Cox, S.I. Ha, G.K. Belka, A. Golant, R.D. Cardiff, L.A. Chodosh (2001): c-MYC induces mammary tumorigenesis by means of a preferred pathway involving spontaneous Kras2 mutations. In: *Nat Med*, 7(2), 235-9

J. **DeGregori**, D.G. Johnson (2006): Distinct and Overlapping Roles for E2F Family Members in Transcription, Proliferation and Apoptosis. In: *Curr Mol Med*, 6 (7), 739-748

L. **Deng**, T. Meng, L. Chen, W. Wei, P. Wang (2020): The role of ubiquitination in tumorigenesis and targeted drug discovery. In: *Signal Transduct Target Ther*, 5(1), 11

R. **Derynck**, E.H. Budi (2019): Specificity, versatility, and control of TGF-β family signaling. In: *Sci Signal*, 12(570):eaav5183

C. **Deschênes**, L. Alvarez, M.-E. Lizotte, A. Vézina, N. Rivard (2004): The nucleocytoplasmic shuttling of E2F4 is involved in the regulation of human intestinal epithelial cell proliferation and differentiation. In: *J Cell Physiol*, 199(2), 262-73

J. **De Vooght**, J.-B. Vulsteke, P. De Haes, X. Bossuyt, R. Lories, E. De Langhe (2020): Anti-TIF1-γ autoantibodies: warning lights of a tumour autoantigen. In: *Rheumatology (Oxford)*, 59(3), 469-477

R. **Dhanasekaran**, J. Park, A. Yevtodiyenko, D.I. Bellovin, S.J. Adam, A.R. Kd, M. Gabay, H. Fernando, J. Arzeno, V. Arjunan, S. Gryanzov, D.W. Felsher (2020): MYC ASO Impedes Tumorigenesis and Elicits Oncogene Addiction in Autochthonous Transgenic Mouse Models of HCC and RCC. In: *Mol Ther Nucleic Acids*, 21, 850-859

Z. **Ding**, G. Jin, W. Wang, W. Chen, Y. Wu, X. Ai, L. Chen, W. Zhang, H. Liang, A. Laurence, M. Zhang, P.K. Datta, B. Zhang, X. Chen (2014): Reduced expression of transcriptional intermediary factor 1 gamma promotes metastasis and indicates poor prognosis of hepatocellular carcinoma. In: *Hepatology*, 60(5), 1620-36

D. **Dingar**, F. Konecny, J. Zou, X. Sun, R. von Harsdorf (2012): Anti-apoptotic function of the E2F transcription factor 4 (E2F4)/p130, a member of retinoblastoma gene family in cardiac myocytes. In: *J Mol Cell Cardiol*, 53(6), 820-8

K.M. **Doherty**, S. Sharma, L.A. Uzdilla, T.M. Wilson, S. Cui, A. Vindigni, R.M. Brosh Jr (2005): RECQ1 helicase interacts with human mismatch repair factors that regulate genetic recombination. In: *J Biol Chem*, 280(30), 28085-94

D. **Dominguez-Sola**, J. Gautier (2014): MYC and the Control of DNA Replication. In: *Cold Spring Harb Perspect Med.*, 4(6): a014423

D. **Dominguez-Sola**, C.Y. Ying, C. Grandori, L. Ruggiero, B. Chen, M. Li, D.A. Galloway, W. Gu, J. Gautier, R. Dalla-Favera (2007): Non-transcriptional control of DNA replication by c-Myc. In: *Nature*, 448(7152), 445-51

M. **Dragoj**, J. Bankovic, A. Podolski-Renic, S.S. Buric, M. Pesic, N. Tanic, T. Stankovic (2019): Association of Overexpressed *MYC* Gene with Altered *PHACTR3* and *E2F4* Genes Contributes to Non-small Cell Lung Carcinoma Pathogenesis. In: *J Med Biochem*, 38(2), 188-195

S. **Dupont**, A. Mamidi, M. Cordenonsi, M. Montagner, L. Zacchigna, M. Adorno, G. Martello, M.J. Stinchfield, S. Soligo, L. Morsut, M. Inui, S. Moro, N. Modena, F. Argenton, S.J. Newfeld, S. Piccolo (2009): FAM/USP9x, a deubiquitinating enzyme essential for TGFbeta signaling, controls Smad4 monoubiquitination. *Cell*, 136 (1), 123-35

S. **Dupont**, L. Zacchigna, M. Cordenonsi, S. Soligo, M. Adorno, M. Rugge, S. Piccolo (2005): Germ-layer Specification And Control Of Cell Growth By ectodermin, A Smad4 Ubiquitin ligase. *Cell* ,121, 87–99.

U. **Eilers**, J. Klumperman, H.-P. Hauri (1989): Nocodazole, a microtubule-active drug, interferes with apical protein delivery in cultured intestinal epithelial cells (Caco-2). In: *J Cell Biol.,* 108(1), 13–22

K. **Engeland** (2017):Cell cycle arrest through indirect transcriptional repression by p53: I have a DREAM. In: *Cell Death Differ*, 25(1), 114-132

G.I. **Evan**, A.H. Wyllie, C.S. Gilbert, T.D. Littlewood, H. Land, M. Brooks, C.M. Waters, L.Z. Penn, D.C. Hancock (1992): Induction of apoptosis in fibroblasts by c-myc protein. In: *Cell*, 69(1), 119-28

S. **Falk**, E. Joosten, V. Kaartinen, L. Sommer (2014):Smad4 and Trim33/Tif1γ redundantly regulate neural stem cells in the developing cortex. In: *Cereb Cortex*, 24(11), 2951-63

P. **Farshi**, R.R. Deshmukh, J.O. Nwankwo, R.T. Arkwright, B. Cvek, J. Liu, Q.P. Dou (2015): Deubiquitinases (DUBs) and DUB inhibitors: a patent review. In: *Expert Opin Ther Pat*, 25(10), 1191-1208

L. **Fattet**, A. Ay, B. Bonneau, L. Jallades, I. Mikaelian, I. Treilleux, G. Gillet, C. Hesling, R. Rimokh (2013): TIF1γ requires sumoylation to exert its repressive activity on TGFβ signaling. In: *J Cell Sci*, 126(Pt 16), 3713-23

Y. **Feng**, L. Li, Y. Du, X. Peng, F. Chen (2020): E2F4 functions as a tumour suppressor in acute myeloid leukaemia via inhibition of the MAPK signalling pathway by binding to EZH2. In: *J Cell Mol Med.*, 24(3), 2157–2168

P.T. **Ferrao**, E.P. Bukczynska, R.W. Johnstone, G.A. McArthur (2012): Efficacy of CHK inhibitors as single agents in MYC-driven lymphoma cells. In: *Oncogene*, 31(13), 1661-72

A. **Finch**, J. Prescott, K. Shchors, A. Hunt, L. Soucek, T.B. Dansen, L.B. Swigart, G.I. Evan (2006): Bcl-xL gain of function and p19 ARF loss of function cooperate oncogenically with Myc in vivo by distinct mechanisms. In: *Cancer Cell*, 10(2), 113-20

N.A. **Forrester**, R.N. Patel, T. Speiseder, P. Groitl, G.G. Sedgwick, N.J. Shimwell, R.I. Seed, P.Ó. Catnaigh, C.J. McCabe, G.S. Stewart, T. Dobner, R.J.A. Grand, A. Martin, A.S. Turnell (2012): Adenovirus E4orf3 targets transcriptional intermediary factor 1γ for proteasome-dependent degradation during infection. In: *J Virol*, 86(6), 3167-79

J. **Freimuth**, N. Gassler, N. Moro, R.W. Günther, C. Trautwein, C. Liedtke, G.A. Krombach (2010): Application of magnetic resonance imaging in transgenic and chemical mouse models of hepatocellular carcinoma. In: *Mol Cancer*, 9:94

K. **Futami**, S. Ogasawara, H. Goto, H. Yano, Y. Furuichi (2010): RecQL1 DNA repair helicase: A potential tumor marker and therapeutic target against hepatocellular carcinoma. In: *Int J Mol Med*, 25(4), 537-45

M. **Gabay**, Y. Li, D.W. Felsher (2014): MYC activation is a hallmark of cancer initiation and maintenance. In: *Cold Spring Harb Perspect Med*, 4(6):a014241

R.Y. **Gadgil**, E.J. Romer, C.C. Goodman, S.D. Rider Jr, F.J. Damewood, J.R. Barthelemy, K. Shin-Ya, H. Hanenberg, M. Leffak (2020): Replication stress at microsatellites causes DNA double-strand breaks and break-induced replication. In: *J Biol Chem*, 295(45), 15378-15397

A. **Gallouet**, F. Ferri, V. Petit, A. Parcelier, D. Lewandowski, N. Gault, V. Barroca, S. Le Gras, E. Soler, F. Grosveld, I. Davidson, P. Romeo (2017): Macrophage production and activation are dependent on TRIM33 . In: *Oncotarget*, 8(3), 5111-5122

H. **Garneau**, M.-C. Paquin, J.C. Carrier, N. Rivard (2009): E2F4 expression is required for cell cycle progression of normal intestinal crypt cells and colorectal cancer cells. In: *J Cell Physiol*, 221(2), 350-8

S. **Gaubatz**, G.J. Lindeman, S. Ishida, L. Jakoi, J.R. Nevins, D.M. Livingston, R.E. Rempel (2000): E2F4 and E2F5 play an essential role in pocket protein-mediated G1 control. In: *Mol Cell*, 6(3), 729-3

A. **Ghirardello**, N. Bassi, L. Palma, E. Borella, M. Domeneghetti, L. Punzi, A. Doria (2013): Autoantibodies in polymyositis and dermatomyositis. In: *Curr Rheumatol Rep*, 15(6), 335

R. **Gillman**, K.L. Floro, M. Wankell, L. Hebbard (2021): The role of DNA damage and repair in liver cancer. In: *Biochim Biophys Acta Rev Cancer*, 1875(1), 188493

D. **Ginsberg**, G. Vairo, T. Chittenden, Z.X. Xiao, G. Xu, K.L. Wydner, J.A. DeCaprio, J.B. Lawrence, D.M. Livingston (1994): E2F-4, a new member of the E2F transcription factor family, interacts with p107. In: *Genes Dev*, 8(22), 2665-79

D. **Gouas**, H. Shi, P. Hainaut (2009): The aflatoxin-induced TP53 mutation at codon 249 (R249S): biomarker of exposure, early detection and target for therapy. In: *Cancer Lett*, 286(1), 29-37

J. **Guo**, W. Qin, Q. Xing, M. Gao, F. Wei, Z. Song, L. Chen, Y. Lin, X. Gao, Z. Lin (2017): TRIM33 is essential for osteoblast proliferation and differentiation via BMP pathway. In: *J Cell Physiol*, 232(11), 3158-3169

J. **Harb**, P.-J. Lin, J. Hao (2019): Recent Development of Wnt Signaling Pathway Inhibitors for Cancer Therapeutics. In: *Curr Oncol Rep*, 21(2), 12

J.A. **Harrigan**, X. Jacq, N.M. Martin, S.P. Jackson (2018): Deubiquitylating enzymes and drug discovery: emerging opportunities. In: *Nat Rev Drug Discov*, 17(1), 57-78

S. **Hatakeyama** (2011): TRIM proteins and cancer. In: *Nat Rev Cancer*, 11(11), 792-804

G. **Hateboer**, A. Wobst, B.O. Petersen, L. Le Cam, E. Vigo, C. Sardet, K. Helin (1998): Cell cycle-regulated expression of mammalian CDC6 is dependent on E2F. In: *Mol Cell Biol*, 18(11), 6679-97

W. **He**, D.C. Dorn, H. Erdjument-Bromage, P. Tempst, M.A. Moore, J. Massaqué (2006): Hematopoiesis controlled by distinct TIF1gamma and Smad4 branches of the TGFbeta pathway. *Cell*, 125 (5), 929-41

L. **He**, H. Zhou, Z. Zeng, H. Yao, W. Jiang, H. Qu (2019): Wnt/β-catenin signaling cascade: A promising target for glioma therapy. In: *J Cell Physiol*, 234(3), 2217-2228

C.-H. **Heldin**, A. Moustakas (2006): A new twist in Smad signaling. In: *Dev Cell*, 10(6), 685-6

B. **Herquel**, K. Ouararhni, K. Khetchoumian, M. Ignat, M. Teletin, M. Mark, G. Béchade, A. Van Dorsselaer, S. Sanglier-Cianférani, A. Hamiche, F. Cammas, I. Davidson, R. Losson (2011): Transcription cofactors TRIM24, TRIM28, and TRIM33 associate to form regulatory complexes that suppress murine hepatocellular carcinoma. *Proc Natl Acad Sci U S A*, 108 (20), 8212-17

C. **Hesling**, J. Lopez, L. Fattet, P. Gonzalo, I. Treilleux, D. Blanchard, R. Losson, V. Goffin, N. Pigat, A. Puisieux, I. Mikaelian, G. Gillet, R. Rimokh (2013): Tif1γ is essential for the terminal differentiation of mammary alveolar epithelial cells and for lactation through SMAD4 inhibition. In: *Development*, 140(1), 167-75

M.R. **Higgs**, H. Lerat, J.-M. Pawlotsky (2013): Hepatitis C virus-induced activation of β-catenin promotes c-Myc expression and a cascade of pro-carcinogenetic events. In: *Oncogene*, 32(39), 4683-93

A.-L. **Hillje**, M.M.A. Worlitzer, T. Palm, J.C. Schwamborn (2011): Neural stem cells maintain their stemness through protein kinase C ζ-mediated inhibition of TRIM32. In: *Stem Cells*, 29(9), 1437-47

B. **Hoffman**, D.A. Liebermann (2008): Apoptotic signaling by c-MYC. In: *Oncogene*, 27(50), 6462-72

R.F. **Holcombe**, J.L. Marsh, M.L. Waterman, F. Lin, T. Milovanovic, T. Truong (2002): Expression of Wnt ligands and Frizzled receptors in colonic mucosa and in colon carcinoma. In: *Mol Pathol*, 55(4), 220-6

J. **Hsu**, J. Arand, A. Chaikovsky, N.A. Mooney, J. Demeter, C.M. Brison, R. Oliverio, H. Vogel, S.M. Rubin, P.K. Jackson, J. Sage (2019): E2F4 regulates transcriptional activation in mouse embryonic stem cells independently of the RB family. In: *Nat Commun*, 10(1), 2939

J. **Hsu**, J. Sage (2016): Novel functions for the transcription factor E2F4 in development and disease. In: *Cell Cycle.*, 15(23), 3183–3190

T. **Hu**, C. Li (2010): Convergence between Wnt-β-catenin and EGFR signaling in cancer. In: *Mol Cancer*, 9:236

T. **Huang**, Y.R. González, D. Qu, E. Huang, F. Safarpour, E. Wang, A. Joselin, D.S. Im, S.M. Callaghan, W. Boonying, L. Julian, S.L. Dunwoodie, R.S. Slack, D.S. Park (2019): The pro-death role of Cited2 in stroke is regulated by E2F1/4 transcription factors. In: *J Biol Chem*, 294(21), 8617-8629

J. **Huang**, Z.-L. Gu, W. Chen, Y.-Y. Xu, M. Chen (2020): Knockdown of ubiquitin-specific peptidase 13 inhibits cell growth of hepatocellular carcinoma by reducing c-Myc expression. In: *Kaohsiung J Med Sci*, doi: 10.1002/kjm2.12209

Z. **Huang**, Q. Wu, O.A. Guryanova, L. Cheng, W. Shou, J.N. Rich, S. Bao (2011): Deubiquitylase HAUSP stabilizes REST and promotes maintenance of neural progenitor cells. In: *Nat Cell Biol*, 13(2), 142-52

Y. **Ikeuchi**, S. Dadakhujaev, A.S. Chandhoke, M.A. Huynh, A. Oldenborg, M. Ikeuchi, L. Deng, E.J. Bennett, J.W. Harper, A. Bonni, S. Bonni (2014): TIF1γ protein regulates epithelial-mesenchymal transition by operating as a small ubiquitin-like modifier (SUMO) E3 ligase for the transcriptional regulator SnoN1. In: *J Biol Chem*, 289(36), 25067-78

H. **Ikushima**, K. Miyazono (2010): TGFbeta signalling: a complex web in cancer progression. In: *Nat Rev Cancer*, 10(6), 415-24

S. **Jain**, S. Singhal, F. Francis, C. Hajdu, J. Wang, A. Suriawinata, Y. Wang, M. Zhang, E.H. Weinshel, F. Francois, Z. Pei, P. Lee, R. Xu (2011): Association of overexpression of TIF1γ with colorectal carcinogenesis and advanced colorectal adenocarcinoma. In: *World J Gastroenterol*, 17(35), 3994-4000

A. **Jemal**, E.M. Ward, C.J. Johnson, K.A. Cronin, J. Ma, A.B. Ryerson, A. Mariotto, A.J. Lake, R. Wilson, R.L. Sherman, R.N. Anderson, S.J. Henley, B.A. Kohler, L. Penberthy, E.J. Feuer, H.K. Weir (2017): Annual Report to the Nation on the Status of Cancer, 1975–2014, Featuring Survival. In: *JNCI*, 109 (9), djx030

X. **Jiang**, Y.H. Tsang, Q. Yu (2007): c-Myc overexpression sensitizes Bim-mediated Bax activation for apoptosis induced by histone deacetylase inhibitor suberoylanilide hydroxamic acid (SAHA) through regulating Bcl-2/Bcl-xL expression. In: *Int J Biochem Cell Biol*, 39(5), 1016-25

A. **Jimenez** (1976): Inhibitors of translation. In: *Nature*., 1(2), 28-30

K. **Jingushi**, Y. Ueda, K. Kitae, H. Hase, H. Egawa, I. Ohshio, R. Kawakami, Y. Kashiwagi, Y. Tsukada, T. Kobayashi, W. Nakata, K. Fujita, M. Uemura, N. Nonomura, K. Tsujikawa (2015): miR-629 Targets TRIM33 to Promote TGFβ/Smad Signaling and Metastatic Phenotypes in ccRCC. In: *Mol Cancer Res*, 13(3), 565-74

W.G. **Kaelin Jr** (1999): Functions of the retinoblastoma protein. In: *Bioessays*, 21(11), 950–958

M. **Kalkat**, D. Resetca, C. Lourenco, P.-K. Chan, Y. Wei, Y.-J. Shiah, N. Vitkin, Y. Tong, M. Sunnerhagen, S.J. Done, P.C. Boutros, B. Raught, L.Z. Penn (2018): MYC Protein Interactome Profiling Reveals Functionally Distinct Regions that Cooperate to Drive Tumorigenesis. In: *Mol Cell*, 72(5), 836-848

A. **Karlsson**, D. Deb-Basu, A. Cherry, S. Turner, J. Ford, D.W. Felsher (2003): Defective double-strand DNA break repair and chromosomal translocations by *MYC* overexpression. In: *Proc Natl Acad Sci U S A*., 100(17), 9974–9979

L. **Kassem**, M. Deygas, L. Fattet, J. Lopez, T. Goulvent, E. Lavergne, S. Chabaud, N. Carrabin, N. Chopin, T. Bachelot, G. Gillet, I. Treilleux, R. Rimokh (2015): TIF1γ interferes with TGFβ1/SMAD4 signaling to promote poor outcome in operable breast cancer patients. In: *BMC Cancer*, 15:453

A. **Kauffmann-Zeh**, P. Rodriguez-Viciana, E. Ulrich, C. Gilbert, P. Coffer, J. Downward, G. Evan (1997): Suppression of c-Myc-induced apoptosis by Ras signalling through PI(3)K and PKB. In: *Nature*, 385(6616), 544-8

L.N. **Kent**, G. Leone (2019): The broken cycle: E2F dysfunction in cancer. In: *Nat Rev Cancer*, 19(6), 326-338

K.M. **Kinross**, A.J. Clark, R.M. Iazzolino, P.O. Humbert (2006): E2f4 regulates fetal erythropoiesis through the promotion of cellular proliferation. In: *Blood*, 108(3),886–895

J. **Kim**, V. Kaartinen (2008): Generation of mice with a conditional allele for Trim33. In: *Genesis*, 46(6), 329-33

S. **Kim**, L. Ma, M.N. Shokhirev, I. Quigley, C. Kintner (2018): Multicilin and activated E2f4 induce multiciliated cell differentiation in primary fibroblasts. In: *Sci Rep*, 8(1), 12369

D. **King**, X.D. Li, G.S. Almeida, C. Kwok, P. Gravells, D. Harrison, S. Burke, A. Hallsworth, Y. Jamin, S. George, S.P. Robinson, C.J. Lord, E. Poon, D. Yeomanson, L. Chesler, H.E. Bryant (2020): MYCN expression induces replication stress and sensitivity to PARP inhibition in neuroblastoma. In: *Oncotarget*, 11(23), 2141-2159

K. **Kliza**, K. Husnjak (2020): Resolving the Complexity of Ubiquitin Networks. In: *Front Mol Biosci*, 7, 21

A. **Koç**, L.J. Wheeler, C.K. Mathews, G.F. Merrill (2004): Hydroxyurea arrests DNA replication by a mechanism that preserves basal dNTP pools. In: *J Biol Chem*, 279(1), 223-30

C. **Köhler**, D. Koalick, A. Fabricius, A.C. Parplys, K. Borgmann, H. Pospiech, F.Grosse (2016): Cdc45 is limiting for replication initiation in humans. In: *Cell Cycle.*, 15(7), 974–985

D. **Komander**, M.J. Clague, S. Urbé (2009): Breaking the chains: structure and function of the deubiquitinases. In: *Nat. Rev. Mol. Cell Biol.*, 10, 550–563

M. **Kudo**, R.S. Finn, S. Qin, K.-H. Han, K. Ikeda, F. Piscaglia, A. Baron, J.-W. Park, G. Han, J. Jassem, J.F. Blanc, A. Vogel, D. Komov, T.R.J. Evans, C. Lopez, C. Dutcus, M. Guo, K. Saito, S. Kraljevic, T. Tamai, M. Ren, A.-L. Cheng (2018): Lenvatinib versus sorafenib in first-line treatment of patients with unresectable hepatocellular carcinoma: a randomised phase 3 non-inferiority trial. In: *Lancet*, 391(10126), 1163-1173

A. **Kulkarni**, J. Oza, M. Yao, H. Sohail, V. Ginjala, A. Tomas-Loba, Z. Horejsi, A.R. Tan, S.J. Boulton, S. Ganesan (2013): Tripartite Motif-containing 33 (TRIM33) Protein Functions in the Poly(ADP-ribose) Polymerase (PARP)-dependent DANN Damage Response through

Interaction with Amplified in Liver Cancer 1 (ALC1) Protein. In: J Biol Chem, 288(45), 32357-69

M. **Kurayoshi**, N. Oue, H. Yamamoto, M. Kishida, A. Inoue, T. Asahara, W. Yasui, A. Kikuchi (2006): Expression of Wnt-5a is correlated with aggressiveness of gastric cancer by stimulating cell migration and invasion. In: *Cancer Res*, 66(21), 10439-48

R.M. **Kypta**, J. Waxman (2012): Wnt/β-catenin signalling in prostate cancer. In: *Nat Rev Urol*, 9(8), 418-28.

Q. **Lan**, X. Tan, P. He, W. Li, S. Tian, W. Dong (2021): TRIM11 Promotes Proliferation, Migration, Invasion and EMT of Gastric Cancer by Activating β-Catenin Signaling. In: *Onco Targets Ther.*, 14, 1429–1440

H.-J. **Lee** (2018): The Role of Tripartite Motif Family Proteins in TGF-β Signaling Pathway and Cancer. In: *J Cancer Prev.*, 23(4), 162–169

E.Y. **Lee**, H. Cam, U. Ziebold, J.B. Rayman, J.A. Lees, B.D. Dynlacht (2002): E2F4 loss suppresses tumorigenesis in Rb mutant mice. In: *Cancer Cell.*, 2(6), 463–472

R. **Lencioni**, T. de Baere, M.C. Soulen, W.S. Rilling, J.-F.H. Geschwind (2016): Lipiodol transarterial chemoembolization for hepatocellular carcinoma: A systematic review of efficacy and safety data. In: *Hepatology*, 64(1), 106-16

R. **Lencioni**, J.M. Llovet, G. Han, W.Y. Tak, J. Yang, A. Guglielmi, S.W. Paik, M. Reig, D.Y. Kim, G.-Y. Chau, A. Luca, L.R. Del Arbol, M.-A. Leberre, W. Niu, K. Nicholson, G. Meinhardt, J. Bruix (2016): Sorafenib or placebo plus TACE with doxorubicin-eluting beads for intermediate stage HCC: The SPACE trial. In: *J Hepatol*, 64(5), 1090-1098

G. **Leone**, J. DeGregori, L. Jakoi, J.G. Cook, J.R. Nevins (1999): c ollaborative role of E2F transcriptional activity and G_1 cyclindependent kinase activity in the induction of S phase. In: *Proc Natl Acad Sci U S A*., 96(12), 6626–6631

G. **Leone**, J. DeGregori, Z. Yan, L. Jakoi, S. Ishida, R.S. Williams, J.R. Nevins (1998): E2F3 activity is regulated during the cell cycle and is required for the induction of S phase. In: *Genes Dev*, 12(14), 2120-30

G. **Leone**, R. Sears, E. Huang, R. Rempel, F. Nuckolls, C.H. Park, P. Giangrande, L. Wu, H.I. Saavedra, S.J. Field, M.A. Thompson, H. Yang, Y. Fujiwara, M.E. Greenberg, S. Orkin, C. Smith, J.R. Nevins (2001): Myc requires distinct E2F activities to induce S phase and apoptosis. In: *Mol Cell*, 8(1), 105-13

A.J. **Levine**, M. Oren (2009): The first 30 years of p53: growing ever more complex. In: *Nat Rev Cancer*, 9(10), 749-58

M. **Levrero**, J. Zucman-Rossi (2016): Mechanisms of HBV-induced hepatocellular carcinoma. In: *J Hepatol*, 64(1 Suppl), 84-S101

T.J. **Liban**, M.J. Thwaites, F.A. Dick, S.M. Rubin (2016): Structural Conservation and E2F Binding Specificity within the Retinoblastoma Pocket Protein Family. In: *J Mol Biol.,* 428(20), 3960–3971

L.P. **Liew**, Z.Y. Lim, M. Cohen, Z. Kong, L. Marjavaara, A. Chabes, S.D. Bell (2016): Hydroxyurea-Mediated Cytotoxicity Without Inhibition of Ribonucleotide Reductase. In: *Cell Rep*, 17(6), 1657-1670

M. **Ligr**, X. Wu, G. Daniels, D. Zhang, H. Wang, C. Hajdu, J. Wang, R. Pan, Z. Pei, L. Zhang, M. Melis, M.R. Pincus, J.K. Saunders, P. Lee, R. Xu (2014): Imbalanced expression of Tif1γ inhibits pancreatic ductal epithelial cell growth. In: *Am J Cancer Res*, 4(3), 196-210

C.-P. **Lin**, C.-R. Liu, C.-N. Lee, T.-S. Chan, H.E. Liu (2010): Targeting c-Myc as a novel approach for hepatocellular carcinoma. In: *World J Hepatol*, 2(1), 16-20

J. **Lin**, J. Shi, H. Guo, X. Yang, Y. Jiang, J. Long, Y. Bai, D. Wang, X. Yang, X. Wan, L. Zhang, J. Pan, K. Hu, M. Guan, L. Huo, X. Sang, K. Wang, H. Zhao (2019): Alterations in DNA Damage Repair Genes in Primary Liver Cancer. In: *Clin Cancer Res*, 25(15), 4701-4711

Y **Liu**, S.M. Kim, Y.Q. Wang, S. Karkashon, A. Lewis-Ballester, S.R. Yeh, M.A. Correia (2021): Characterization of the Structural Determinants of the Ubiquitin-Dependent Proteasomal Degradation of Human Hepatic Tryptophan 2,3-Dioxygenase. In: *Biochem J*, BCJ20210213

J. **Liu**, R. Xu, S.-J. Mai, Y.-S. Ma, M.-Y. Zhang, P.-S. Cao, N.-Q. Weng, R.-Q. Wang, D. Cao, W. Wei, R.-P. Guo, Y.-J. Zhang, L. Xu, M.-S. Chen, H.-Z. Zhang, L. Huang, D. Fu, H.-Y.

Wang (2020): LncRNA CSMD1-1 promotes the progression of Hepatocellular Carcinoma by activating MYC signaling. In: *Theranostics*, 10(17), 7527-7544

J.M. **Llovet**, M.I. Real, X. Montaña, R. Planas, S. Coll, J. Aponte, C. Ayuso, M. Sala, J. Muchart, R. Solà, J. Rodés, J. Bruix, Barcelona Liver Cancer Group (2002): Arterial embolisation or chemoembolisation versus symptomatic treatment in patients with unresectable hepatocellular carcinoma: a randomised controlled trial. In: *Lancet*, 359(9319), 1734-9

J.M. **Llovet**, S. Ricci, V. Mazzaferro, P. Hilgard, E. Gane, J.-F. Blanc, A.C. de Oliveira, A. Santoro, J.-L. Raoul, A. Forner, M. Schwartz, C. Porta, S. Zeuzem, L. Bolondi, T.F. Greten, P.R. Galle, J.-F. Seitz, I. Borbath, D. Häussinger, T. Giannaris, M. Shan, M. Moscovici, D. Voliotis, J. Bruix, SHARP Investigators Study Group (2008): Sorafenib in advanced hepatocellular carcinoma. In: *N Engl J Med*, 359(4), 378-90

C.-M. **Lo**, H. Ngan, W.-K. Tso, C.-L. Liu, C.-M. Lam, R.T.-P. Poon, S.-T. Fan, J. Wong (2002): Randomized controlled trial of transarterial lipiodol chemoembolization for unresectable hepatocellular carcinoma. In: *Hepatology*, 35(5), 1164-71

X. **Lu**, S. Parvathaneni, T. Hara, A. Lal, S. Sharma (2013): Replication stress induces specific enrichment of RECQ1 at common fragile sites FRA3B and FRA16D. In: *Mol Cancer*, 12(1), 29

M. **Luo**, J. Bai, B. Liu, P. Yan, F. Zuo, H. Sun, Y. Sun, X. Xu, Z. Song, Y. Yang, J. Massagué, X. Lan, Z. Lu, Y. Chen, H. Deng, W. Xie, Q. Xi: H3K18ac Primes Mesendodermal Differentiation upon Nodal Signaling. In: *Stem Cell Reports*, 13(4), 642-656

Y. **Ma**, S.N. Freeman, W.D. Cress (2004): E2F4 deficiency promotes drug-induced apoptosis. In: *Cancer Biol Ther*, 3(12), 1262-9

L. **Ma**, I. Quigley, H. Omran, C. Kintner (2014): Multicilin drives centriole biogenesis via E2f proteins. In: *Genes Dev*, 28(13), 1461–1471

S.K. **Madden**, A.D. de Araujo, M. Gerhardt, D.P. Fairlie, J.M. Mason (2021): Taking the Myc out of cancer: toward therapeutic strategies to directly inhibit c-Myc. In: *Mol Cancer*, 20(1), 3

H.H. **Mady**, S. Hasso, M.F. Melhem (2002): Expression of E2F-4 gene in colorectal adenocarcinoma and corresponding covering mucosa: an immunohistochemistry, image analysis, and immunoblot study. In: *Appl Immunohistochem Mol Morphol*, 10 (3), 225-230

M. **Manandhar**, K.S. Boulware, R.D. Wood (2015): The ERCC1 and ERCC4 (XPF) genes and gene products. In: *Gene*, 569(2), 153-61

T. **Manicum**, F. Ni, Y. Ye, X. Fan, B.-C. Chen (2018):Prognostic values of *E2F* mRNA expression in human gastric cancer. In: *Biosci Rep*, 38(6):BSR20181264

J. **Massagué** (2012): TGFβ signalling in context. In: *Nat Rev Mol Cell Biol*, 13(10), 616-30

J. **Massagué**, S.W. Blain, R.S. Lo (2000): TGFbeta signaling in growth control, cancer, and heritable disorders. In: *Cell*, 103(2), 295-309

Y. **Matsushita**, Y. Yokoyama, H. Yoshida, Y. Osawa, M. Mizunuma, T. Shigeto, M. Futagami, T. Imaizumi, H. Mizunuma (2014): The level of RECQL1 expression is a prognostic factor for epithelial ovarian cancer. In: *J Ovarian Res*, 7, 107

V. **Mazzaferro**, E. Regalia, R. Doci, S. Andreola, A. Pulvirenti, F. Bozzetti, F. Montalto, M. Ammatuna, A. Morabito, L. Gennari (1996): Liver transplantation for the treatment of small hepatocellular carcinomas in patients with cirrhosis. In: *N Engl J Med*, 334(11), 693-9

R. **Mendoza-Maldonado**, V. Faoro, S. Bajpai, M. Berti, F. Odreman, M. Vindigni, T. Ius, A. Ghasemian, S. Bonin, M. Skrap, G. Stanta, A. Vindigni (2011): The human RECQ1 helicase is highly expressed in glioblastoma and plays an important role in tumor cell proliferation. In: *Mol Cancer*, 10, 83

G. **Meroni**, G. Diez-Roux (2005): TRIM/RBCC, a novel class of 'single protein RING finger' E3 ubiquitin ligases. In: *Bioessays*, 27(11), 1147-57

T.E.T. **Mevissen**, D. Komander (2017): Mechanisms of Deubiquitinase Specificity and Regulation. In: *Annu Rev Biochem*, 86, 159-192

N. **Meyer**, L.Z. Penn (2008): Reflecting on 25 years with MYC. In: *Nat Rev Cancer*, 8(12), 976-90

R.M. **McAvera**, L.J. Crawford (2020): TIF1 Proteins in Genome Stability and Cancer. In: *Cancers (Basel)*, 12(8), 2094

N.J. **McHugh**, S.L. Tansley (2018): Autoantibodies in myositis. In: *Nat Rev Rheumatol*, 14(5), 290-302

S.B. **McMahon** (2014): MYC and the Control of Apoptosis. In: Cold Spring Harb Perspect Med., 4(7): a014407

D.M. **Miller**, S.D. Thomas, A. Islam, D. Muench, K. Sedoris (2012): c-Myc and cancer metabolism. In: *Clin Cancer Res*, 18(20), 5546-53

J. **Min**, J. Hu, C. Luo, J. Zhu, J. Zhao, Z. Zhu, L. Wu, R. Yuan (2020): IFITM3 upregulates c-myc expression to promote hepatocellular carcinoma proliferation via the ERK1/2 signalling pathway. In: *Biosci Trends*, 13(6), 523-529

S. **Mittnacht** (1998): Control of pRB phosphorylation. In: *Curr. Opin. Genet. Dev.*, 8(1), 21–27

E. **Morgunova,** Y. Yin, A. Jolma, K. Dave, B. Schmierer, A. Popov, N. Eremina, L. Nilsson, J. Taipale (2015): Structural insights into the DNA-binding specificity of E2F family transcription factors. In : *Nat Commun.*, 6:10050

S.F. **Muakkassah-Kelly**, D.A. Jans, N. Lydon, F. Bieri, F. Waechter, P. Bentley, W. Stäubli (1988): Electroporation of cultured adult rat hepatocytes with the c-myc gene potentiates DNA synthesis in response to epidermal growth factor. In: *Exp Cell Res*, 178(2), 296-306

T. **Murayama**, Y. Takeuchi, K. Yamawaki, T. Natsume, M. Li, R.-C.N. Marcela, T. Nishimura, Y. Kogure, A. Nakata, K. Tominaga, A. Sasahara, M. Yano, S. Ishikawa, T. Ohta, K. Ikeda, K. Horie-Inoue, S. Inoue, M. Seki, Y. Suzuki, S. Sugano, T. Enomoto, M. Tanabe, K.-I. Tada, M.T. Kanemaki, K. Okamoto, A. Tojo, N. Gotoh (2020): MCM10 compensates for Myc-induced DNA replication stress in breast cancer stem-like cells. In: *Cancer Sci*, doi: 10.1111/cas.14776

Y. **Muro**, A. Ishikawa, K. Sugiura, M. Akiyama (2012): Clinical features of anti-TIF1-α antibody-positive dermatomyositis patients are closely associated with coexistent dermatomyositis-specific autoantibodies and anti-TIF1-γ or anti-Mi-2 autoantibodies. In: *Rheumatology*, 51(8), 1508-13

N. **Muthalagu**, M.R. Junttila, K.E. Wiese, E. Wolf, J. Morton, B. Bauer, G.I. Evan, M. Eilers, D.J. Murphy (2014): BIM is the primary mediator of MYC-induced apoptosis in multiple solid tissues. In: *Cell Rep*, 8(5), 1347-53

J.R. **Nevins** (1998): Toward an understanding of the functional complexity of the E2F and retinoblastoma families. In: *Cell Growth Differ.,* 9(8), 585–593

Y.A. **Nevzorova**, F.J. Cubero, W. Hu, F. Hao, U. Haas, P. Ramadori, N. Gassler, M. Hoss, P. Strnad, H.W. Zimmermann, F. Tacke, C. Trautwein, C. Liedtke (2016): Enhanced expression of c-myc in hepatocytes promotes initiation and progression of alcoholic liver disease. In: *J Hepatol*, 64(3), 628-40

Y.A. **Nevzorova**, W. Hu, F.J. Cubero, U. Haas, J. Freimuth, F. Tacke, C. Trautwein, C. Liedtke (2013): Overexpression of c-myc in hepatocytes promotes activation of hepatic stellate cells and facilitates the onset of liver fibrosis. In: *Biochim Biophys Acta*, 1832(10), 1765-75

A.W.T. **Ng**, S.L. Poon, M.N. Huang, J.Q. Lim, A. Boot, W. Yu, Y. Suzuki, S. Thangaraju, C.C.Y. Ng, P. Tan, S.-T. Pang, H.-Y. Huang, M.-C. Yu, P.-H. Lee, S.-Y. Hsieh, A.Y. Chang, B.T. Teh, S.G. Rozen (2017): Aristolochic acids and their derivatives are widely implicated in liver cancers in Taiwan and throughout Asia. In: *Sci Transl Med*, 9(412):eaan6446

H. **Ongen**, C.L. Andersen, J.B. Bramsen, B. Oster, M.H. Rasmussen, P.G. Ferreira, J. Sandoval, E. Vidal, N. Whiffin, A. Planchon, I. Padioleau, D. Bielser, L. Romano, I. Tomlinson, R.S. Houlston, M. Esteller, T.F. Orntoft, E.T. Dermitzakis (2014): Putative cis-regulatory drivers in colorectal cancer. In: *Nature*, 512(7512), 87—90

K. **Ohtani**, R. Iwanaga, M. Nakamura, M. Ikeda, N. Yabuta, H. Tsuruga, H. Nojima (1999): Cell growth-regulated expression of mammalian MCM5 and MCM6 genes mediated by the transcription factor E2F. In: *Oncogene*, 18(14), 2299-309

J.T. **Opferman**, A. Kothari (2018): Anti-apoptotic BCL-2 family members in development. In: *Cell Death Differ*., 25(1), 37–45

K. **Ozato**, D.-M. Shin, T.-H. Chang, H.C. Morse (2008): TRIM family proteins and their emerging roles in innate immunity. In: *Nat Rev Immunol.*, 8(11), 849–860

T. **Parisi**, R.T. Bronson, J.A. Lees (2009): Inhibition of pituitary tumors in Rb mutant chimeras through E2f4loss reveals a key suppressive role for the pRB/E2F pathway in urothelium and ganglioniccarcinogenesis. In: *Oncogene.*, 28(4), 500–508

S. **Parvathaneni**, S. Sharma (2019): The DNA repair helicase RECQ1 has a checkpoint-dependent role in mediating DNA damage responses induced by gemcitabine. In: *J Biol Chem*, 294(42), 15330-15345

S. **Parvathaneni**, A. Stortchevoi, J.A. Sommers, R.M. Brosh Jr, S. Sharma (2013): Human RECQ1 interacts with Ku70/80 and modulates DNA end-joining of double-strand breaks. In: *PLoS One*, 8(5):e62481

J.-W. **Park**, M. Chen, M. Colombo, L.R. Roberts, M. Schwartz, P.-J. Chen, M. Kudo, P. Johnson, S. Wagner, L.S. Orsini, M. Sherman (2015): Global patterns of hepatocellular carcinoma management from diagnosis to death: the BRIDGE Study. In: *Liver Int*, 35(9), 2155-66

S. **Pelengaris**, M. Khan (2003): The many faces of c-MYC. In: *Arch Biochem Biophys*, 416(2), 129-36

C.M. **Pfeffer**, A.T.K. Singh (2018): Apoptosis: A Target for Anticancer Therapy. In: *Int J Mol Sci*., 19(2), 448

C.M. **Pickart** (2001): Mechanisms underlying ubiquitination. In: *Annu Rev Biochem*, 70, 503-533

M. **Podhorecka**, A. Skladanowski, P. Bozko (2010): H2AX Phosphorylation: Its Role in DNA Damage Response and Cancer Therapy. In: *J Nucleic Acids*., 920161

S. **Polager**, Y. Kalma, E. Berkovich, D. Ginsberg (2002): E2Fs up-regulate expression of genes involved in DNA replication, DNA repair and mitosis. In: *Oncogene*, 21(3), 437-46

R.M. **Pommier**, J. Gout, D.F. Vincent, L.B. Alcaraz, N. Chuvin, V. Arfi, S. Martel, B. Kaniewski, G. Devailly, G. Fourel, P. Bernard, C. Moyret-Lalle, S. Ansieau, A. Puisieux, U. Valcourt, S. Sentis, L. Bartholin (2015): TIF1γ Suppresses Tumor Progression by Regulating Mitotic Checkpoints and Chromosomal Stability. In: *Cancer Res*, 75(20), 4335-50

N. **Popov**, M. Wanzel, M. Madiredjo, D. Zhang, R. Beijersbergen, R. Bernards, R. Moll, S.J. Elledge, M. Eilers (2007): The ubiquitin-specific protease USP28 is required for MYC stability. In: *Nat Cell Biol*, 9, 765–774

V. **Popuri**, D.L. Croteau, R.M. Brosh Jr, V.A. Bohr (2012): RECQ1 is required for cellular resistance to replication stress and catalyzes strand exchange on stalled replication fork structures. In: *Cell Cycle*, 11(22), 4252-65

L.M.F. **Primo**, L.K. Teixeira (2019): DNA replication stress: oncogenes in the spotlight. In: *Genet Mol Biol*, 43(1 suppl 1):e20190138

C. **Pucci**, C. Martinelli, G. Ciofani (2019): Innovative approaches for cancer treatment: current perspectives and new challenges. In: *Ecancermedicalscience*, 13, 961

G. **Qi**, G. Lu, J. Yu, Y. Zhao, C. Wang, H. Zhang, Q. Xia (2019): Up-regulation of TIF1γ by valproic acid inhibits the epithelial mesenchymal transition in prostate carcinoma through TGF-β/Smad signaling pathway. In: *Eur J Pharmacol*, 860:172551

A. **Qu**, C. Jiang, Y. Cai, J.-H. Kim, N. Tanaka, J.M. Ward, Y.M. Shah, F.J. Gonzalez (2014): Role of Myc in hepatocellular proliferation and hepatocarcinogenesis. In: *J Hepatol*, 60(2), 331-8

R. **Quéré**, L. Saint-Paul, V. Carmignac, R.Z. Martin, M.-L. Chrétien, A. Largeot, A. Hammann, J.-P. Pais de Barros, J.-N. Bastie, L. Delva (2014): Tif1γ regulates the TGF-β1 receptor and promotes physiological aging of hematopoietic stem cells. In: *Proc Natl Acad Sci U S A*, 111(29), 10592-7

S. **Qiu**, G. Jiang, L. Cao, J. Huang (2021): Replication Fork Reversal and Protection. In: *Front Cell Dev Biol*, 9, 670392

E.A. **Rakha**, S.E. Pinder, E.C. Paish, J.F. Robertson, I.O. Ellis (2004): Expression of E2F-4 in invasive breast carcinomas is associated with poor prognosis. In: *J Pathol*, 203 (3), 754-61

D.G. **Ransom**, N. Bahary, K. Niss, D. Traver, C. Burns, N.S. Trede, N. Paffett-Lugassy, W.J. Saganic, C.A. Lim, C. Hersey, Y. Zhou, B.A. Barut, S. Lin, P.D. Kingsley, J. Palis, S.H. Orkin, L.I. Zon (2004): The zebrafish moonshine gene encodes transcriptional intermediary factor 1gamma, an essential regulator of hematopoiesis. In: *PLoS Biol*, 2(8):E237

S. **Rajderkar**, J.M. Mann, C. Panaretos, K. Yumoto, H. Li, Y. Mishina, B. Ralston, V. Kaartinen (2019): Trim33 is required for appropriate development of pre-cardiogenic mesoderm. In: *Dev Biol*, 450(2), 101-114

S. **Rajderkar**, C. Panaretos, V. Kaartinen (2017): Trim33 regulates early maturation of mouse embryoid bodies in vitro. In: *Biochem Biophys Rep*, 12, 185-192

L. **Reavie**, G.D. Gatta, K. Crusio, B. Aranda-Orgilles, S.M. Buckley, B. Thompson, E. Lee, J. Gao, A.L. Bredemeyer, B.A. Helmink, J. Zavadil, B.P. Sleckman, T. Palomero, A. Ferrando, I. Aifantis (2010): Hematopoietic Stem Cell Differentiation Regulated by a Single Ubiquitin Ligase: Substrate Complex. In: *Nat Immunol.*, 11(3), 207–215

R.E. **Rempel**, S. Mori, M. Gasparetto, M.A. Glozak, E.R. Andrechek, S.B. Adler, N.M. Laakso, A.S. Lagoo, R. Storms, C. Smith, J.R. Nevins (2009): A role for E2F activities in determining the fate of Myc-induced lymphomagenesis. In: *PLoS Genet*, 5(9):e1000640

S. **Rennoll**, G. Yochum (2015): Regulation of *MYC* gene expression by aberrant Wnt/β-catenin signaling in colorectal cancer. In: *World J Biol Chem*., 6(4), 290–300

F.E. **Reyes-Turcu**, K.H. Ventii, K.D. Wilkinson (2009): Regulation and cellular roles of ubiquitin-specific deubiquitinating enzymes. In: *Annu Rev Biochem*, 78, 363-397

A. **Reymond**, G. Meroni, A. Fantozzi, G. Merla, S. Cairo, L. Luzi, D. Riganelli, E. Zanaria, S. Messali, S. Cainarca, A. Guffanti, S. Minucci, P.G. Pelicci, A. Ballabio (2001): The tripartite motif family identifies cell compartments. In: *EMBO J*, 20(9), 2140-51

D.A. **Rhodes**, G. Ihrke, A.T. Reinicke, G. Malcherek, M. Towey, D.A. Isenberg, J. Trowsdale (2002): The 52 000 MW Ro/SS-A autoantigen in Sjögren's syndrome/systemic lupus erythematosus (Ro52) is an interferon-gamma inducible tripartite motif protein associated with membrane proximal structures. In: *Immunology*, 106(2), 246-56

C. **Ribeiro-Silva**, W. Vermeulen, H. Lans (2019): SWI/SNF: Complex complexes in genome stability and cancer. In: *DNA Repair* (*Amst),* 77, 87-95

S. **Roayaie**, G. Jibara, P. Tabrizian, J.-W. Park, J. Yang, L. Yan, M. Schwartz, G. Han, F. Izzo, M. Chen, J.-F. Blanc, P. Johnson, M. Kudo, L.R. Roberts, M. Sherman (2015): The role of hepatic resection in the treatment of hepatocellular cancer. In: *Hepatology*, 62(2), 440-51

P.A. **Roelofs**, C.Y. Goh, B.H. Chua, M.C. Jarvis, T.A. Stewart, J.L. McCann, R.M. McDougle, M.A. Carpenter, J.W. Martens, P.N. Span, D. Kappei, R.S. Harris (2020): Characterization of the mechanism by which the RB/E2F pathway controls expression of the cancer genomic DNA deaminase APOBEC3B. In: *Elife*, 9:e61287

S. **Rohban**, S. Campaner (2015): Myc induced replicative stress response: How to cope with it and exploit it. In: *Biochim Biophys Acta*, 1849(5), 517-24T.A. **Rosenquist**, A.P. Grollman (2016): Mutational signature of aristolochic acid: Clue to the recognition of a global disease. In: *DNA Repair (Amst)*, 44, 205-211

S. **Sadasivam**, J.A. DeCaprio (2013): The DREAM complex: master coordinator of cell cycle-dependent gene expression. In: *Nat Rev Cancer*, 13(8), 585-95

D. **Samanta**, P.K. Datta (2012): Alterations in the Smad pathway in human cancers. In: *Front Biosci (Landmark Ed)*, 17:1281-93

S. **Sanada**, K. Futami, A. Terada, K. Yonemoto, S. Ogasawara, J. Akiba, M. Yasumoto, A. Sumi, K. Ushijima, T. Kamura, Y. Furuichi, H. Yano (2013): RECQL1 DNA repair helicase: a potential therapeutic target and a proliferative marker against ovarian cancer. In: *PLoS One*, 8(8):e72820

R. **Sanchez**, M.-M. Zhou (2009): The role of human bromodomains in chromatin biology and gene transcription. In: *Curr Opin Drug Discov Devel.*,12(5), 659–665

R. **Sanchez**, M.-M. Zhou (2011): The PHD finger: a versatile epigenome reader. In: *Trends Biochem Sci*, 36(7), 364-72

E. **Santoni-Rugiu**, D. Duro, T. Farkas, I.S. Mathiasen, M. Jäättelä, J. Bartek, J. Lukas (2002): E2F activity is essential for survival of Myc-overexpressing human cancer cells. In: *Oncogene*, 21(42), 6498-509

T. **Sato**, F. Okumura, T. Ariga, S. Hatakeyama (2012): TRIM6 interacts with Myc and maintains the pluripotency of mouse embryonic stem cells. In: *J Cell Sci*, 125(6), 1544-55

A.E. **Schade**, M. Fischer, J.A. DeCaprio (2019): RB, p130 and p107 differentially repress G1/S and G2/M genes after p53 activation. In: *Nucleic Acids Res*, 47(21), 11197-11208

F.X. **Schaub**, V. Dhankani, A.C. Berger, M. Trivedi, A.B. Richardson, R. Shaw, W.Zhao, X. Zhang, A. Ventura, Y. Liu, D.E. Ayer, P.J. Hurlin, A.D. Cherniack, R.N. Eisenman, B. Bernard, C. Grandori, Cancer Genome Atlas Network (2018): Pan-cancer alterations of the MYC oncogene and its proximal network across the Cancer Genome Atlas. In: *Cell Syst*., 6, 282–300

M. **Scheffner**, U. Nuber, J.M. Huibregtse (1995): Protein ubiquitination involving an E1-E2-E3 enzyme ubiquitin thioester cascade. In: *Nature*, 373(6509), 81-3

G.G. **Sedgwick**, K. Townsend, A. Martin, N.J. Shimwell, R.J.A. Grand, G.S. Stewart, J. Nilsson, A.S. Turnell (2013): Transcriptional intermediary factor 1γ binds to the anaphase-promoting complex/cyclosome and promotes mitosis. In: *Oncogene*, 32(39), 4622-33

J. **Seoane**, R.R. Gomis (2017): TGF-β Family Signaling in Tumor Suppression and Cancer Progression. In: *Cold Spring Harb Perspect Biol.*, 9(12): a022277

M. **Serrano**, A.W. Lin, M.E. McCurrach, D. Beach, S.W. Lowe (1997): Oncogenic ras provokes premature cell senescence associated with accumulation of p53 and p16INK4a. In: *Cell*, 88(5), 593-602

H.B. **El-Serag** (2012): Epidemiology of viral hepatitis and hepatocellular carcinoma. In: *Gastroenterology*, 142(6), 1264-1273

H.B. **El-Serag**, K.L. Rudolph (2007): Hepatocellular carcinoma: epidemiology and molecular carcinogenesis. In: *Gastroenterology*, 132(7), 2557-76

C.M. **Shachaf**, A.M. Kopelman, C. Arvanitis, A. Karlsson, S. Beer, S. Mandl, M.H. Bachmann, A.D. Borowsky, B. Ruebner, R.D. Cardiff, Q. Yang, J.M. Bishop, C.H. Contag, D.W. Felsher (2004): MYC inactivation uncovers pluripotent differentiation and tumour dormancy in hepatocellular cancer. In: *Nature*, 431(7012), 1112-7

S. **Sharma**, R.M. Brosh Jr (2007): Human RECQ1 is a DNA damage responsive protein required for genotoxic stress resistance and suppression of sister chromatid exchanges. In: *PLoS One*, 2(12):e1297

S. **Sharma**, P. Phatak, A. Stortchevoi, M. Jasin, J.R. Larocque (2012): RECQ1 plays a distinct role in cellular response to oxidative DNA damage. In: *DNA Repair (Amst)*, 11(6), 537-49

S. **Sharma**, D.J. Stumpo, A.S. Balajee, C.B. Bock, P.M. Lansdorp, R.M. Brosh Jr, P.J. Blackshear (2007): RECQL, a member of the RecQ family of DNA helicases, suppresses chromosomal instability. In: *Mol Cell Biol*, 27(5), 1784-94

S. **Sharma**, J.A. Sommers, S. Choudhary, J.K. Faulkner, S. Cui, L. Andreoli, L. Muzzolini, A. Vindigni, R.M. Brosh Jr (2005): Biochemical analysis of the DNA unwinding and strand annealing activities catalyzed by human RECQ1. In: *J Biol Chem*, 280(30), 28072-84

W. **Shi**, L. Feng, S. Dong, Z. Ning, Y. Hua, L. Liu, Z. Chen, Z. Meng (2020): FBXL6 governs c-MYC to promote hepatocellular carcinoma through ubiquitination and stabilization of HSP90AA1. In: *Cell Commun Signal*, 18(1), 100

S. **Shiina**, K. Sato, R. Tateishi, M. Shimizu, H. Ohama, T. Hatanaka, M. Takawa, H. Nagamatsu, Y. Imai (2018): Percutaneous Ablation for Hepatocellular Carcinoma: Comparison of Various Ablation Techniques and Surgery. In: *Can J Gastroenterol Hepatol.*, 4756147

K.M. **Short**, T.C. Cox (2006): Subclassification of the RBCC/TRIM superfamily reveals a novel motif necessary for microtubule binding. In: *J Biol Chem*, 281(13), 8970-80

K.M. **Short**, B. Hopwood, Z. Yi, T.C. Cox (2002): MID1 and MID2 homo- and heterodimerise to tether the rapamycin-sensitive PP2A regulatory subunit, Alpha 4, to microtubules: implications for the clinical variability of X-linked Opitz GBBB syndrome and other developmental disorders. In: *BMC Cell Biol*, 3:1.doi: 10.1186/1471-2121-3-1

W.A. **Siddiqui**, A. Ahad, H. Ahsan (2015): The mystery of BCL2 family: Bcl-2 proteins and apoptosis: an update. In: *Arch Toxicol*, 89(3), 289-317

M.M. **Simile**, M.R. De Miglio, M.R. Muroni, M. Frau, G. Asara, S. Serra, M.D. Muntoni, M.A. Seddaiu, L. Daino, F. Feo, R.M. Pascale (2004): Down-regulation of c-myc and Cyclin D1

genes by antisense oligodeoxy nucleotides inhibits the expression of E2F1 and in vitro growth of HepG2 and Morris 5123 liver cancer cells. In: *Carcinogenesis*, 25(3), 333-41

S. **Sohn**, P. Hearing (2016): The adenovirus E4-ORF3 protein functions as a SUMO E3 ligase for TIF-1γ sumoylation and poly-SUMO chain elongation. In: *Proc Natl Acad Sci U S A*, 113(24), 6725-30

C. **Speck**, Z. Chen, H. Li, B. Stillman (2005): ATPase-dependent cooperative binding of ORC and Cdc6 to origin DNA. In: *Nat Struct Mol Biol*, 12(11), 965-71

S.V. **Srinivasan**, D. Dominguez-Sola, L.C. Wang, O. Hyrien, J. Gautier (2013): Cdc45 is a critical effector of myc-dependent DNA replication stress. In: *Cell Rep*, 3(5), 1629-39

J. **Srivastava**, A. Siddiq, R. Gredler, X.-N. Shen, D. Rajasekaran, C.L. Robertson, M.A. Subler, J.J. Windle, C.I. Dumur, N.D. Mukhopadhyay, D. Garcia, Z. Lai, Y. Chen, U. Balaji, P.B. Fisher, D. Sarkar (2015): Astrocyte elevated gene-1 (AEG-1) and c-Myc cooperate to promote hepatocarcinogenesis. In: *Hepatology*, 61(3), 915–929

R.V. **Stevens**, D. Esposito, K. Rittinger (2019): Characterisation of class VI TRIM RING domains: linking RING activity to C-terminal domain identity. In: *Life Sci Alliance*, 2(3):e201900295

Z.E. **Stine**, Z.E. Walton, B.J. Altman, A.L. Hsieh, C.V. Dang (2015): MYC, Metabolism, and Cancer. In: *Cancer Discov.*, 5(10), 1024–1039

A. **Tarangelo**, N. Lo, R. Teng, E. Kim, L. Le, D. Watson, E.E. Furth, P. Raman, U. Ehmer, P. Viatour (2015): Recruitment of Pontin/Reptin by E2f1 amplifies E2f transcriptional response during cancer progression. In: *Nat Commun*, 6, 10028

M.B. **Stope** (2021): Phosphorylation of histone H2A.X as a DNA-associated biomarker (Review). In: *World Academy of Sciences Journal*, DOI: 10.3892/wasj.2021.102

T.H. **Stracker** (2019): E2F4/5-mediated transcriptional control of multiciliated cell differentiation: redundancy or fine-tuning? In: *Dev Biol*, 446(1), 20-21

M. **Stremlau**, C.M. Owens, M.J. Perron, M. Kiessling, P. Autissier, J. Sodroski (2004): The cytoplasmic body component TRIM5alpha restricts HIV-1 infection in Old World monkeys. In: *Nature*, 427(6977), 848-53

B. **Suresh**, J. Lee, K.-S. Kim, S. Ramakrishna (2016): The Importance of Ubiquitination and Deubiquitination in Cellular Reprogramming. In: *Stem Cells Int*, 6705927

A. **Tarangelo**, N. Lo, R. Teng, E. Kim, L. Le, D. Watson, E.E. Furth, P. Raman, U. Ehmer, P. Viatour (2015): Recruitment of Pontin/Reptin by E2f1 amplifies E2f transcriptional response during cancer progression. In: *Nat Commun*, 6, 10028

P. **Tabrizian**, G. Jibara, B. Shrager, M. Schwartz, S. Roayaie (2015): Recurrence of hepatocellular cancer after resection: patterns, treatments, and prognosis. In: *Ann Surg*, 261(5), 947-55

S. **Thangavel**, R. Mendoza-Maldonado, E. Tissino, J.M. Sidorova, J. Yin, W. Wang, R.J. Monnat Jr, A. Falaschi, A. Vindigni (2010): Human RECQ1 and RECQ4 helicases play distinct roles in DNA replication initiation. In: *Mol Cell Biol*, 30(6), 1382-96

J.M. **Trimarchi**, J.A. Lees (2002): Sibling rivalry in the E2F family. In: *Nat. Rev. Mol.Cell Biol.*, 3(1), 11–20

P.K. **Tsantoulis**, V.G. Gorgoulis (2005): Involvement of E2F transcription factor family in cancer. In: *Eur J Cancer*, 41(16), 2403-14

M. **Tsuneoka**, E. Mekada (2000): Ras/MEK signaling suppresses Myc-dependent apoptosis in cells transformed by c-myc and activated ras. In: *Oncogene*, 19(1), 115-23

R. **Taub**, I. Kirsch, C. Morton, G. Lenoir, D. Swan, S. Tronick, S. Aaronson, P. Leder (1982): Translocation of the c-myc gene into the immunoglobulin heavy chain locus in human Burkitt lymphoma and murine plasmacytoma cells. In: *Proc Natl Acad Sci U S A*, 79(24), 7837-41

T. **Ubhi**, G.W. Brown (2019): Exploiting DNA Replication Stress for Cancer Treatment. In: *Cancer Res*, 79(8), 1730-1739

M.J. **van Amerongen**, F. Diehl, T. Novoyatleva, C. Patra, F.B. Engel (2010): E2F4is required for cardiomyocyte proliferation. In: *Cardiovasc. Res.*, 86(1), 92–102

S. **Van Den Heuvel**, N.J. Dyson (2008): Conserved functions of the pRB and E2F families. In: *Nat. Rev. Mol.Cell Biol.*, 9(9), 713—724

L. **Venturini**, J. You, M. Stadler, R. Galien, V. Lallemand, M.H. Koken, M.G. Mattei, A. Ganser, P. Chambon, R. Losson, H. de Thé (1999): TIF1gamma, a novel member of the transcriptional intermediary factor 1 family. In: *Oncogene*, 18(5), 1209-17

L. **Verlinden**, I.V. Bempt, G. Eelen, M. Drijkoningen, I. Verlinden, K. Marchal, C. De Wolf-Peeters, M.-R. Christiaens, L. Michiels, R. Bouillon, A. Verstuyf (2007): The E2F-regulated gene Chk1 is highly expressed in triple-negative estrogen receptor /progesterone receptor /HER-2 breast carcinomas. In: *Cancer Res*, 67(14), 6574-81

R. **Verona**, K. Moberg, S. Estes, M. Starz, J.P. Vernon, J.A. Lees (1997): E2F activity is regulated by cell cycle-dependent changes in subcellular localization. In: *Mol Cell Biol*, 17 (12), 7268-7282

A. **Villanueva** (2019): Hepatocellular Carcinoma. In: *N Engl J Med*, 380(15), 1450-62

D.F. **Vincent**, J. Gout, N. Chuvin, V. Arfi, R.M. Pommier, P. Bertolino, N. Jonckheere, D. Ripoche, B. Kaniewski, S. Martel, J.-B. Langlois, S. Goddard-Léon, A. Colombe, M. Janier, I. Van Seuningen, R. Losson, U. Valcourt, I. Treilleux, P. Dubus, N. Bardeesy, L. Bartholin (2012): Tif1γ Suppresses Murine Pancreatic Tumoral Transformation by a Smad4-Independent Pathway. *Am erican Journal of Pathology*, 180 (6), 2214-21

D.F. **Vincent**, K.-P. Yan, I. Treilleux, F. Gay, V. Arfi, B. Kaniewsky, J.C. Marie, F. Lepinasse, S. Martel, S. Goddard-Leon, J.L. Iovanna, P. Dubus, S. Garcia, A. Puisieux, R. Rimokh, N. Bardeesy, J.-Y. Scoazec, R. Losson, L. Bartholin (2009): Inactivation of TIF1γ Cooperates with $Kras^{G12D}$ to Induce Cystic Tumors of the Pancreas. *PLoS Genetics*, 5 (7): e1000575

E. **Viziteu**, B. Klein, J. Basbous, Y.-L. Lin, C. Hirtz, C. Gourzones, L. Tiers, A. Bruyer, L. Vincent, C. Grandmougin, A. Seckinger, H. Goldschmidt, A. Constantinou, P. Pasero, D. Hose, J. Moreaux (2017): RECQ1 helicase is involved in replication stress survival and drug resistance in multiple myeloma. In: *Leukemia*, 31(10), 2104-2113

T. **Wahlström**, M.A. Henriksson (2015): Impact of MYC in regulation of tumor cell metabolism. In: *Biochim Biophys Acta*, 1849(5), 563-9

E. **Wang**, S. Kawaoka, J. Roe, J. Shi, A.F. Hohmann, Y. Xu, A.S. Bhagwat, Y. Suzuki, J.B. Kinney, C.R. Vakoc (2015): The transcriptional cofactor TRIM33 prevents apoptosis in B lymphoblastic leukemia by deactivating a single enhancer. In: *Elife*, 4:e06377

D. **Wang**, J. Russell, H. Xu, D.G. Johnson (2001): Deregulated expression ofDP1 induces epidermal proliferation and enhances skin carcinogenesis. In: *Mol Carcinog*, 31(2), 90-100

J. **Wang**, Y. Tian, H. Chen, H. Li, S. Zheng (2018): Key signaling pathways, genes and transcription factors associated with hepatocellular carcinoma. In: *Mol Med Rep*, 17(6), 8153-8160

B. **Wang**, T. Tian, K.-H. Kalland, X. Ke, Y. Qu (2018): Targeting Wnt/β-Catenin Signaling for Cancer Immunotherapy. In: *Trends Pharmacol Sci*, 39(7), 648-658

L. **Wang**, X. Tong, Z. Zhou, S. Wang, Z. Lei, T. Zhang, Z. Liu, Y. Zeng, C. Li, J. Zhao, Z. Su, C. Zhang, X. Liu, G. Xu, H.-T. Zhang (2018): Circular RNA hsa_circ_0008305 (circPTK2) inhibits TGF-β-induced epithelial-mesenchymal transition and metastasis by controlling TIF1γ in non-small cell lung cancer. In: *Mol Cancer*, 17(1), 140

R. **Wang**, X. Wang, L. Zhuang (2019): Gene expression profiling reveals key genes and pathways related to the development of non-alcoholic fatty liver disease. In: *Ann Hepatol*, 15(2), 190-9

Y. **Wang**, M.-C. Wu, J.S.T. Sham, W. Zhang, W.-Q. Wu, X.-Y. Guan (2002): Prognostic significance of c-myc and AIB1 amplification in hepatocellular carcinoma. A broad survey using high-throughput tissue microarray. In: *Cancer*, 95(11), 2346-52

L. **Wang**, H. Yang, Z. Lei, J. Zhao, Y. Chen, P. Chen, C. Li, Y. Zeng, Z. Liu, X. Liu, H.-T. Zhang (2016): Repression of TIF1γ by SOX2 promotes TGF-β-induced epithelial-mesenchymal transition in non-small-cell lung cancer. In: *Oncogene*, 35(7), 867-77

C. **Wang**, J. Zhang, J. Yin, Y. Gan, S. Xu, Y. Gu, W. Huang (2021): Alternative approaches to target Myc for cancer treatment. In: *Signal Transduct Target Ther*, 6(1), 117

J.D. **Warren**, B. Orr, D.A. Compton (2020): A comparative analysis of methods to measure kinetochore-microtubule attachment stability. In: *Methods Cell Biol*, 158, 91-116

X. **Wei**, W. Zheng, P. Tian, Y. He, H. Liu, M Peng, X. Li, X. Liu (2020): Oncogenic hsa_circ_0091581 promotes the malignancy of HCC cell through blocking miR-526b from degrading c-MYC mRNA. In: *Cell Cycle*, 19(7), 817-824

J. **West**, T.R. Card, G.P. Aithal, K.M. Fleming (2017): Risk of hepatocellular carcinoma among individuals with different aetiologies of cirrhosis: a population-based cohort study. In: *Aliment Pharmacol Ther*, 45(7), 983-990

D. **Westphal**, R.M. Kluck, G. Dewson (2014): Building blocks of the apoptotic pore: how Bax and Bak are activated and oligomerize during apoptosis. In: *Cell Death Differ*, 21(2), 196-205

J. **Whitfield**, T. Littlewood, G.I. Evan, L. Soucek (2015): The estrogen receptor fusion system in mouse models: a reversible switch. In: *Cold Spring Harb Protoc*, 3, 227-34

C.P. **Wild**, J.D. Miller, J.D. Groopman (2015): MYCOTOXIN CONTROL IN LOW- AND MIDDLE-INCOME COUNTRIES. In: *International Agency for Research on Cancer*, IARC Working Group Reports, No9

E. **Wiśnik**, T. Płoszaj, A. Robaszkiewicz (2017): Downregulation of PARP1 transcription by promoter-associated E2F4-RBL2-HDAC1-BRM complex contributes to repression of pluripotency stem cell factors in human monocytes. In: *Sci Rep*, 7(1), 9483

D.K. **Woo**, H.S. Kim, H.S. Lee, Y.H. Kang, H.K. Yang, W.H Kim (2001): Altered expression and mutation of beta-catenin gene in gastric carcinomas and cell lines. In: *Int J Cancer*, 95(2), 108-13

M.Y. **Wu**, C.S. Hill (2009): Tgf-beta superfamily signaling in embryonic development and homeostasis. In: *Dev Cell*, 16(3), 329-43

C.-H. **Wu**, J. van Riggelen, A. Yetil, A.C. Fan, P. Bachireddy, D.W. Felsher (2007): Cellular senescence is an important mechanism of tumor regression upon c-Myc inactivation. In: *Proc Natl Acad Sci U S A*, 104(32), 13028-33

M. **Wu**, Y. Zhou, C. Fei, T. Chen, X. Yin, L. Zhang, Z. Ren (2020): ID1 overexpression promotes HCC progression by amplifying the AURKA/Myc signaling pathway. In: *Int J Oncol*, 57(3), 845-857

A. **Xanthoulis**, D.G. Tiniakos (2013): E2F transcription factors and digestive system malignancies: how much do we know? In: *World J Gastroenterol*, 19(21), 3189-98

Z. **Yan**, J. DeGregori, R. Shohet, G. Leone, B. Stillman, J.R. Nevins, R.S. Williams (1998): Cdc6 is regulated by E2F and is essential for DNA replication in mammalian cells. In: *Proc Natl Acad Sci U S A*, 95(7), 3603-8

W.-X. **Yang**, Y.-Y. Pan, C.-G. You (2019): CDK1, CCNB1, CDC20, BUB1, MAD2L1, MCM3, BUB1B, MCM2, and RFC4 May Be Potential Therapeutic Targets for Hepatocellular Carcinoma Using Integrated Bioinformatic Analysis. In: *Biomed Res Int*., 1245072

Q. **Xi**, Z. Wang, A.-I. Zaromytidou, X.H.-F. Zhang, L.-F. Chow-Tsang, J.X. Liu, H. Kim, A. Barlas, K. Manova-Todorova, V. Kaartinen, L. Studer, W. Mark, D.J. Patel, J. Massagué (2011): A poised chromatin platform for TGF-β access to master regulators., *Cell*, 147 (7), 1511-24

B. **Xin**, M. Yamamoto, K. Fujii, T. Ooshio, X. Chen, Y. Okada, K. Watanabe, N. Miyokawa, H. Furukawa, Y. Nishikawa (2017): Critical role of Myc activation in mouse hepatocarcinogenesis induced by the activation of AKT and RAS pathways. In: *Oncogene*., 36, 5087-97

X. **Xia**, F. Zuo, M. Luo, Y. Sun, J. Bai, Q. Xi (2017): Role of TRIM33 in Wnt signaling during mesendoderm differentiation. In: *Sci China Life Sci*, 60(10), 1142-1149

X.J. **Xie**, H.J. Li, J.J. Pan, X. Han (2021): Knockdown of TRIM26 inhibits the proliferation, migration and invasion of bladder cancer cells through the Akt/GSK3β/β-catenin pathway. In: *Chem Biol Interact*, 337:109366

Y. **Xu**, G. Wu, J. Zhang, J. Li, N. Ruan, J. Zhang, Z. Zhang, Y. Chen, Q. Zhang, Q. Xia (2020): TRIM33 Overexpression Inhibits the Progression of Clear Cell Renal Cell Carcinoma In Vivo and In Vitro. In: *Biomed Res Int*, 2020:8409239

J. **Xue**, Y. Chen, Y. Wu, Z. Wang, A. Zhou, S. Zhang, K. Lin, K. Aldape, S. Majumder, Z. Lu, S. Huang (2015): Tumour suppressor TRIM33 targets nuclear β-catenin degradation. In: Nat Commun, 6:6156

J. **Xue**, X. Lin, W.-T. Chiu, Y.-H. Chen, G. Yu, M. Liu, X.-H. Feng, R. Sawaya, R.H. Medema, M.-C. Hung, S. Huang (2014): Sustained activation of SMAD3/SMAD4 by FOXM1 promotes TGF-β-dependent cancer metastasis. In: *J Clin Invest,* 124(2), 564-79

K. **Yan**, P. Dollé, M. Mark, T. Lerouge, O. Wendling, P. Chambon, R. Losson (2004): Molecular cloning, genomic structure, and expression analysis of the mouse transcriptional intermediary factor 1 gamma gene. In: *Gene*, 334, 3-13

S.-F. **Yang**, C.-W. Chang, R.-J. Wei, Y.-L. Shiue, S.-N. Wang, Y.-T. Yeh (2014): Involvement of DNA Damage Response Pathways in Hepatocellular Carcinoma. In: *Biomed Res Int.*, 153867

J.D. **Yang**, P. Hainaut, G.J. Gores, A. Amadou, A. Plymoth, L.R. Roberts (2019): A global view of hepatocellular carcinoma: trends, risk, prevention and management. In: *Nat Rev Gastroenterol Hepatol*, 16(10), 589-604

J.D. **Yang**, J.J. Larson, K.D. Watt, A.M. Allen, R.H. Wiesner, G.J. Gores, L.R. Roberts, J.A. Heimbach, M.D. Leise (2017): Hepatocellular Carcinoma Is the Most Common Indication for Liver Transplantation and Placement on the Waitlist in the United States. In: *Clin Gastroenterol Hepatol*, 15(5), 767-775

J.D. **Yang**, H.A. Mohammed, W.S. Harmsen, F. Enders, G.J. Gores, L.R. Roberts (2017): Recent Trends in the Epidemiology of Hepatocellular Carcinoma in Olmsted County, Minnesota: A US Population-based Study. In: *J Clin Gastroenterol*, 51(8), 742-748

H. **Yang**, Q. Peng, L. Yin, S. Li, J. Shi, Y. Zhang, X. Lu, X. Shu, S. Zhang, G. Wang (2017): Identification of multiple cancer-associated myositis-specific autoantibodies in idiopathic inflammatory myopathies: a large longitudinal cohort study. In: *Arthritis Res Ther*, 19(1), 259

J.D. **Yang**, L.R. Roberts (2010): Hepatocellular carcinoma: A global view. In: *Nat Rev Gastroenterol Hepatol*, 7(8), 448-58

H. **Yao**, E. Ashihara, T. Maekawa (2011): Targeting the Wnt/β-catenin signaling pathway in human cancers. In: *Expert Opinion on Therapeutic Targets*, 15(7), 873-87

X. **Yin**, C. Xu, X. Zheng, H. Yuan, M. Liu, Y. Qiu, J. Chen (2016): SnoN suppresses TGF-β-induced epithelial-mesenchymal transition and invasion of bladder cancer in a TIF1γ-dependent manner. In: *Oncol Rep*, 36(3), 1535-41

Z.M. **Younossi**, D. Blissett, R. Blissett, L. Henry, M. Stepanova, Y. Younossi, A. Racila, S. Hunt, R. Beckerman (2016): The economic and clinical burden of nonalcoholic fatty liver disease in the United States and Europe. In: *Hepatology*, 64(5), 1577-1586

Z.M. **Younossi**, A.B. Koenig, D. Abdelatif, Y. Fazel, L. Henry, M. Wymer (2016): Global epidemiology of nonalcoholic fatty liver disease-Meta-analytic assessment of prevalence, incidence, and outcomes. In: *Hepatology*, 64(1), 73-84

Z.M. **Younossi**, M. Otgonsuren, L. Henry, C. Venkatesan, A. Mishra, M. Erario, S. Hunt (2015): Association of nonalcoholic fatty liver disease (NAFLD) with hepatocellular carcinoma (HCC) in the United States from 2004 to 2009. In: *Hepatology*, 62(6), 1723-30.

C. **Yu**, Z. Ding, H. Liang, B. Zhang, X. ChenThe (2019): Roles of TIF1γ in Cancer. In:*Front Oncol*, 9:979

J. **Yu**, X.-L. Yu, Z.-Y. Han, Z.-G. Cheng, F.-Y. Liu, H.-Y. Zhai, M.-J. Mu, Y.-M. Liu, P. Liang (2017): Percutaneous cooled-probe microwave versus radiofrequency ablation in early-stage hepatocellular carcinoma: a phase III randomised controlled trial. In: *Gut*, 66(6), 1172-1173

L. **Yu**, T.-T. Yu, K.H. Young (2019): Cross-talk between Myc and p53 in B-cell lymphomas. In: *Chronic Dis Transl Med.*, 5(3), 139–154

M.-F. **Yuen**, D.-S. Chen, G.M. Dusheiko, H.L.A. Janssen, D.T.Y. Lau, S.A. Locarnini, M.G. Peters, C.-L. Lai (2018): Hepatitis B virus infection. In: *Nat Rev Dis Primers*, 4:18035

R. **Yuk**, T. Tatewaki, N. Yamaguchi, K. Aoyama, T. Honda, S. Kubota, M. Morii, I. Manabe, T. Kuga, T. Tomonaga, N. Yamaguchi (2019): Desuppression of TGF-β signaling via nuclear c-Abl-mediated phosphorylation of TIF1γ/TRIM33 at Tyr-524, -610, and -1048. In: *Oncogene*, 38(5), 637-655

R. **Yuki**, T. Tatewaki, N. Yamaguchi, K. Aoyama, T. Honda, S. Kubota, M. Morii, I. Manabe, T. Kuga, T. Tomonaga, N. Yamaguchi (2019): Desuppression of TGF-β signaling via nuclear c-

Abl-mediated phosphorylation of TIF1γ/TRIM33 at Tyr-524, -610, and -1048. In: *Oncogene*, 38(5), 637-655

A. **Zachou**, V. Zouvelou, G.K. Papadimas, M. Rentzos, C. Papadopoulos (2018): Anti-TIF1-γ autoantibodies-positive dermatomyositis: where is the malignancy? In: *Rheumatology*, 57(4), 756

Z.A. **Zahr**, A.N. Baer (2011): Malignancy in myositis. In: *Curr Rheumatol Rep*, 13(3), 208-15

J. **Zhang**, Q. Dai, D. Park, X. Deng (2016): Targeting DNA Replication Stress for Cancer Therapy. In: *Genes (Basel)*., 7(8), 51

X.-Y. **Zhang**, H.K. Pfeiffer, H.S. Mellert, T.J. Stanek, R.T. Sussman, A. Kumari, D. Yu, I. Rigoutsos, A. Thomas-Tikhonenko, H.E. Seidel, L.A. Chodosh, G. Packham, R. Baserga, S.B. McMahon (2011): Inhibition of the single downstream target BAG1 activates the latent apoptotic potential of MYC. In: *Mol Cell Biol*, 31(24), 5037-45

L. **Zhang**, B. Qin, B. Zou, S. Wang, X. Quan, J. Wang, H. Zhao (2021): Knockdown of TRIM15 inhibits the proliferation, migration and invasion of esophageal squamous cell carcinoma cells through inactivation of the Wnt/β-catenin signaling pathway. In: *J Bioenerg Biomembr*, 53(2), 213-222

F. **Zhang**, S.M. Zakaria, V.H. Tabor, M. Singh, S. Tronnersjö, J. Goodwin, G. Selivanova, J. Bartek, A. Castell, L.-G. Larsson (2018): MYC and RAS are unable to cooperate in overcoming cellular senescence and apoptosis in normal human fibroblasts. In: *Cell Cycle.*, 17(24), 2697–2715

Z. **Zhen**, M. Zhang, X. Yuan, M. Li (2019): Transcription factor E2F4 is a positive regulator of milk biosynthesis and proliferation of bovine mammary epithelial cells. In: *Cell Biol Int*, doi: 10.1002/cbin.11225

K. **Zheng**, F.J. Cubero, Y.A. Nevzorova (2017): c-MYC-Making Liver Sick: Role of c-MYC in Hepatic Cell Function, Homeostasis and Disease. In: *Genes (Basel)*, 8(4), 123

N. **Zheng**, N. Shabek (2017): Ubiquitin Ligases: Structure, Function, and Regulation. In: *Annu Rev Biochem*, 86, 129-157

Z. **Zhou**, Y. Liu, M. Ma, L. Chang (2017): Knockdown of TRIM44 inhibits the proliferation and invasion in papillary thyroid cancer cells through suppressing the Wnt/β-catenin signaling pathway. In: *Biomed Pharmacother*, 96, 98-103

D. **Zhuang**, S. Mannava, V. Grachtchouk, W.-H. Tang, S. Patil, J.A. Wawrzyniak, A.E. Berman, T.J. Giordano, E.V. Prochownik, M.S. Soengas, M.A. Nikiforov (2008): C-MYC overexpression is required for continuous suppression of oncogene-induced senescence in melanoma cells. In: *Oncogene*, 27(52), 6623-34

D.B. **Zimonjic**, N.C. Popescu (2012): Role of DLC1 tumor suppressor gene and MYC oncogene in pathogenesis of human hepatocellular carcinoma: Potential prospects for combined targeted therapeutics. In: *Int J Oncol.*, 41(2), 393–406

J. **Zugazagoitia**, C. Guedes, S. Ponce, I. Ferrer, S. Molina-Pinelo, L. Paz-Ares (2016): Current Challenges in Cancer Treatment. In: *Clin Ther*, 38(7), 1551-66

8 Affidavit / Eidesstaattliche Erklärung

I hereby confirm that my thesis entitled “Influence of the E3 ligase Trim33 on the development and the therapy resistance of liver cancer” is the result of my own work. I did not receive any help or support from commercial consultants. All sources and/or materials are listed and specified in the thesis.

Furthermore, I confirm that this thesis has not yet been submitted as part of another examination process neither in identical nor in similar form.

Place, Date Signature

Hiermit erkläre ich an Eides statt, die Dissertation “Influence of the E3 ligase Trim33 on the development and the therapy resistance of liver cancer ” eigenständig, d.h. insbesondere selbständig und ohne Hilfe eines kommerziellen Promotionsberaters, angefertigt und keine anderen als die von mir angegebenen Quellen und Hilfsmittel verwendet zu haben.

Ich erkläre außerdem, dass die Dissertation weder in gleicher noch in ähnlicher Form bereits in einem anderen Prüfungsverfahren vorgelegen hat.

Ort, Datum Unterschrift